University of Maryland Electron Ring (UMER)

June 23, 2016

Brian L. Beaudoin
UMER Faculty and Students
Institute for Research in Electronics & Applied Physics
Energy Research Facility
College Park, MD, USA

Background on UMER

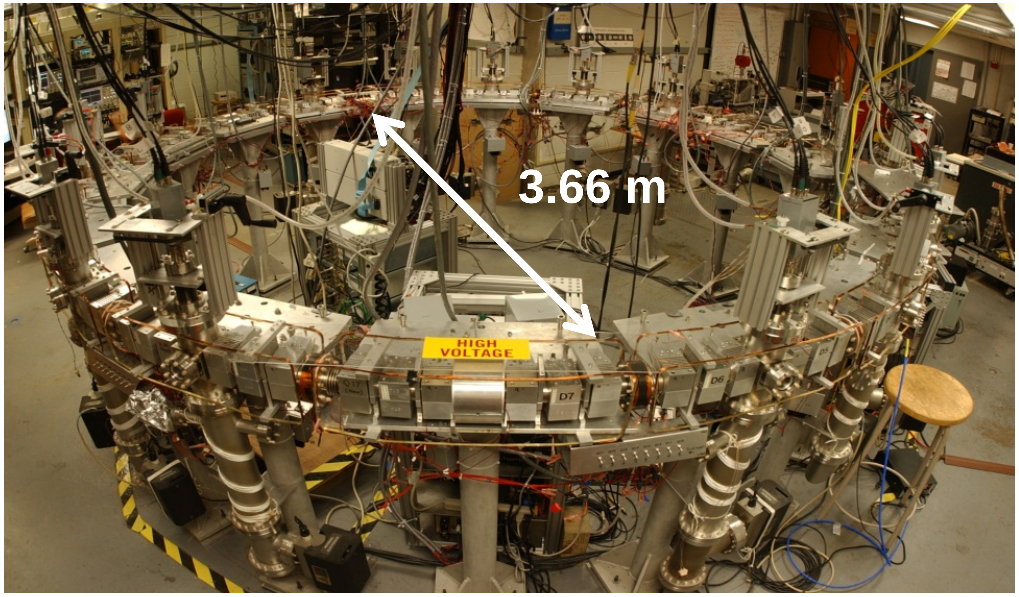

UMER spans a broad range of intensities through the use of the aperture plate

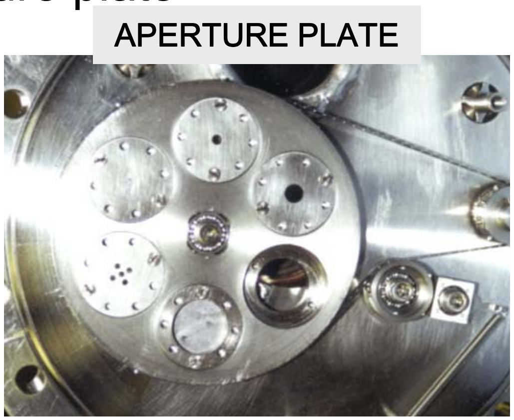

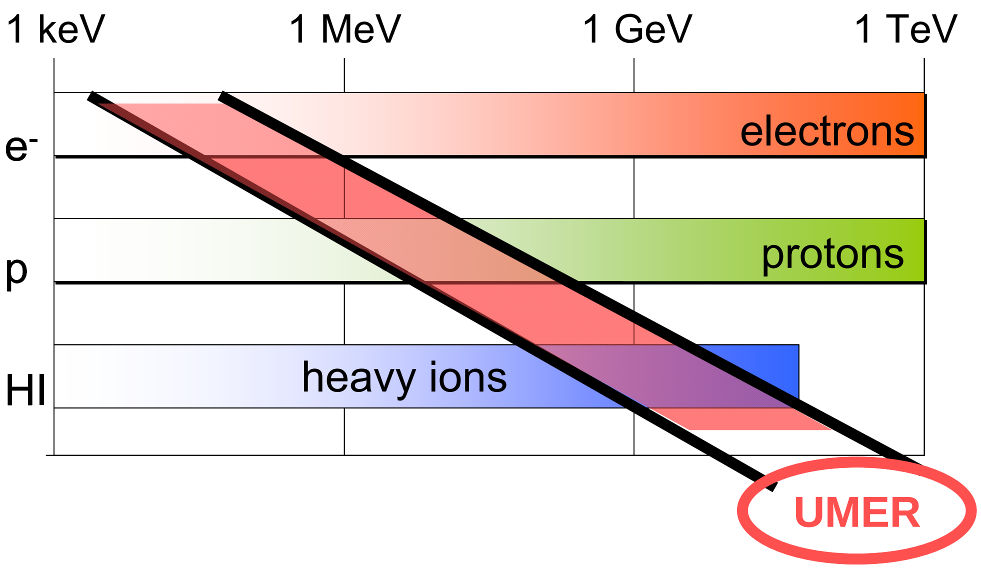

Parameters

Energy: 10keV
Rigidity: 3.38E-4T-m
Current: 0.06-100mA
Tune: 6.76
Tune Shift: 0.045-0.96
Chromaticity: -7.9
Momentum Compaction Factor: 0.0204
Size: 1.5-10mm
Emittance: 7.6-64 mm mr
Avg Earth Field: 400mG

University of Maryland Electron Ring

70	DC Magnetic Quadrupoles
2	P P	Wide Pulsed Quadrupoles
35		DC Bending Dipole
1		Solenoid
1		Pulsed Dipole
1		Bergoz Coil
3		Induction Gap
16		Diagnostic Chamber

Circulation Time 197 ns

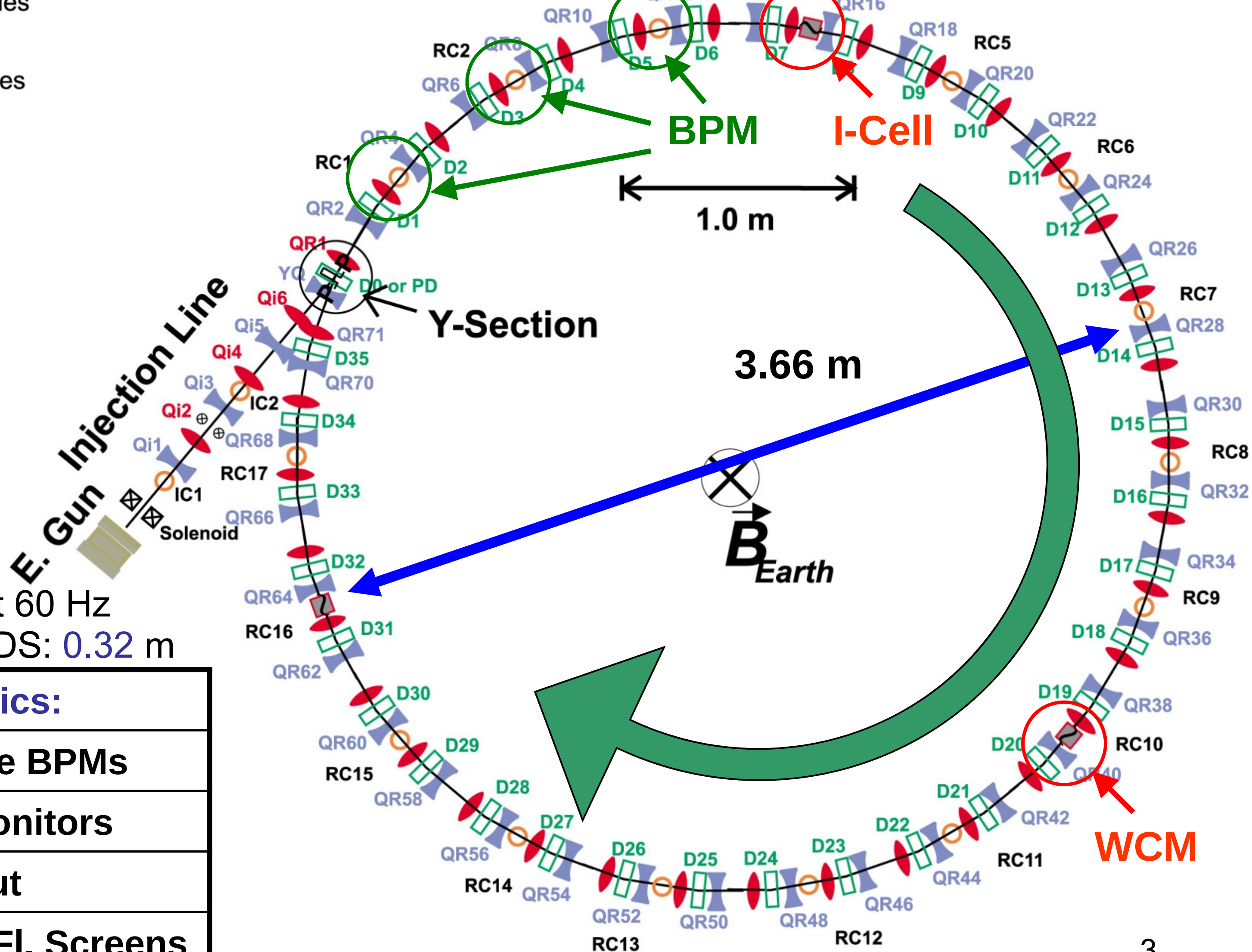

Single turn injection at 60 Hz
FULL LATTICE PERIODS: 0.32 m

Ring Diagnostics:
14 Fast, Capacitive BPMs
1 Wall Current Monitors
RF-Knockout
Slow and Fast Fl. Screens
OTR Screens

Thermionic Electron Sources

Standard Dispenser Cathodes (3-5A/cm^2 CW emission, 15A/cm^2 pulsed)

-HeatWave Labs (www.cathode.com)

Triode Gun

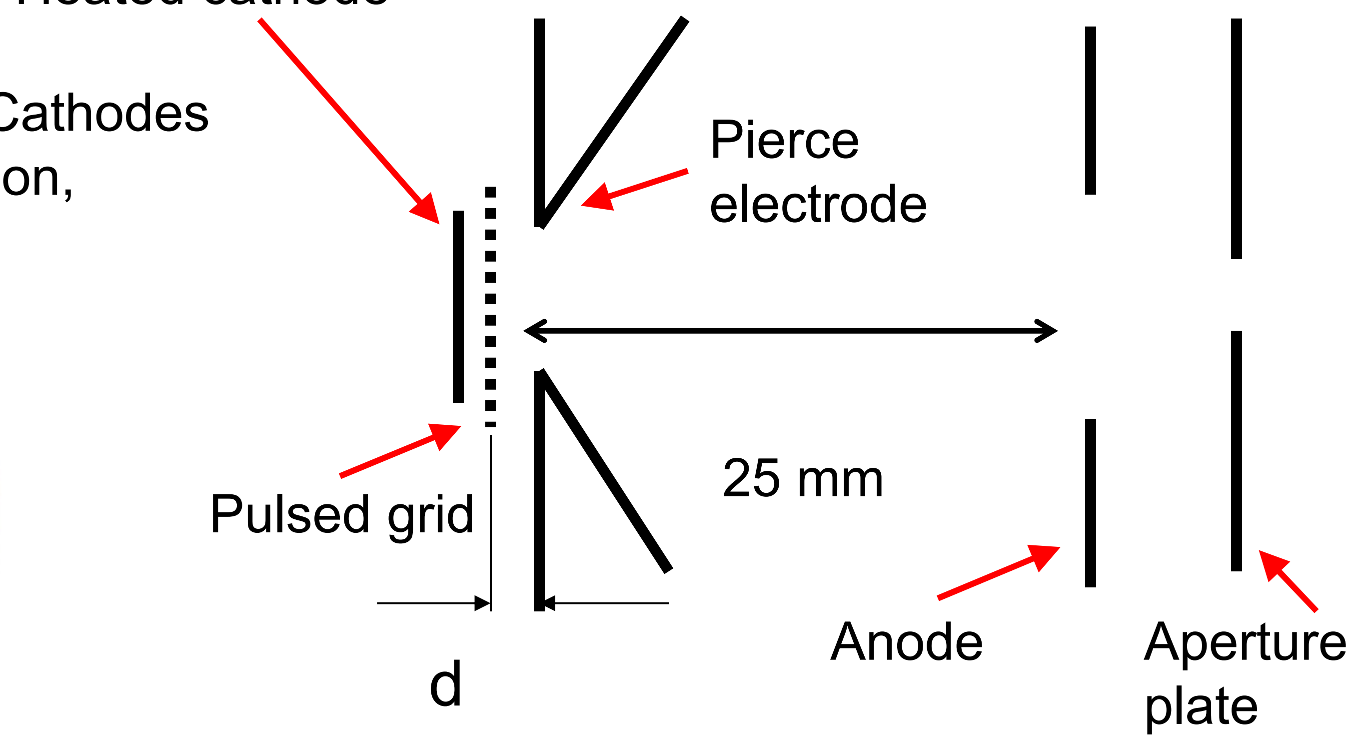

Cross-sectional view of a dispenser cathode

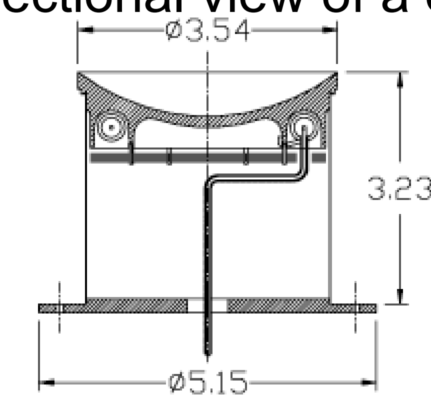

UMERs Pulsed Electron Gun

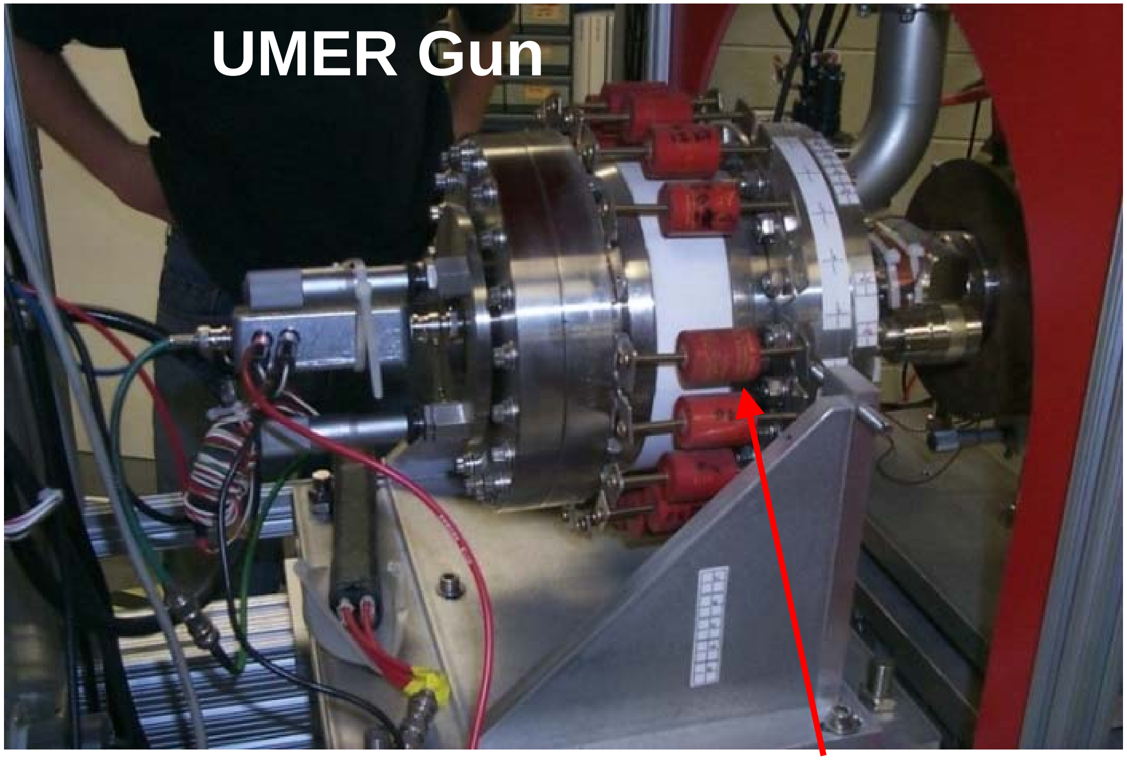

Capacitor bank between cathode and anode

Grid

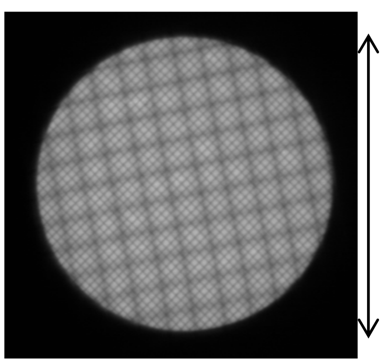

8 mm

Extracted current pulse with a Pulse Forming Line (PFL)

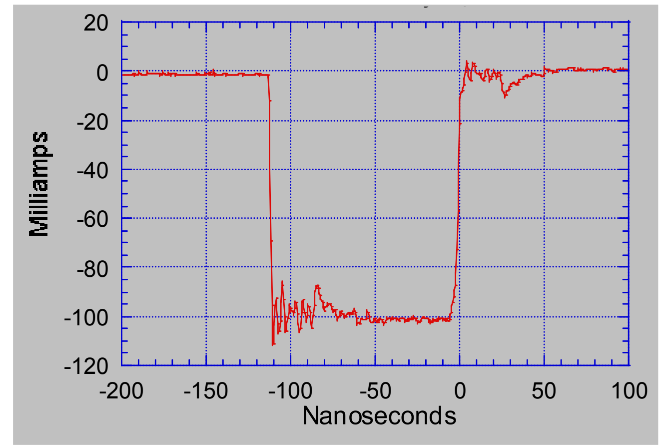

Extracted current pulse with a laser and thermionic pulse

5 ns laser pulse

Pierce Electrode Geometry

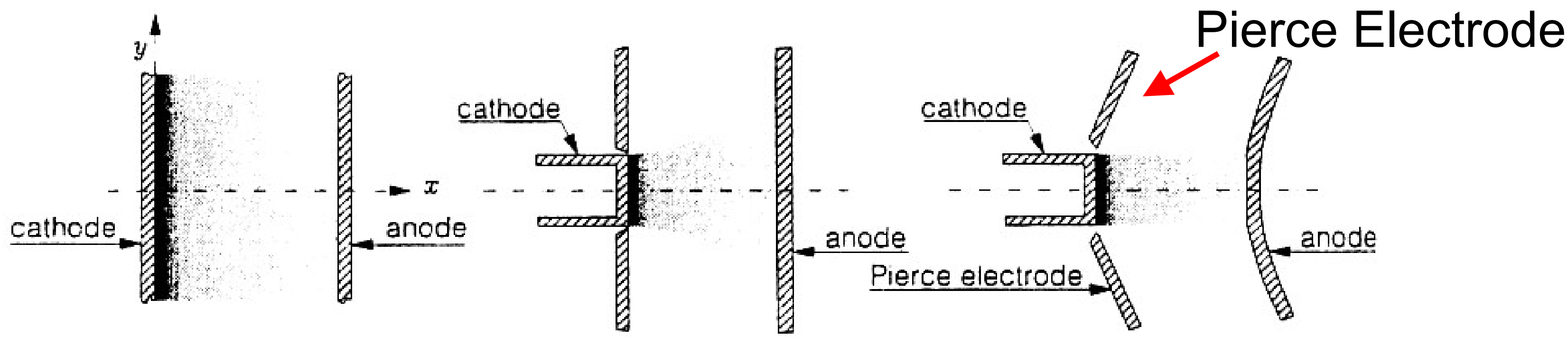

"Infinite" Diode "finite" Diode Pierce Diode

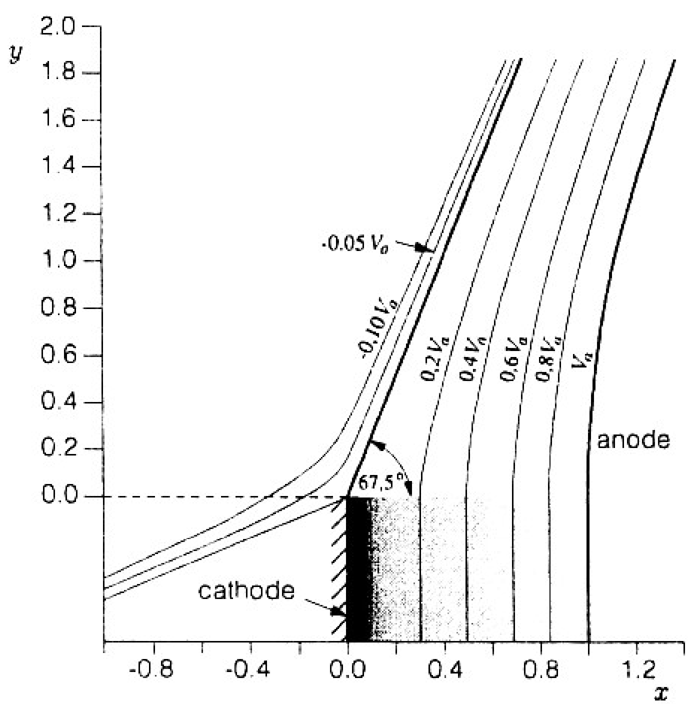

Assume $V(x) \propto x^{4/3}$, outside beam for finite (in y-direction) diode.

Use complex formalism $x \rightarrow re^{i\varphi} = \varsigma + i\xi$, $V \rightarrow W = V_R + iV_R$.

Then $V_R \propto r^{2/3} \cos[(4/3)\arctan(\varsigma/\ \xi)]$.

Since cathode is grounded, $V_R=0$, so we need
$(4/3)\arctan(\varsigma/\ \xi)] = \pi/2$, or slope at x=0 is

$(3/4)\ \pi/2 = 67.5^0$

*Miroslav Sedlacek, Electron Physics of Vacuum and Gaseous Devices, Sec. 6.2 (1996).

Printed Circuit (PC) Dipole and Quadrupole

On a circular cylindrical surface, we want: $\int K_z dz \propto \cos n\theta$

n=order of multipole.

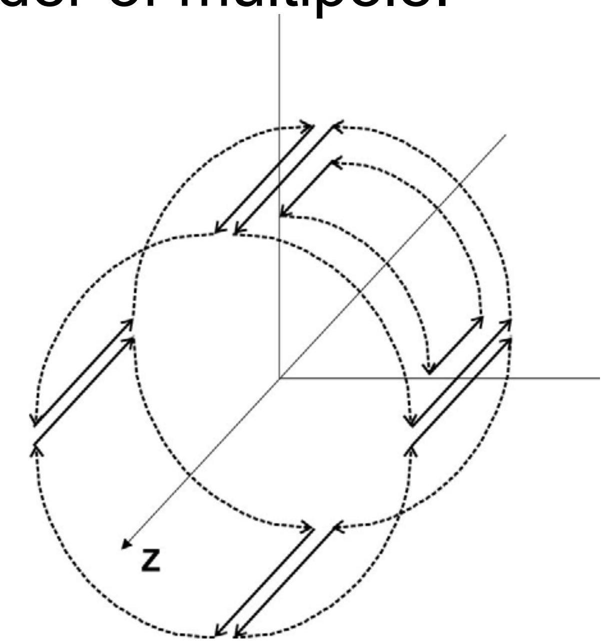

Only conductors parallel to z-axis contribute to integrated B-field.

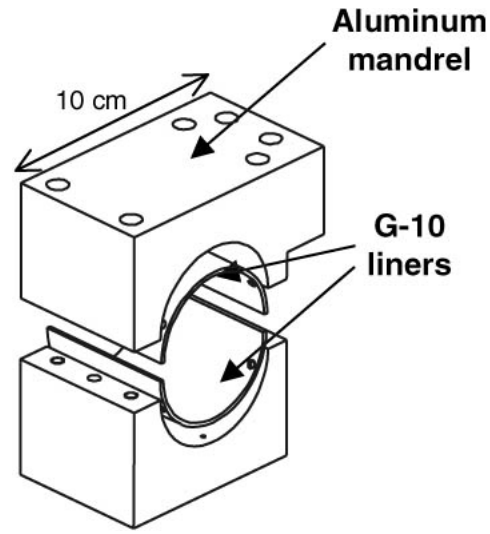

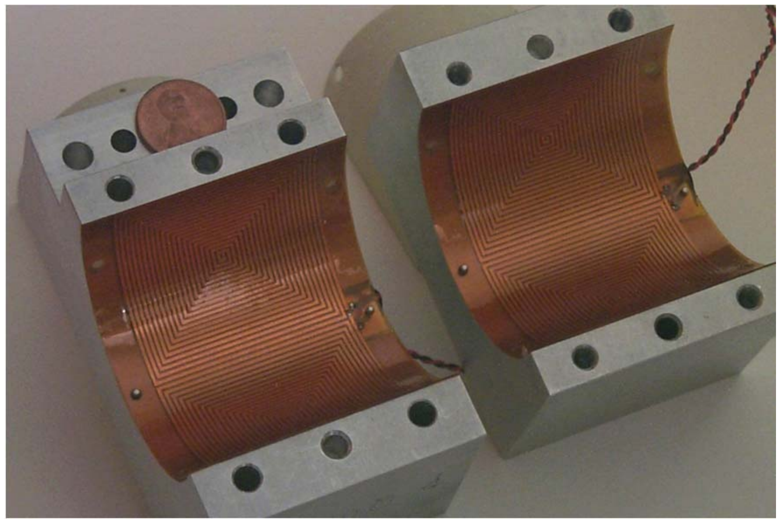

UMER PC quadrupole

*W.W. Zhang, et al, Phys, Rev. ST Accel. Beams, 3, 122401 (2000).

Standard UMER Magnets & Lattice

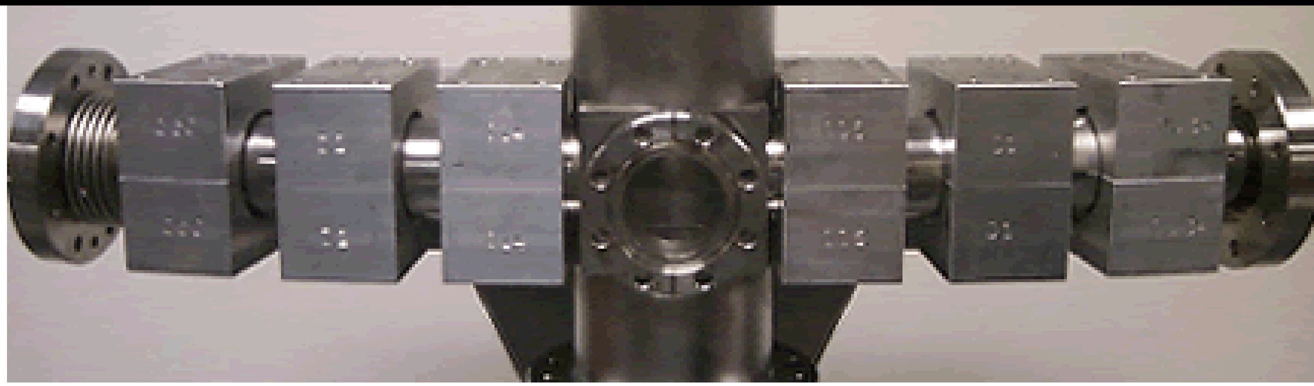

72 Quads
(~ 30 G peak)

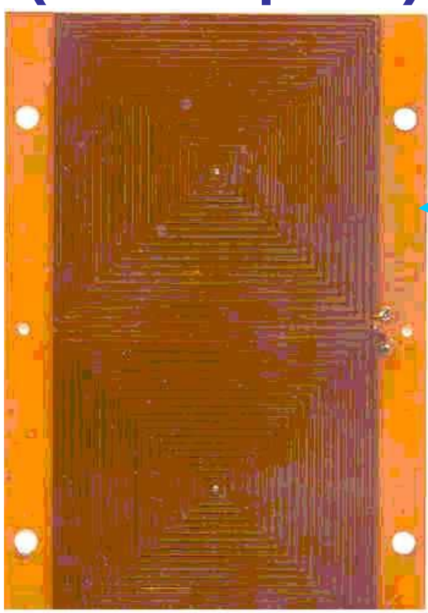

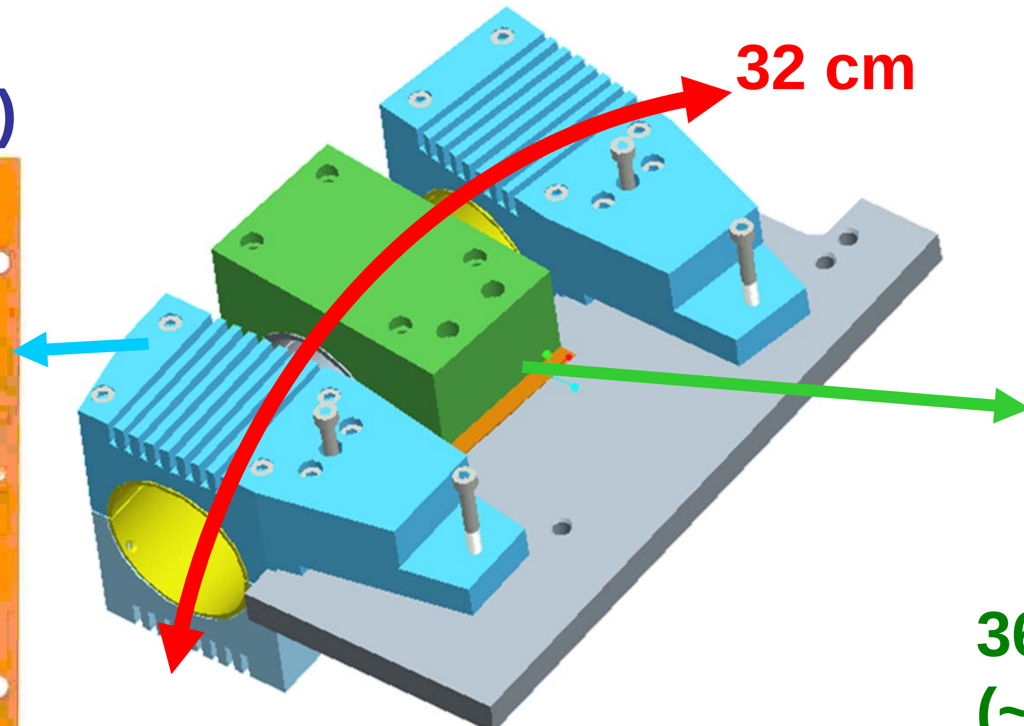

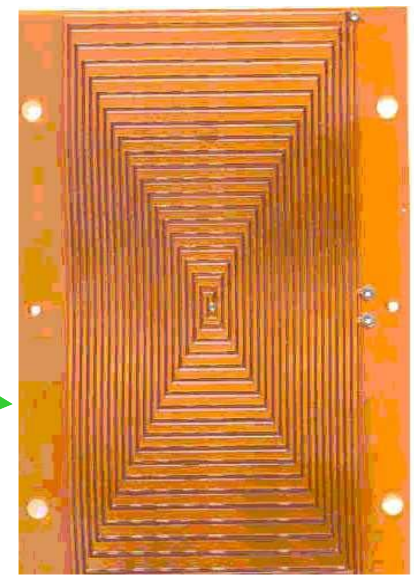

36 Dipoles
(~ 15 G peak)

Multiple Conductors in a PC Dipole

These conductors are contributing most to the total field

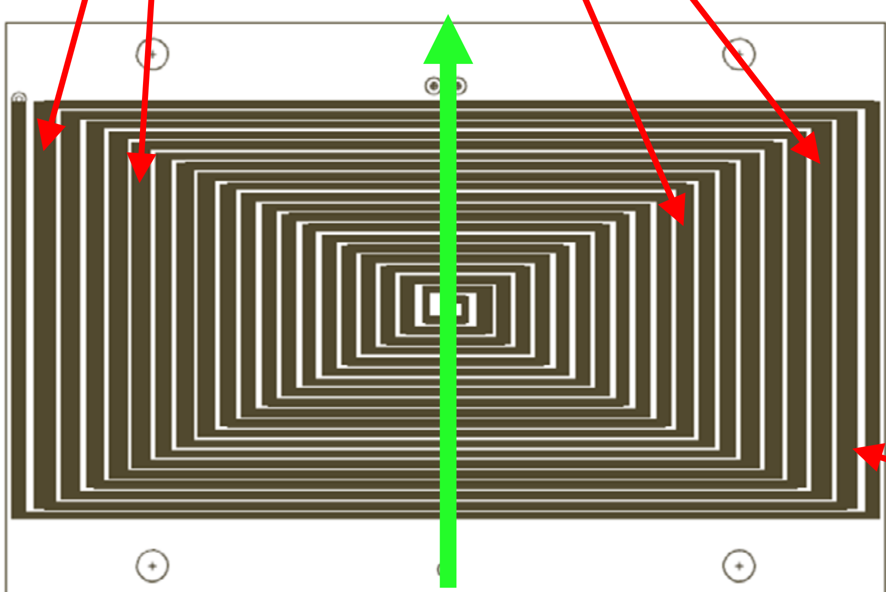

Beam

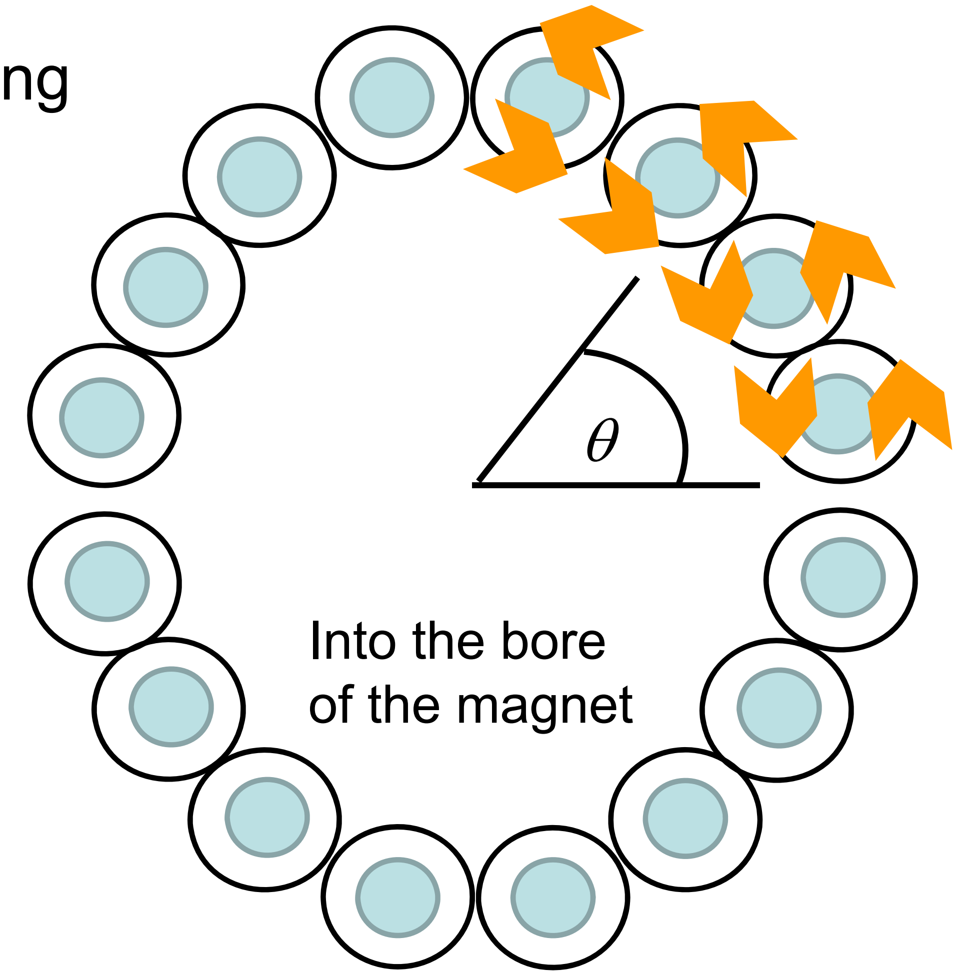

Half Lengths

$$z_{1/2}(\theta) = \frac{l}{2}\left[1 - \left|\sin((n+1)\theta)\right|\right]^{1/2}$$

Multipole Expansion

2D Multipole Expansion:

K_n is complex

r is real

$$B_y + iB_x = \sum_{n=0}^{\infty} K_n (x+iy)^n \quad = \sum_{n=0}^{\infty} K_n r^n e^{in\theta}$$

$$= \sum_{n=0}^{\infty} |K_n| e^{i\delta_n} r^n e^{in\theta}$$

Amplitude

rotation

$$
\begin{array}{llll}
n=0 \;\Rightarrow & B_x = 0 & ; B_y = |K_0| & \equiv \text{dipole} \\
n=1 \;\Rightarrow & B_x(r,0) = 0 & ; B_y(r,0) = r|K_1| & \equiv \text{quadrupole} \\
 & B_x(r,\pi/2) = r|K_1| & ; B_y(r,\pi/2) = 0 & \\
 & B_{x,y}(r,\theta+\pi) & = -B_{x,y}(r,\theta) & \\
n=2 \;\Rightarrow & B_x(r,0) = 0 & ; B_y(r,0) = r^2|K_2| & \equiv \text{sextupole} \\
 & B_x(r,\pi/4) = r^2|K_2| & ; B_y(r,\pi/4) = 0 & \\
 & B_{x,y}(r,\theta+\pi/2) & = -B_{x,y}(r,\theta) &
\end{array}
$$

UMER Rotating Coil*

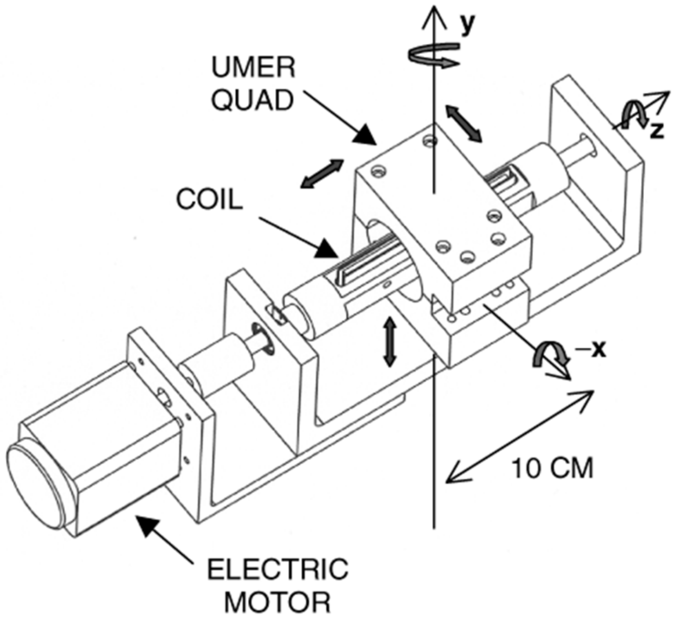

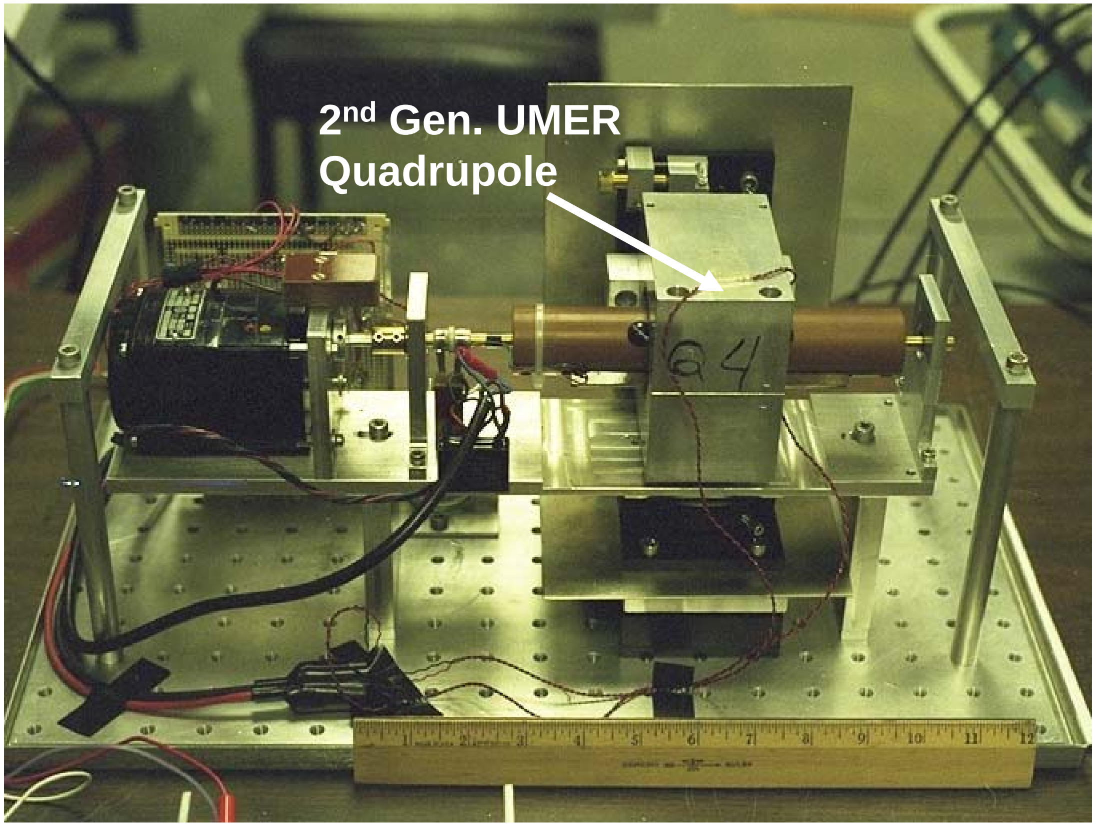

The coil contains ~3000 turns of very fine wire. The whole of the rotating coil apparatus is normally enclosed in mu-metal box.

A rectangular rotating coil is positioned along the axis of the magnet. An FFT of the induced voltage details the harmonic content of the magnetic field.

*W.W. Zhang, et al, Phys, Rev. ST Accel. Beams, 3, 122401 (2000).

FFT of Rotating Coil Signal

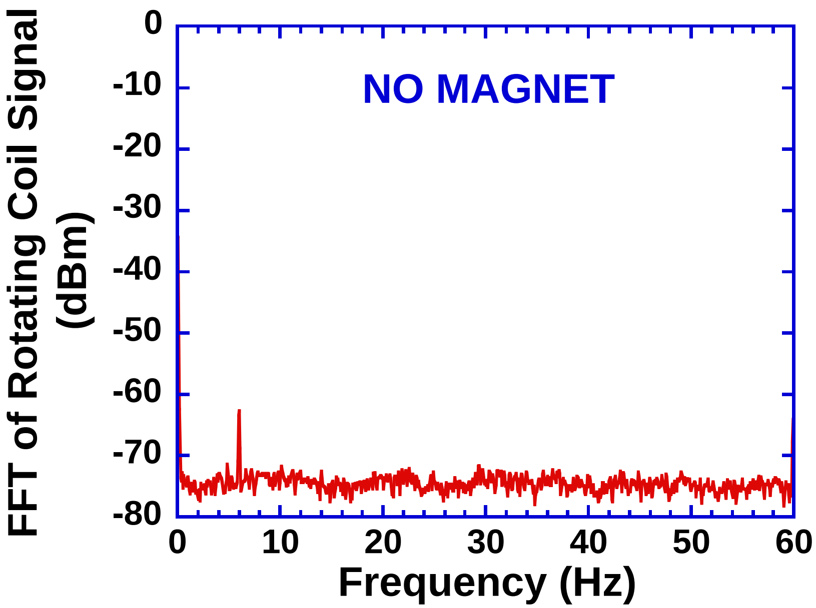

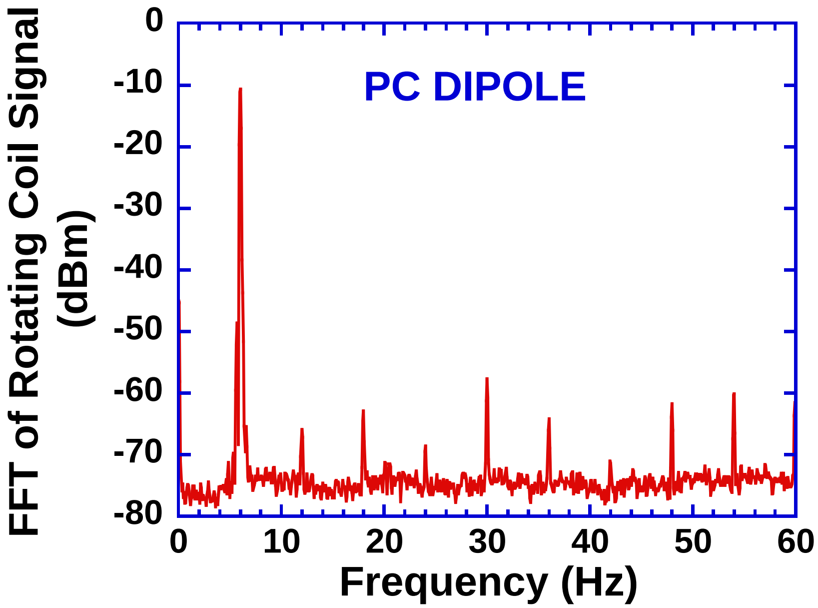

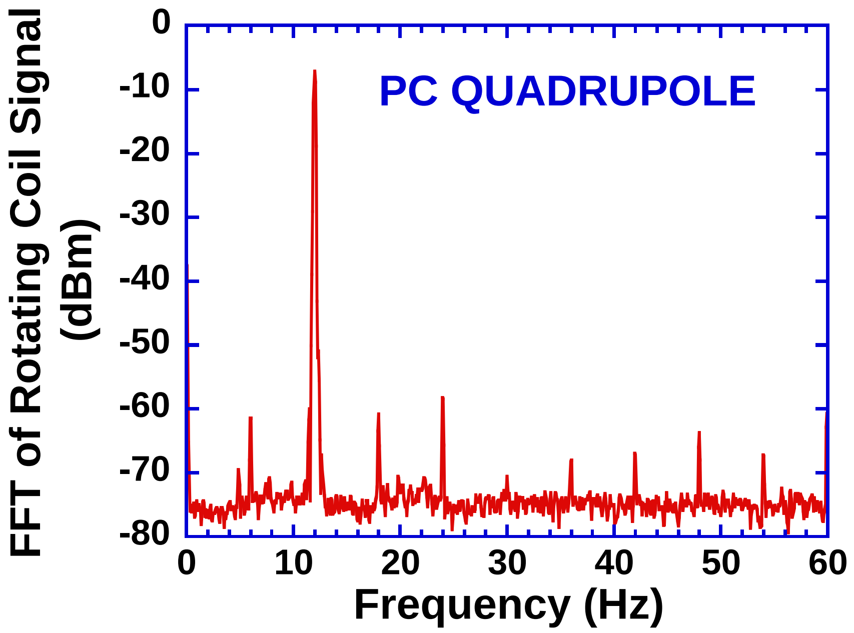

1st Generation PC Octupoles

Designed by (UG) David Matthew and Kiersten Ruisard

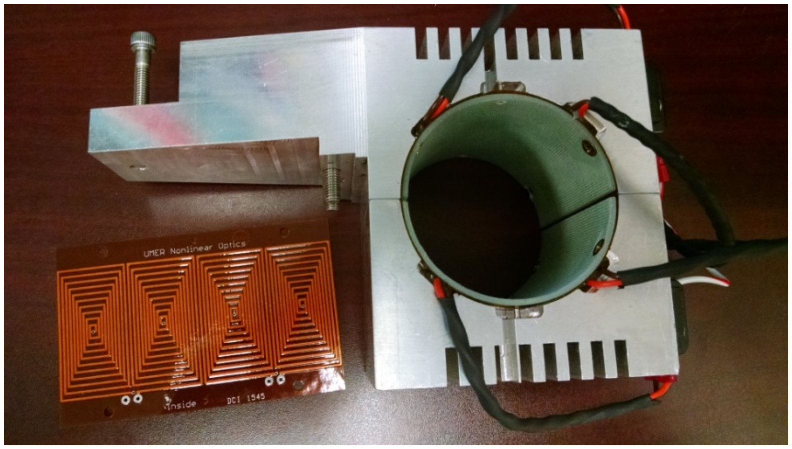

Maxwell model

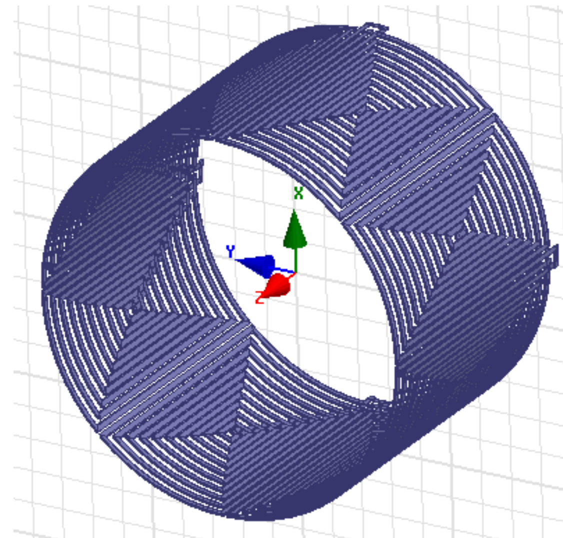

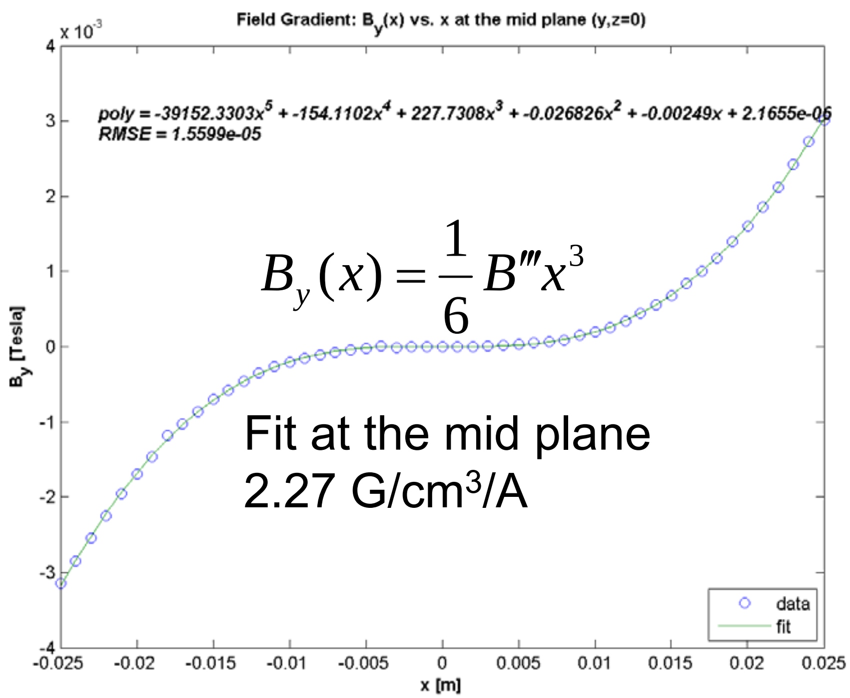

$$B_y(x) = \frac{1}{6} B''' x^3$$

Fit at the mid plane
2.27 G/cm^3/A

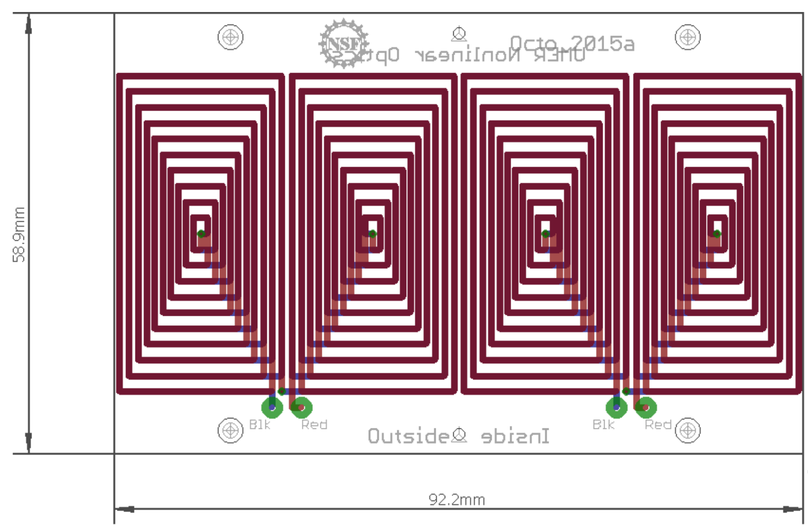

Measuring the Multipole Content of the Octupole

FFT Scope Data

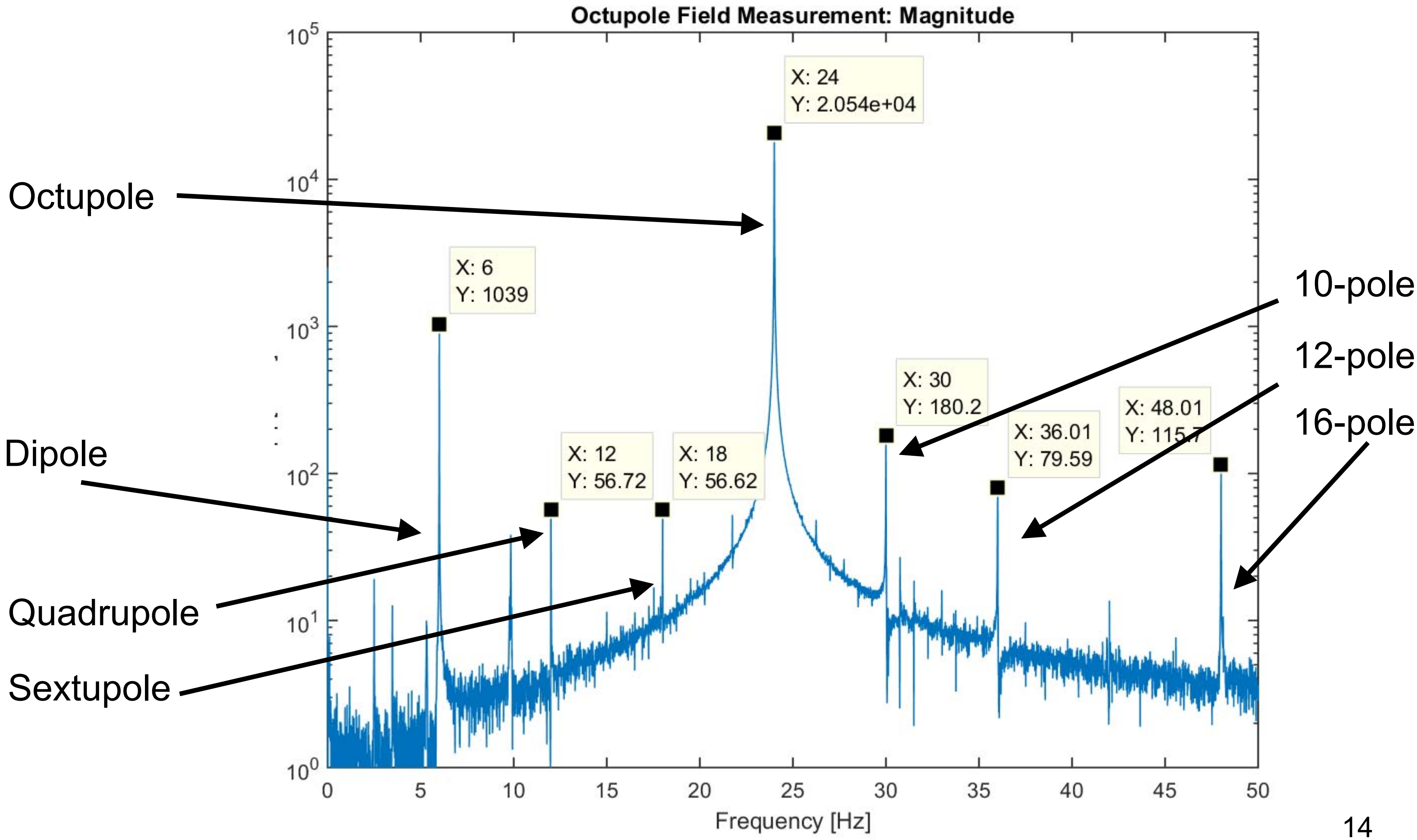

Transverse Dynamics

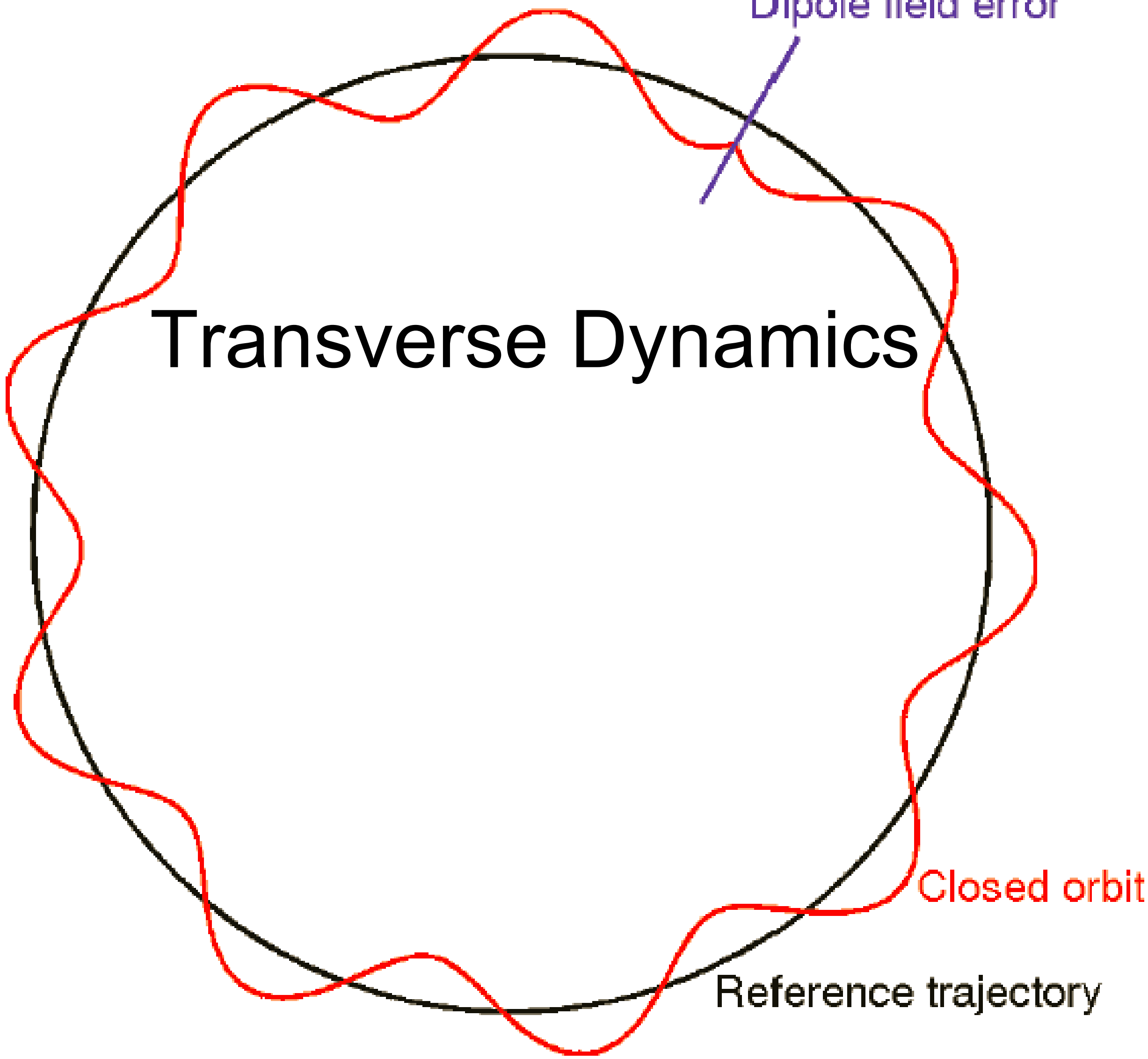

Beam Transport Down Quadrupole Line

Phosphor screen images of the beam

Gun

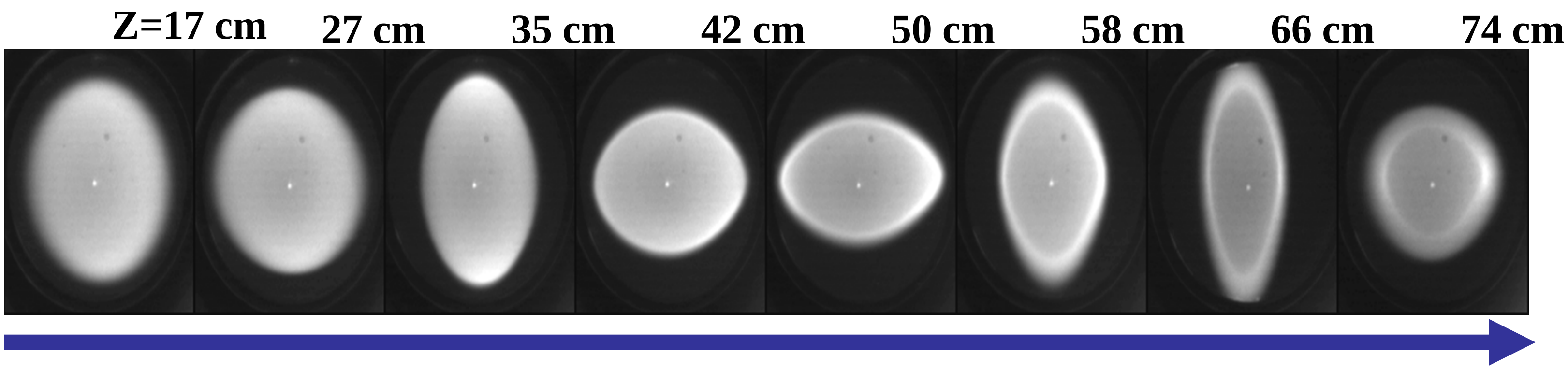

z ~ 0.15 – 1 m

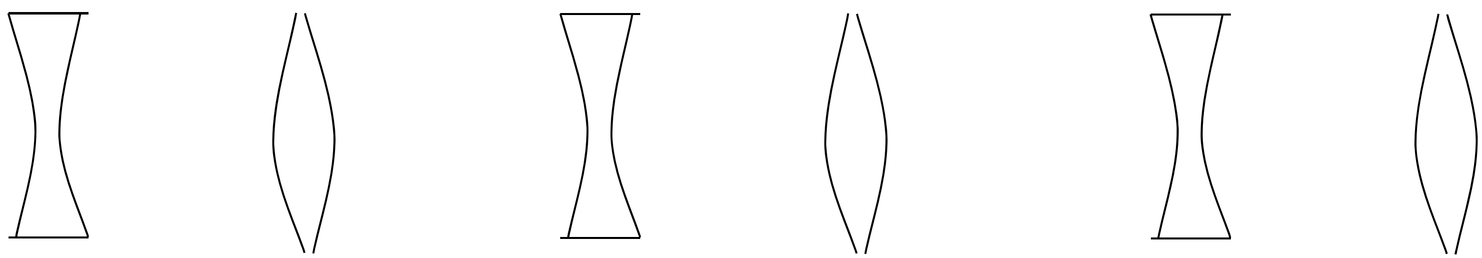

*Bernal, Kishek, Haber, and Reiser, PRL, **82**, 4002 (1999).*

*Kishek, O'Shea, Reiser, PRL, **85**, 4514 (2000).*

Reiser, Sec. 7.3.5, 7.3.6.1

Integer and Half-Integer Resonances

Integer Resonance

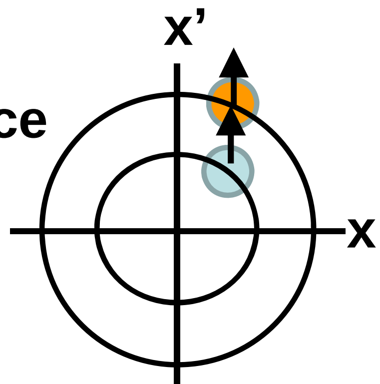

Dipole errors in the accelerator perturbs beam motion

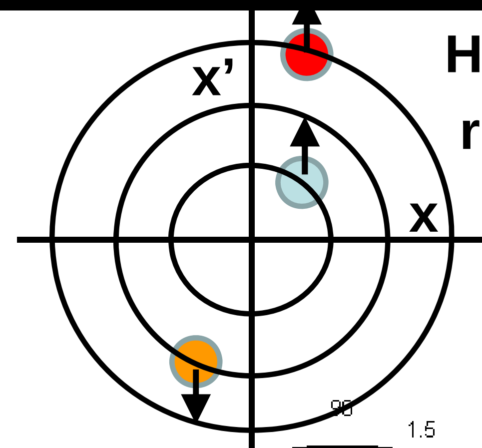

Half-Integer resonance

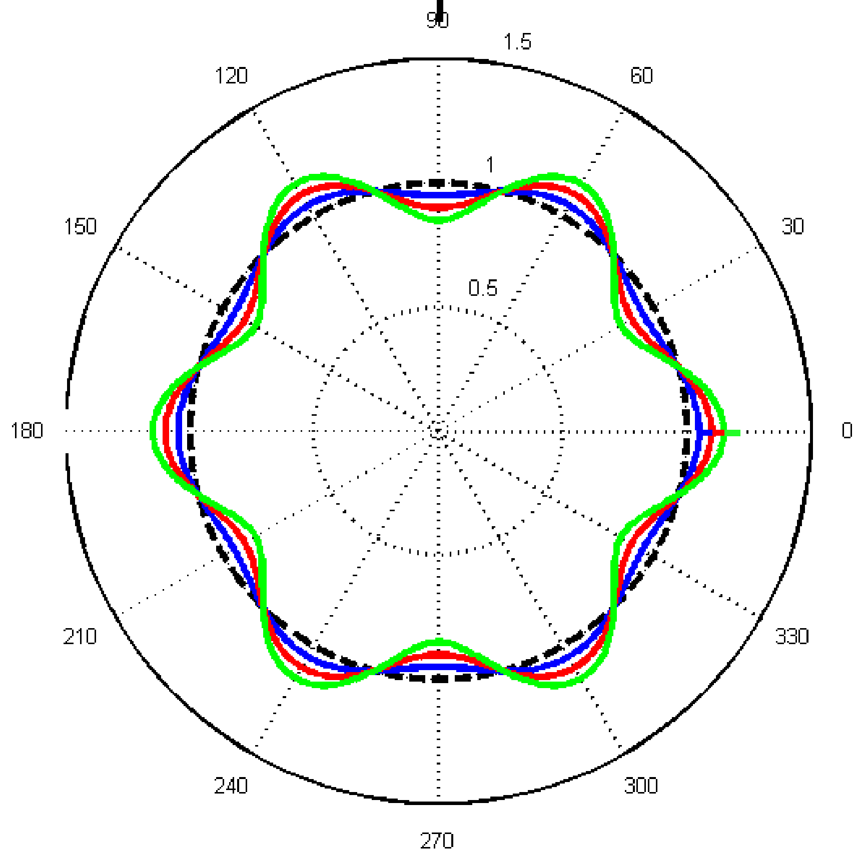

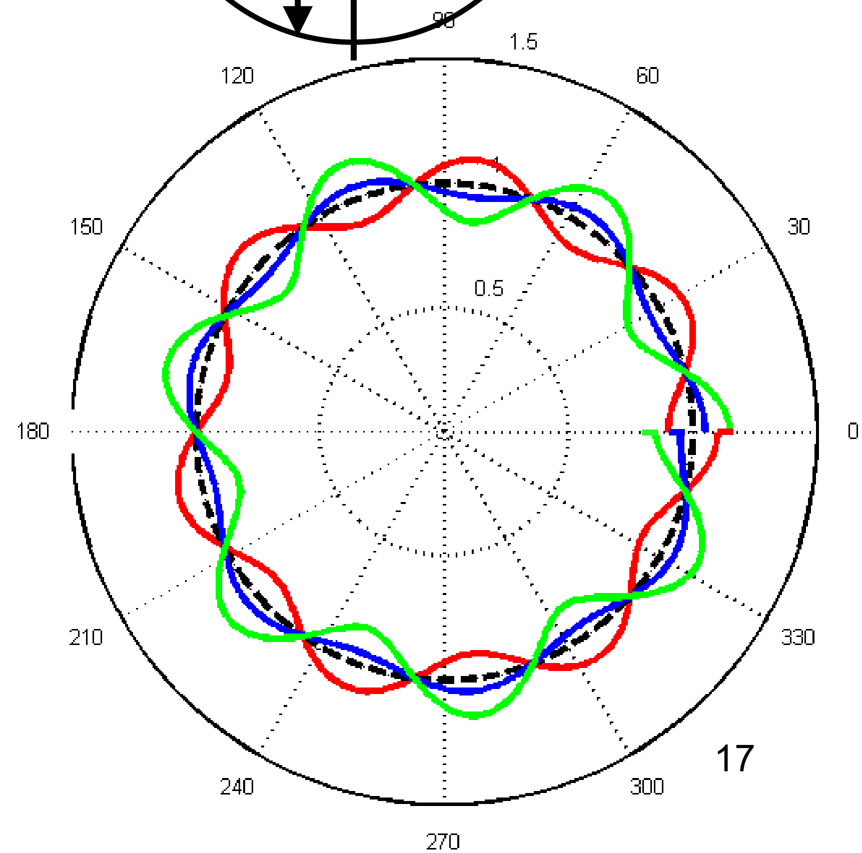

Quadrupole Tune Scans

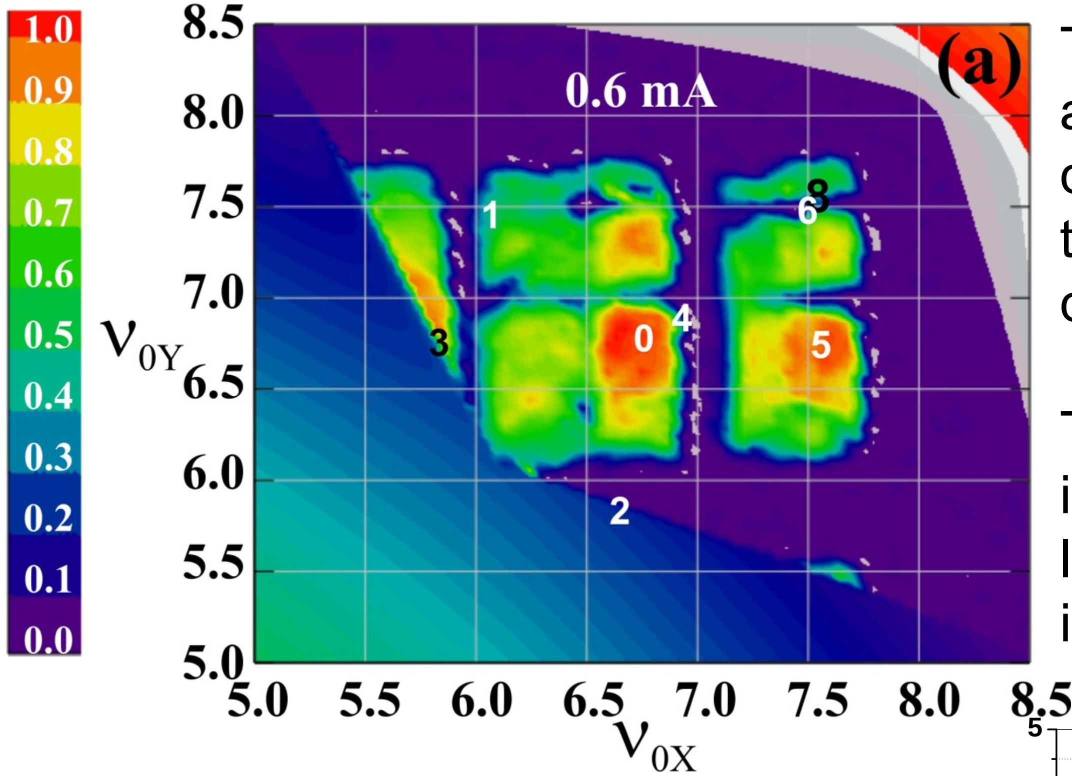

The current traces shown below are taken as a function of the quadrupole currents. We vary both the horizontal and vertical quadrupoles.

The regions of no transmission indicate current loss at the integer lines, the beam resonantly kicked itself out of the machine.

$$Intensity_{Turn} = I_{Turn} / I_1$$

Duration the beam survives over multiple turns

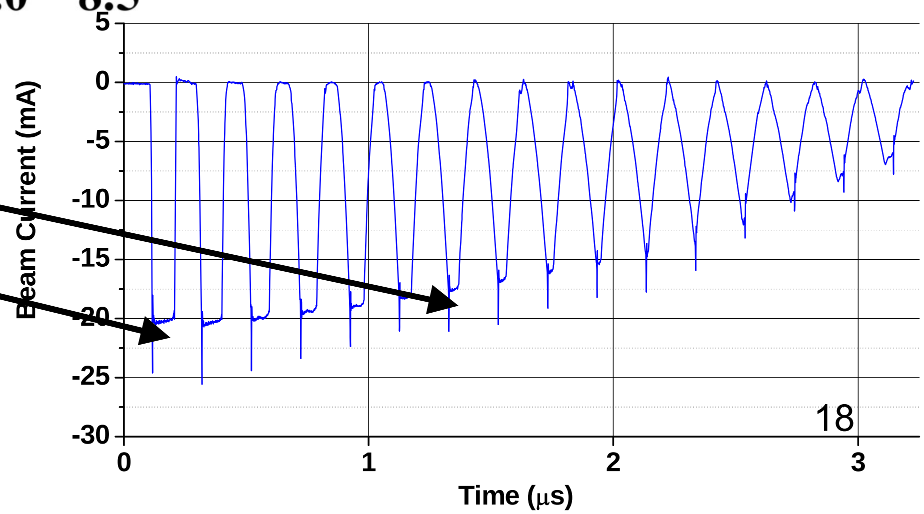

Quadrupole Tune Scans vs Beam Current

Beam Current Transmission Plots at 10th turn

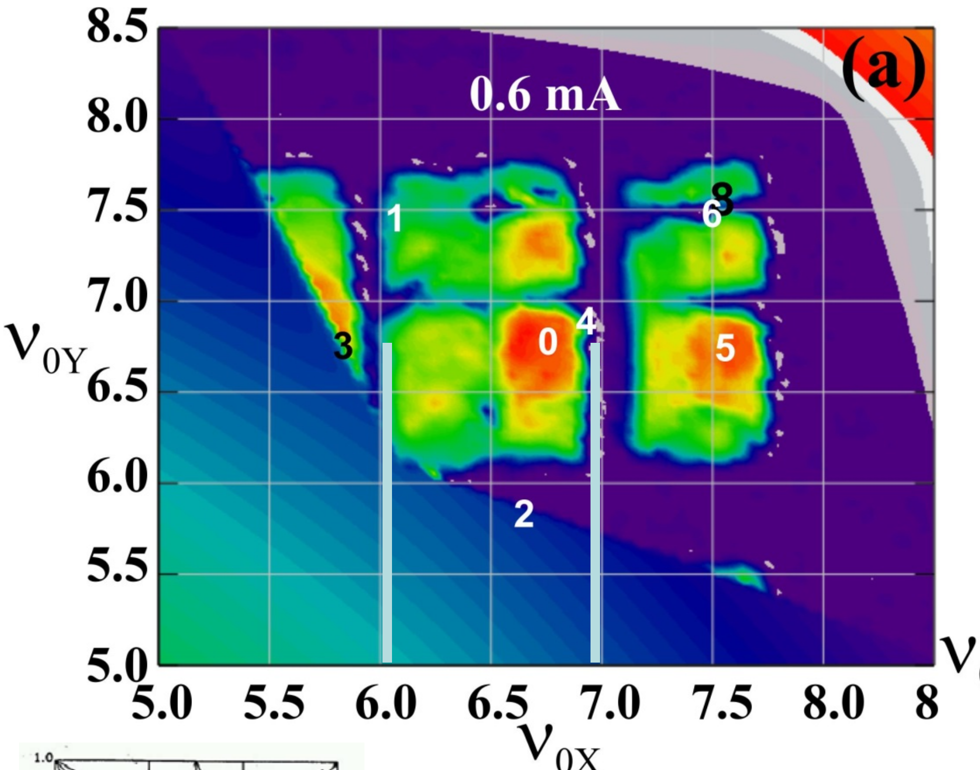

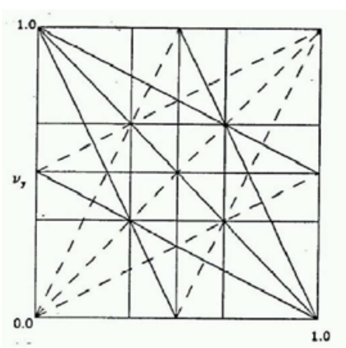

Integer

$$\nu_x + \nu_y = 13$$

Half-Integer

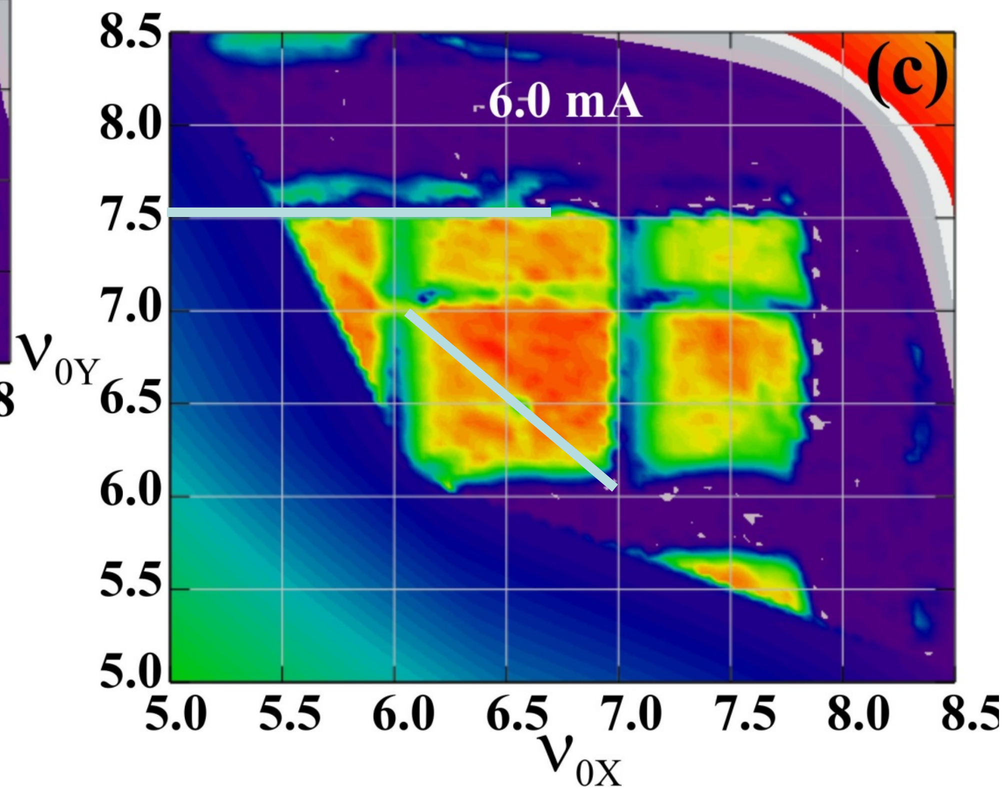

*S. Bernal, B. Beaudoin, M. Cornacchia and D. Sutter, Proceedings of PAC2013, TUPAC31.

Longitudinal Dynamics without Barrier Buckets

Longitudinal Space-Charge Forces Diminishes the Bunch Shape

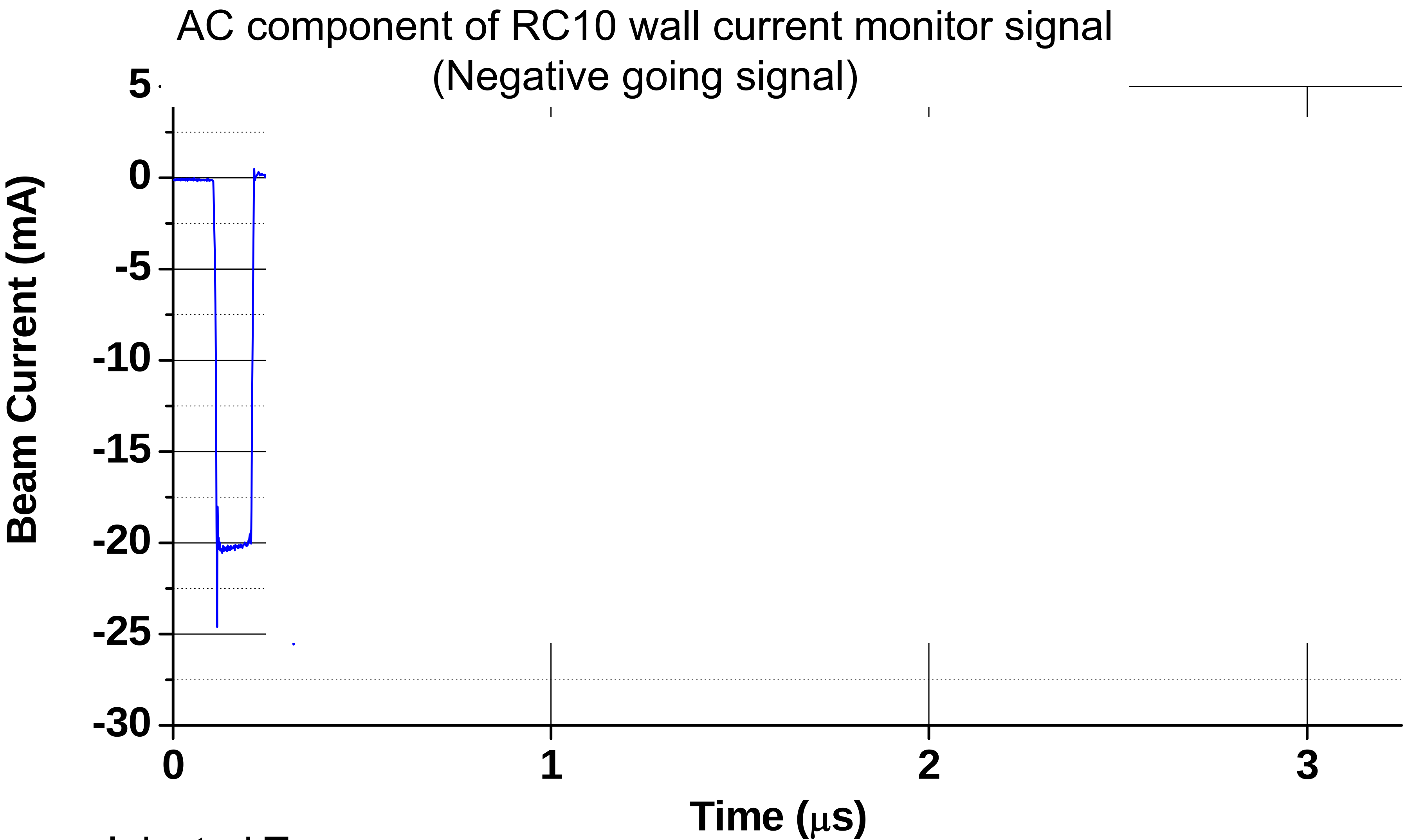

Injected Turn
21 mA

Longitudinal Bunch Erosion of Bunch Current

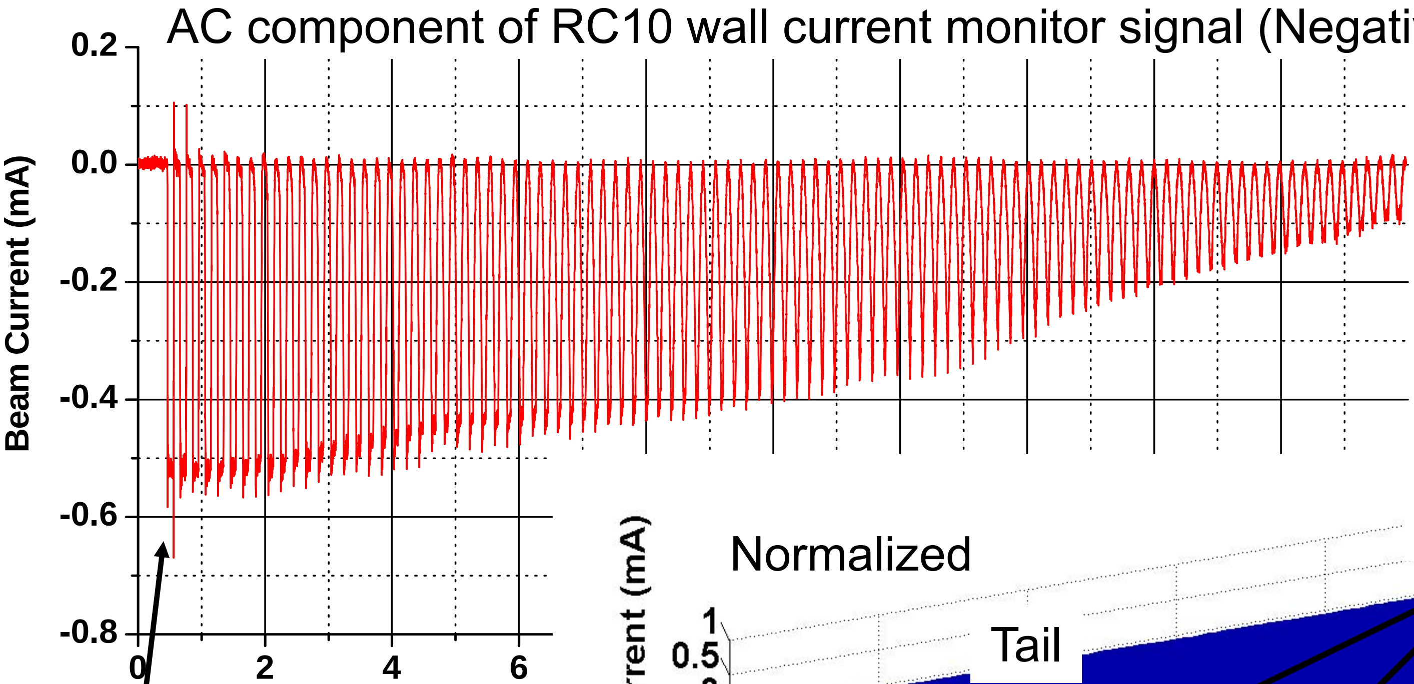

$$c_s = \sqrt{\frac{qg\lambda_o}{4\pi\varepsilon_o\gamma_o^5 m}}$$

The 0.6 mA beam

$$\frac{c_s}{v_o} = 0.0049$$

Injected Turn

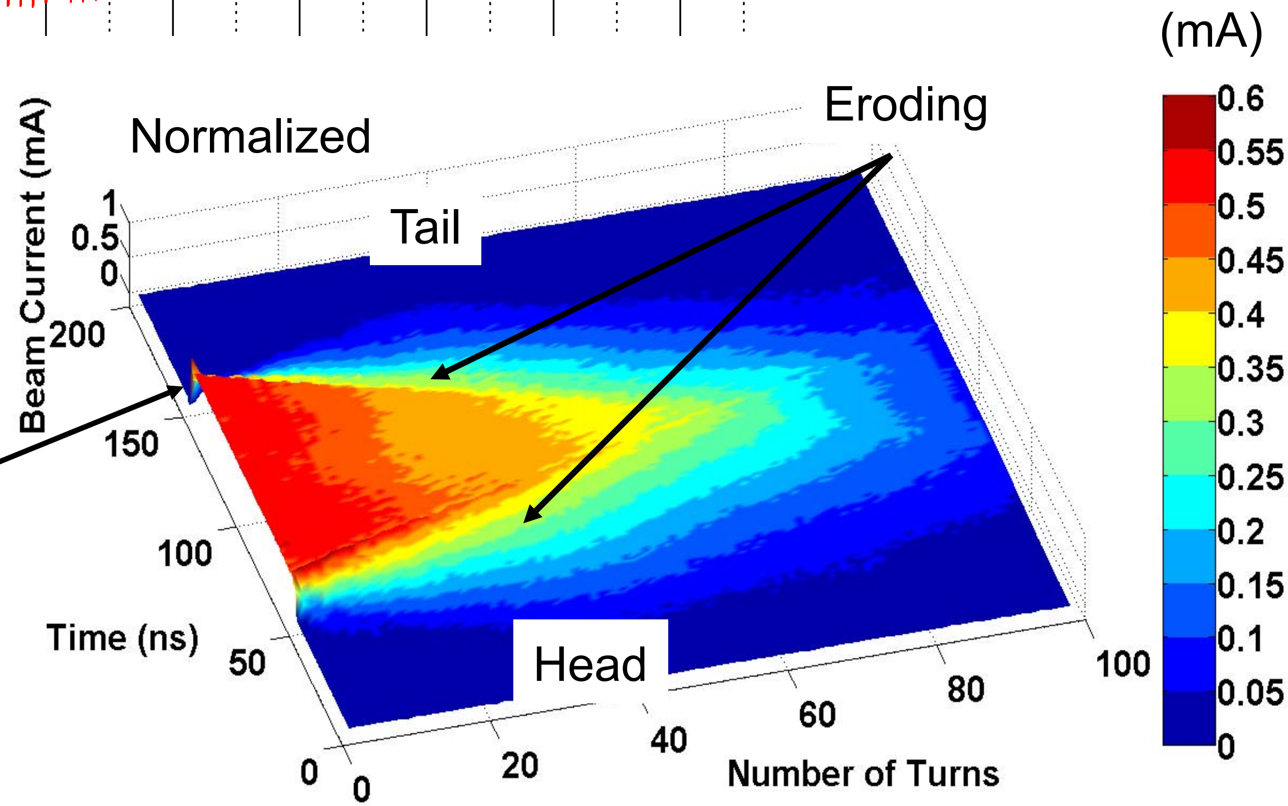

Longitudinal Space-Charge Physics

One - Dimensional

$$E_z \propto -\frac{d\lambda}{dz}$$

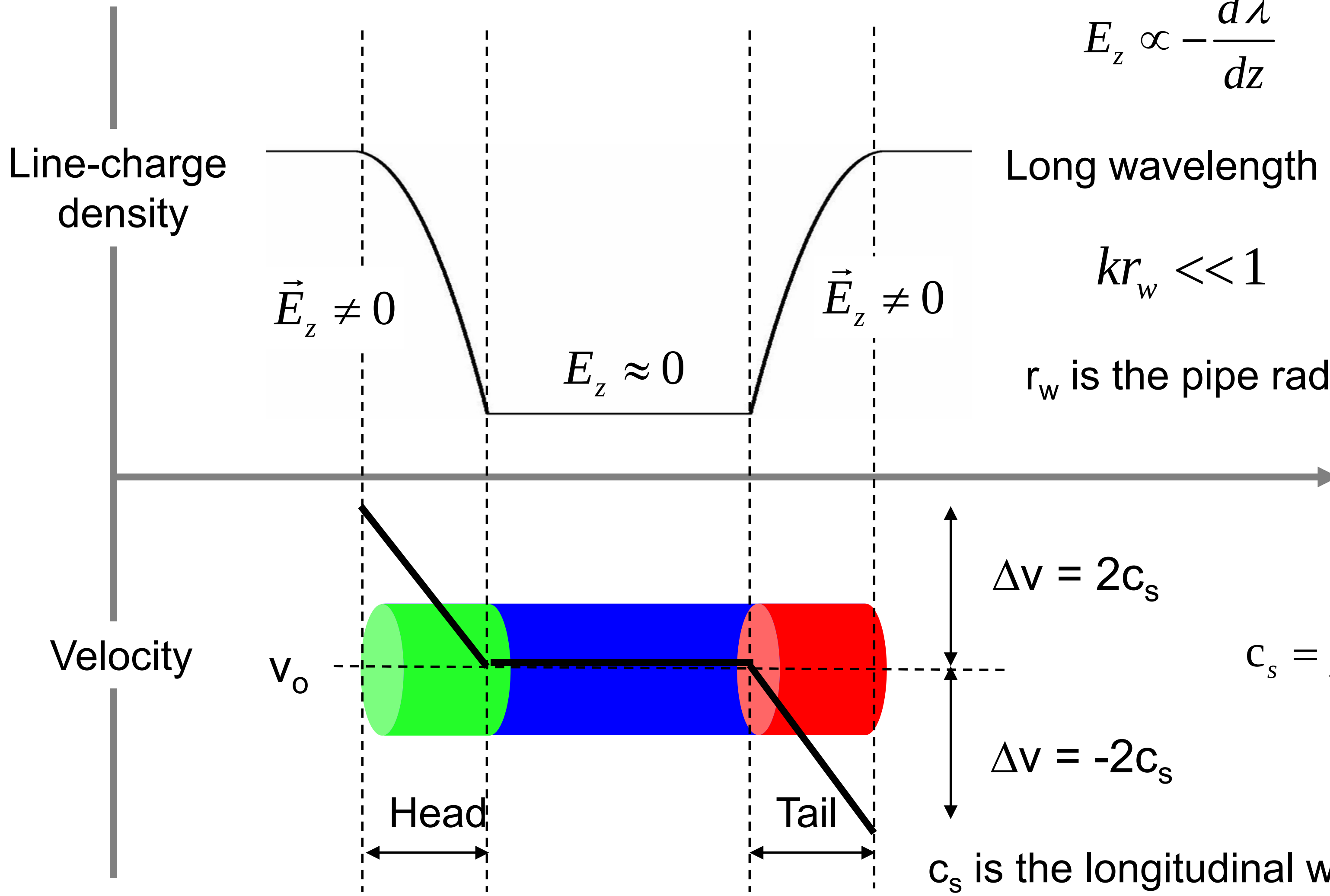

Long wavelength limit

$$kr_w << 1$$

r_w is the pipe radius

$$c_s = \sqrt{\frac{qg\lambda_o}{4\pi\varepsilon_o\gamma_o^5 m}}$$

c_s is the longitudinal wave speed of a perturbation on the bunch.

-CERN 77-13, 19 July 1977,
"Theoretical Aspects of the Behavior of Beams in Accelerators and Storage Rings
-A. Faltens, E.P. Lee, and S.S. Rosenblum, Journal of Applied Physics, 61, 5219, (1987).

Space-Charge Driven Transverse-Longitudinal Correlation

$$\rho = \frac{p}{eB}$$

$$\Delta\theta \approx \frac{p_\perp}{p} = \frac{Bl}{(B\rho)}$$

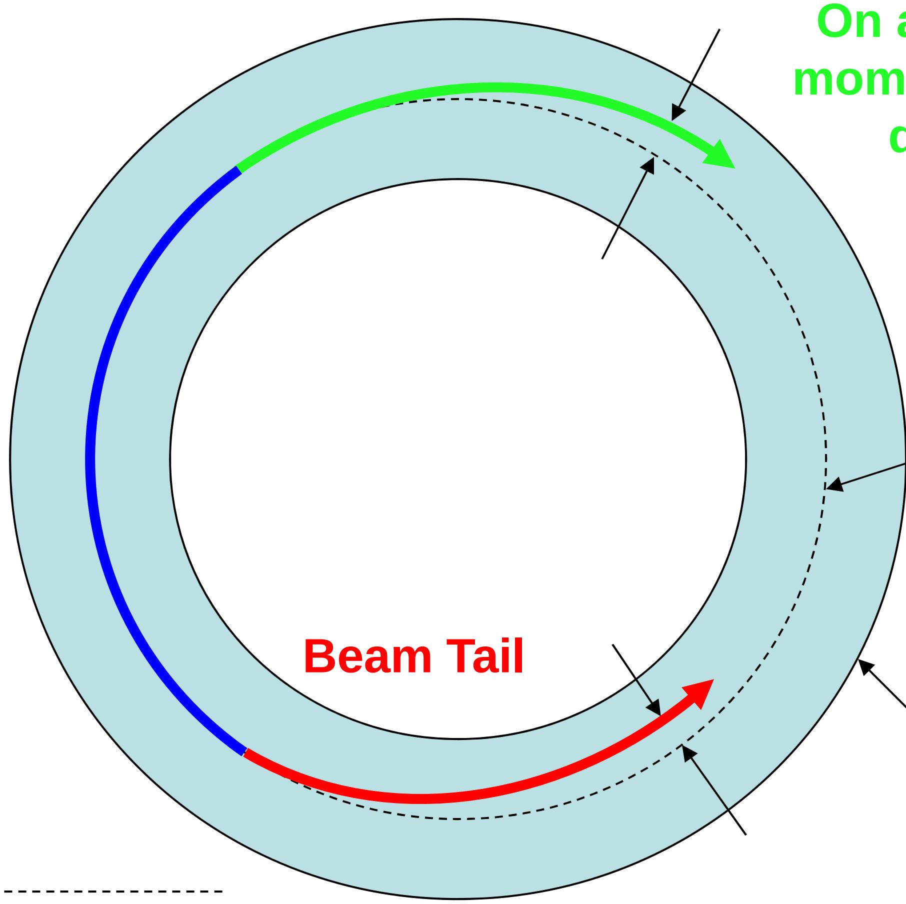

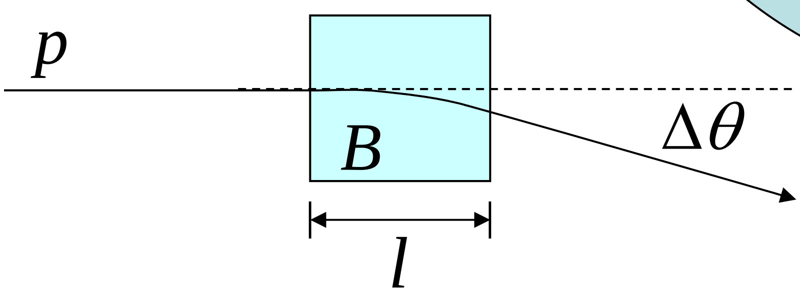

Time Resolved Measurement of Beam Ends

21 mA Beam

Multiple images are taken every 3 ns along the ~110 ns beam

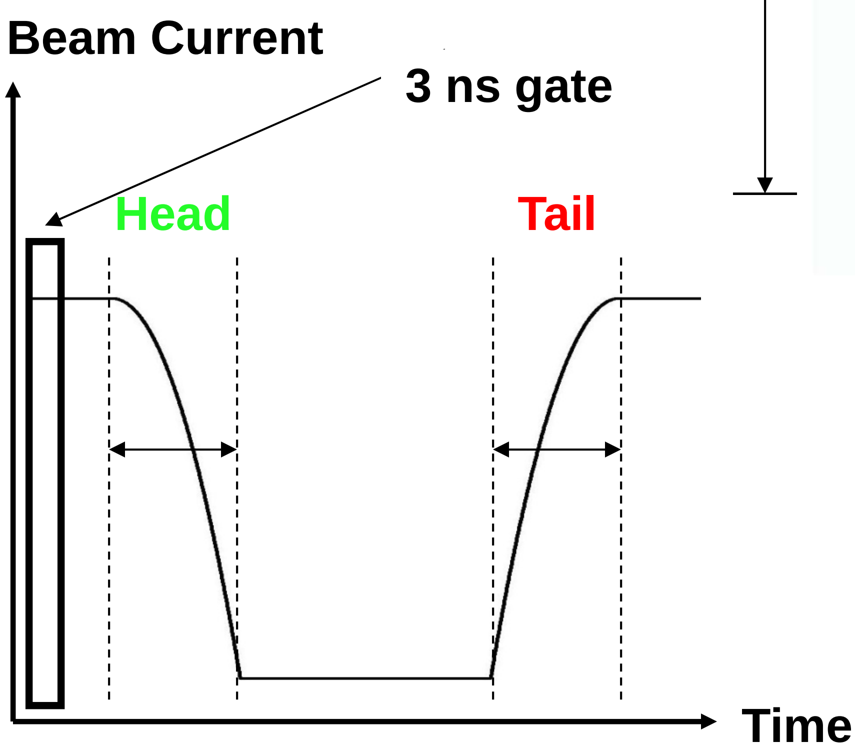

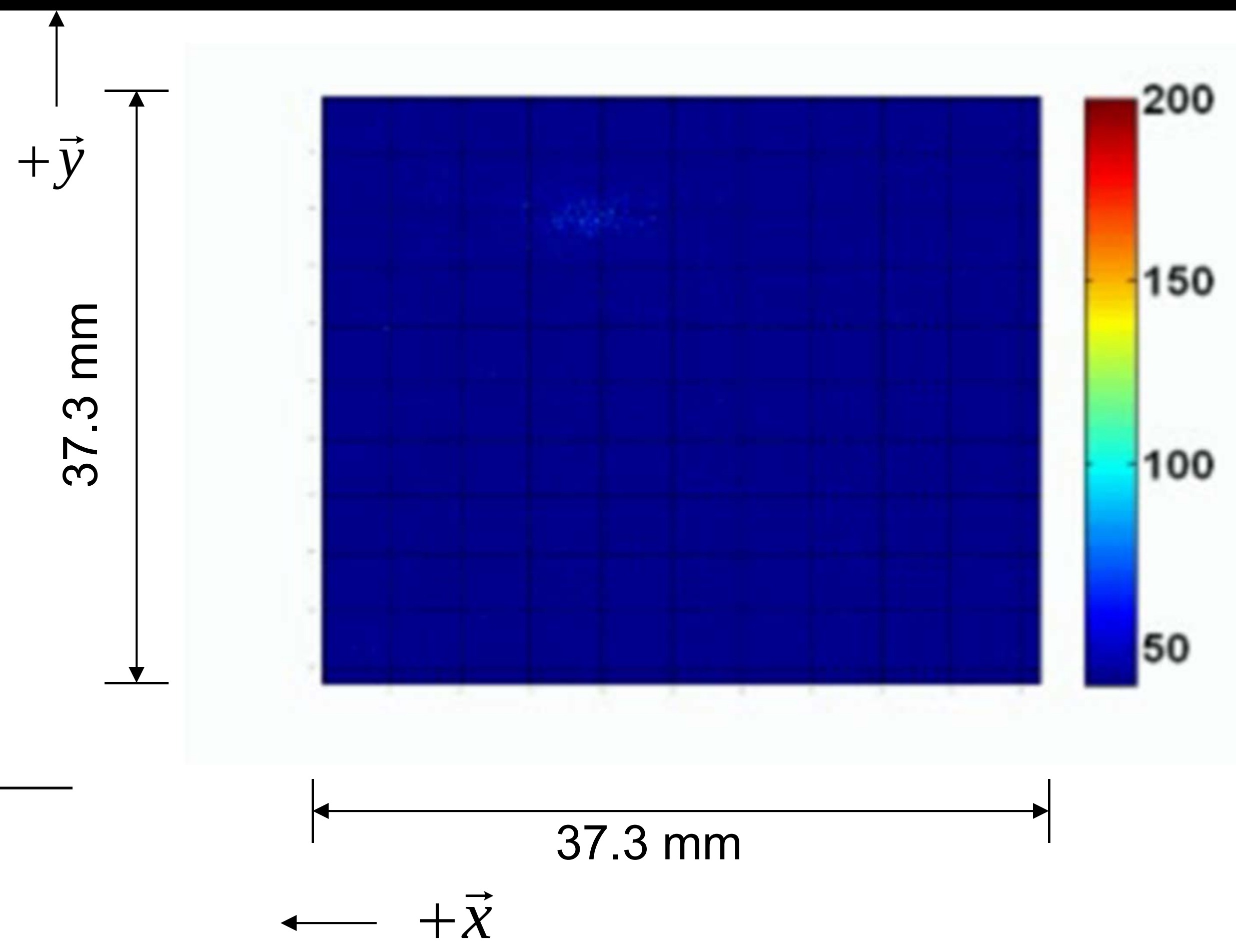

1st Turn Intercepting Diagnostic Measured at Ring Chamber 15

Centroid Deflection across the Bunch Length

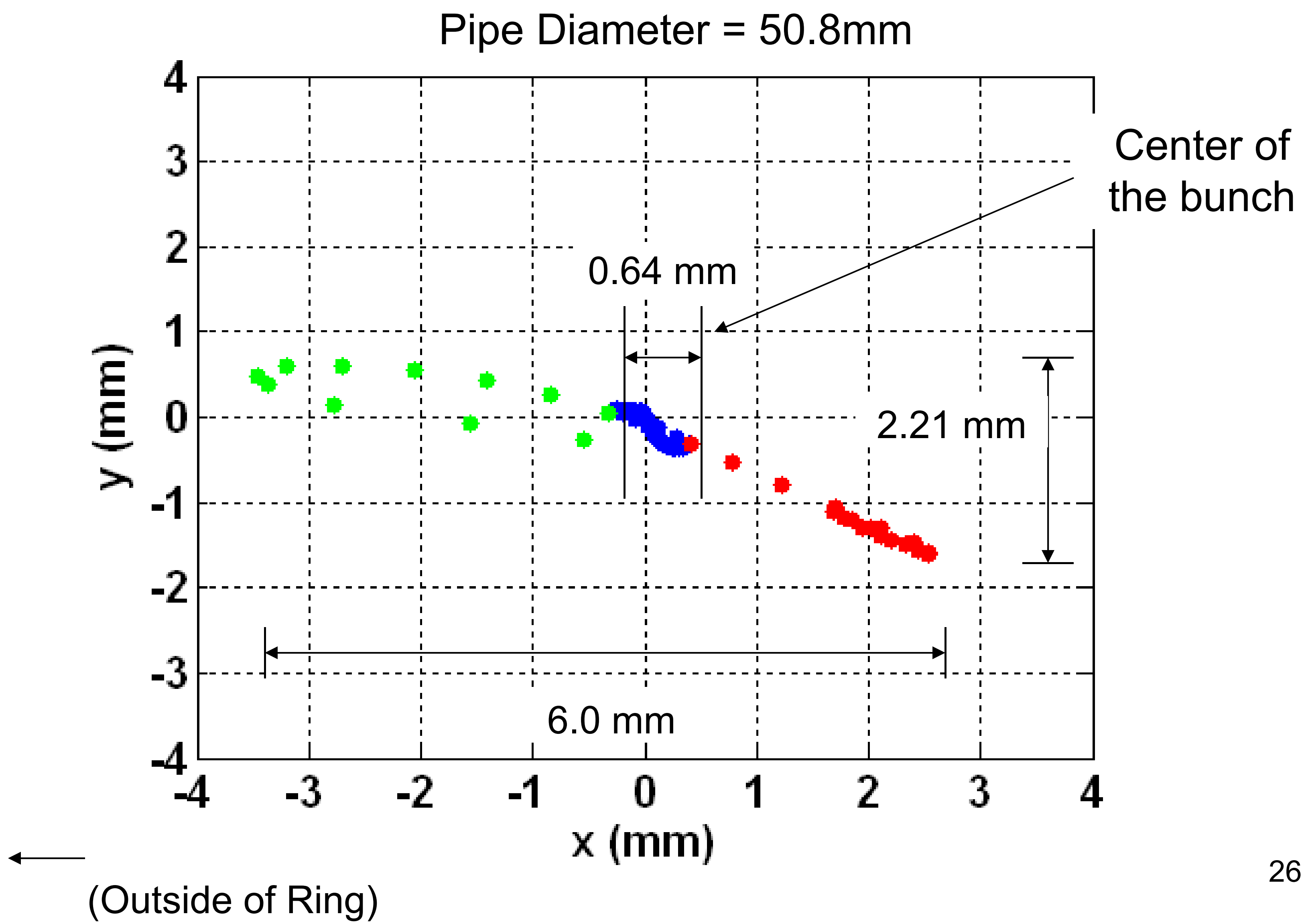

Quadrupole Focusing Dependence on Momentum

$$\Delta\theta \approx -\frac{B_x(x)l}{(B\rho)} = -\frac{B'lx}{(B\rho)} \Rightarrow$$

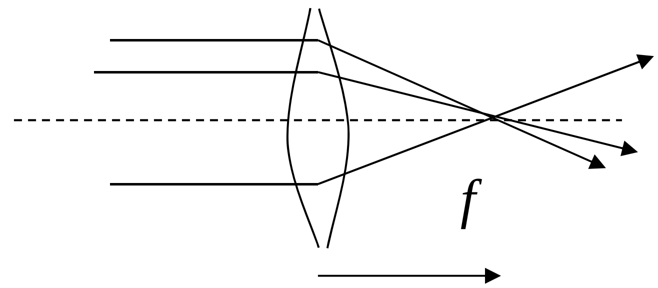

$$f = \frac{(B\rho)}{B'l}$$

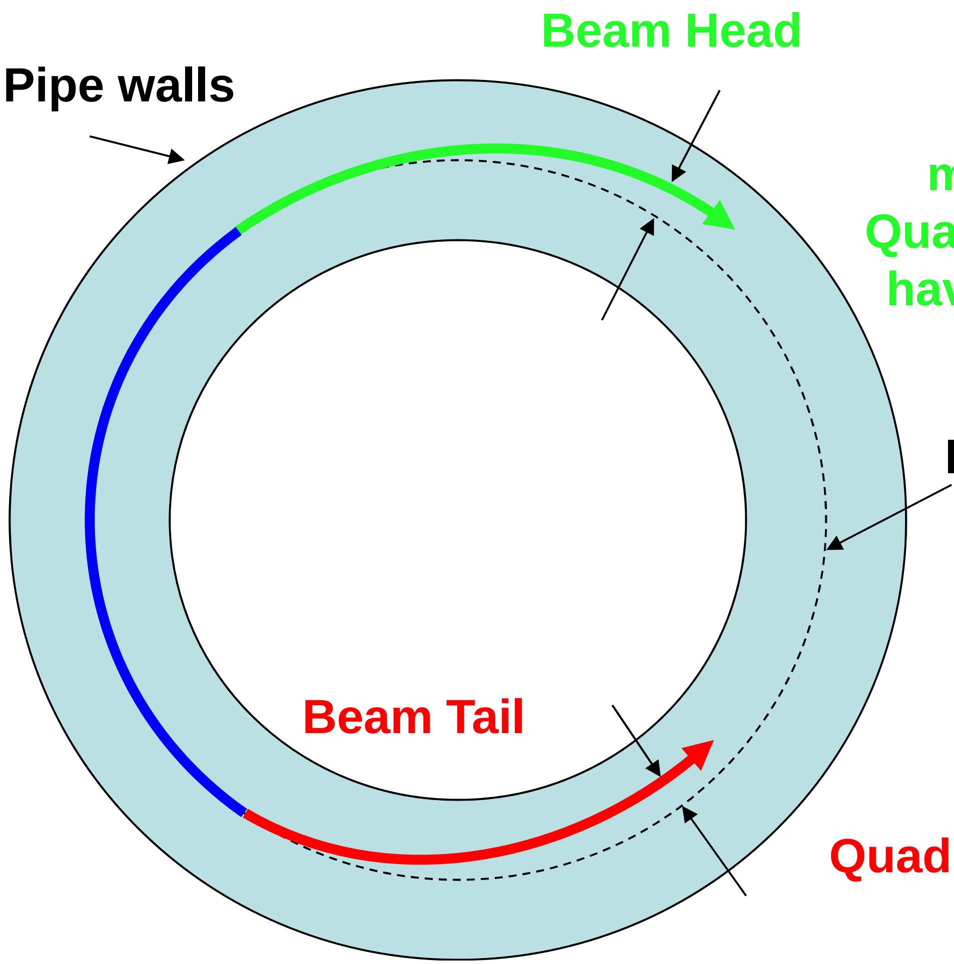

On average higher momentum particles = Quadrupoles will effectively have a longer focal length

$$\sin\frac{\mu}{2} = \frac{L}{2f}$$

$$\nu \equiv \frac{1}{2\pi}\oint\frac{ds}{\beta(s)} = \frac{1}{2\pi}N_{cell}\mu_{cell}$$

On average lower momentum particles = Quadrupoles will effectively have a shorter focal length

Fractional Tune-Shift at the Ends of the Beam

Direction beam position monitor signal

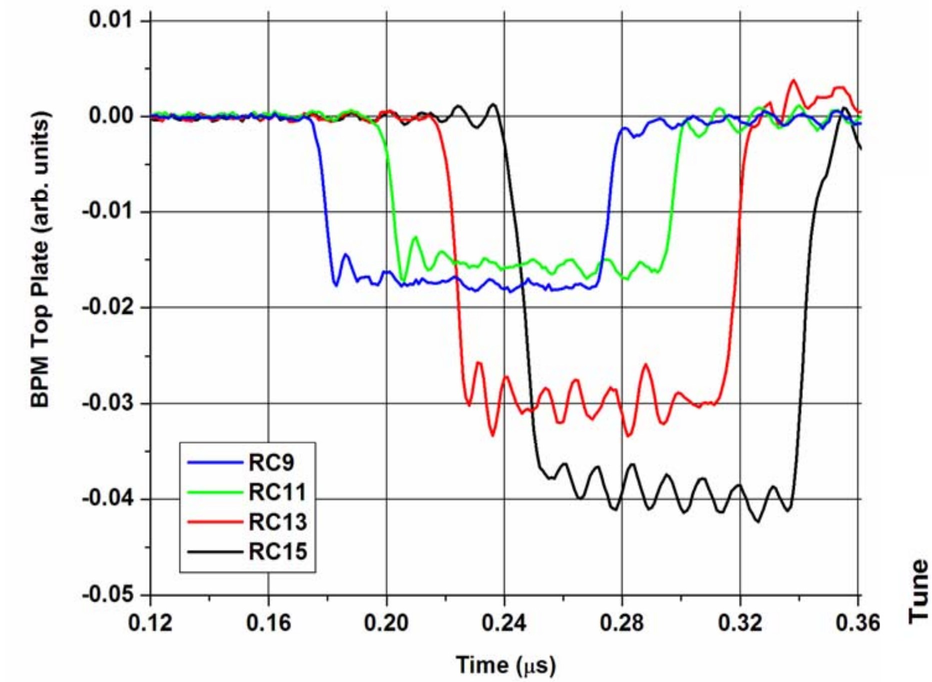

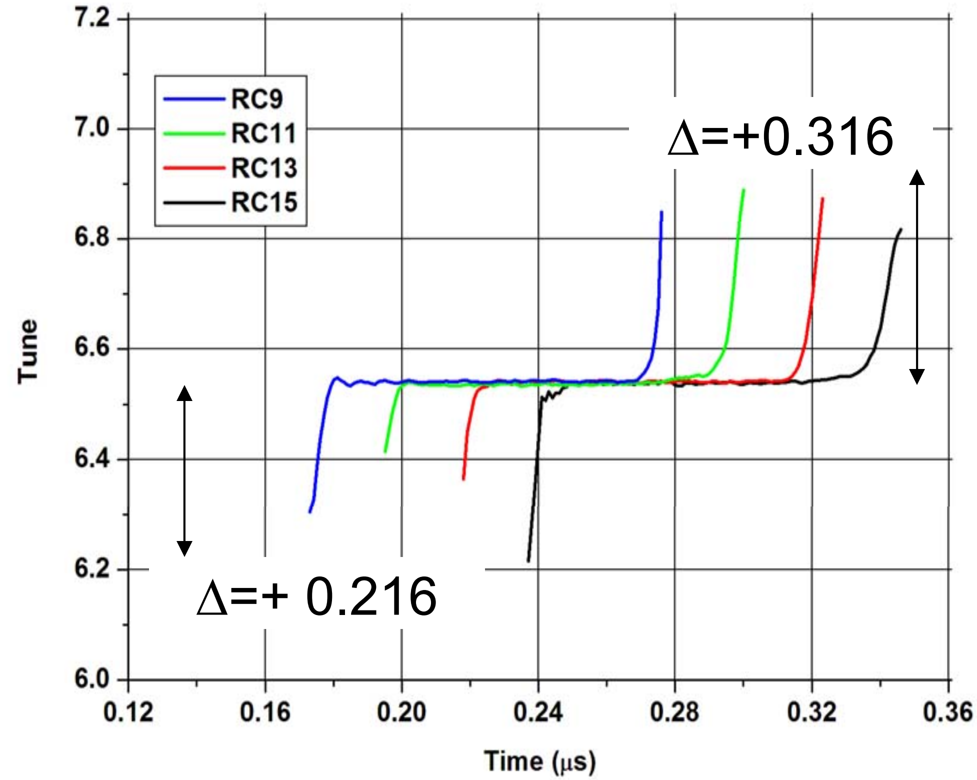

A fractional tune shift appears at the ends of the bunch, corresponding to the momentum deviations at the ends.

-B. Beaudoin and R.A. Kishek, PRSTAB 16,114201 (2013).

Allowing the Beam to Coast Indefinitely

Inter-Stream Spacing Shrinks as the Bunch wraps

Simulated Phase Space

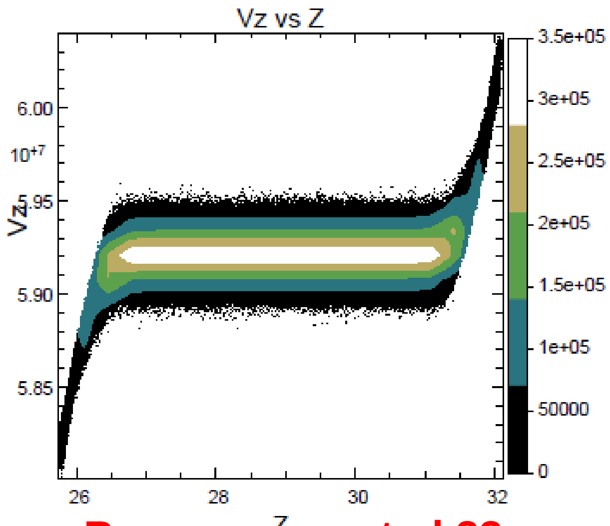

Beam propagated 23 m

ΔL > 0.56C

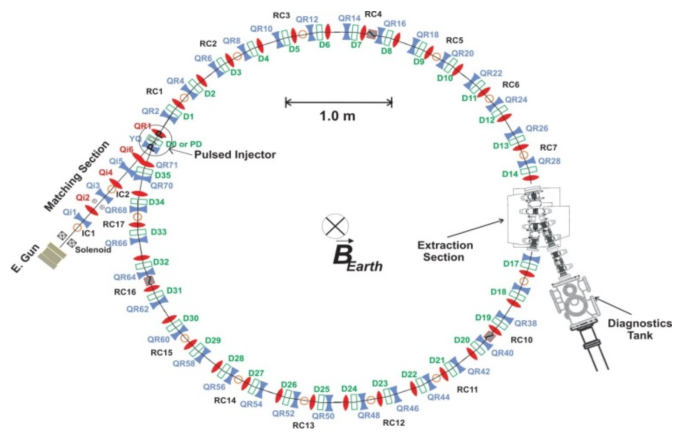

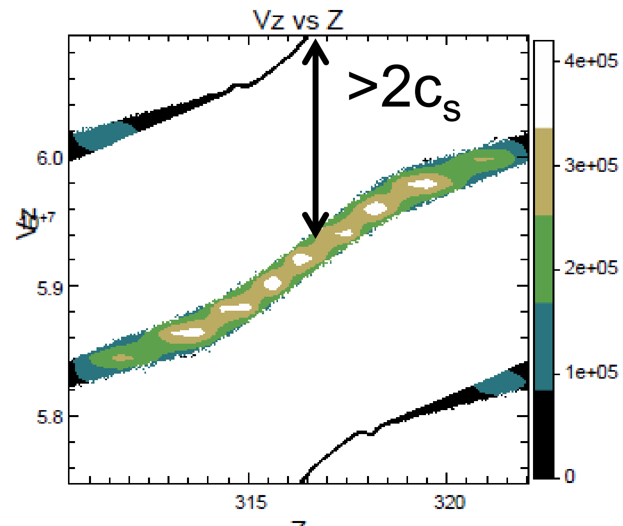

Beam propagated 310.5 m

ΔL = 2C

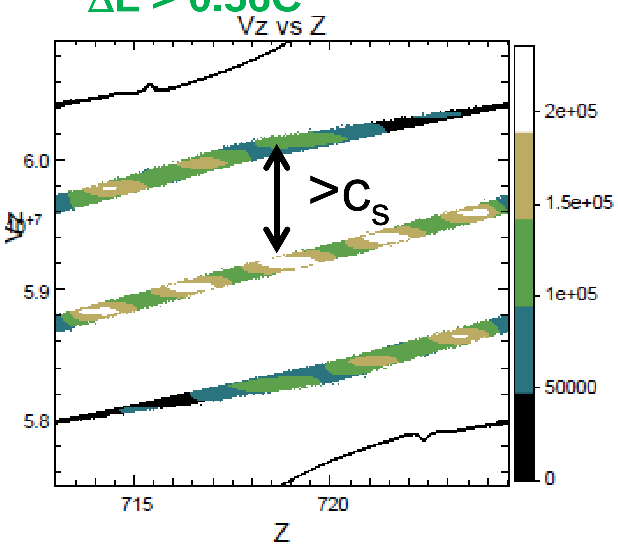

Beam propagated 713 m

ΔL > 4C

ΔL = Bunch length

C = Ring circumference

Injected length
ΔL = 0.5C

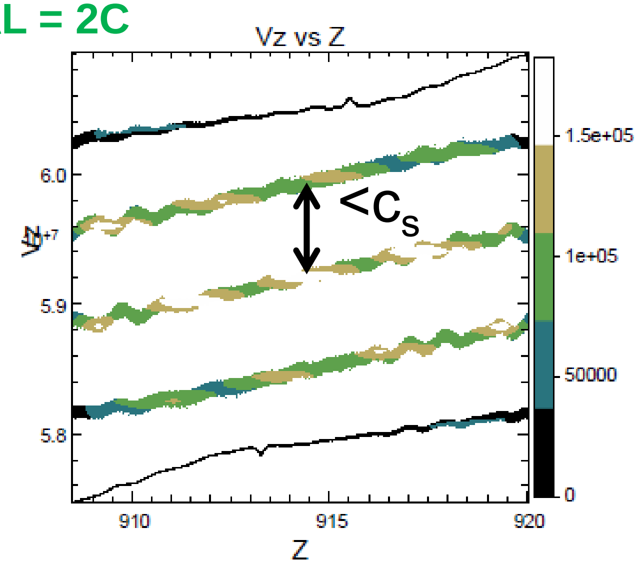

Beam propagated 908.5 m

ΔL = 5C

Wrapped Streams Couple to Subsequent Streams

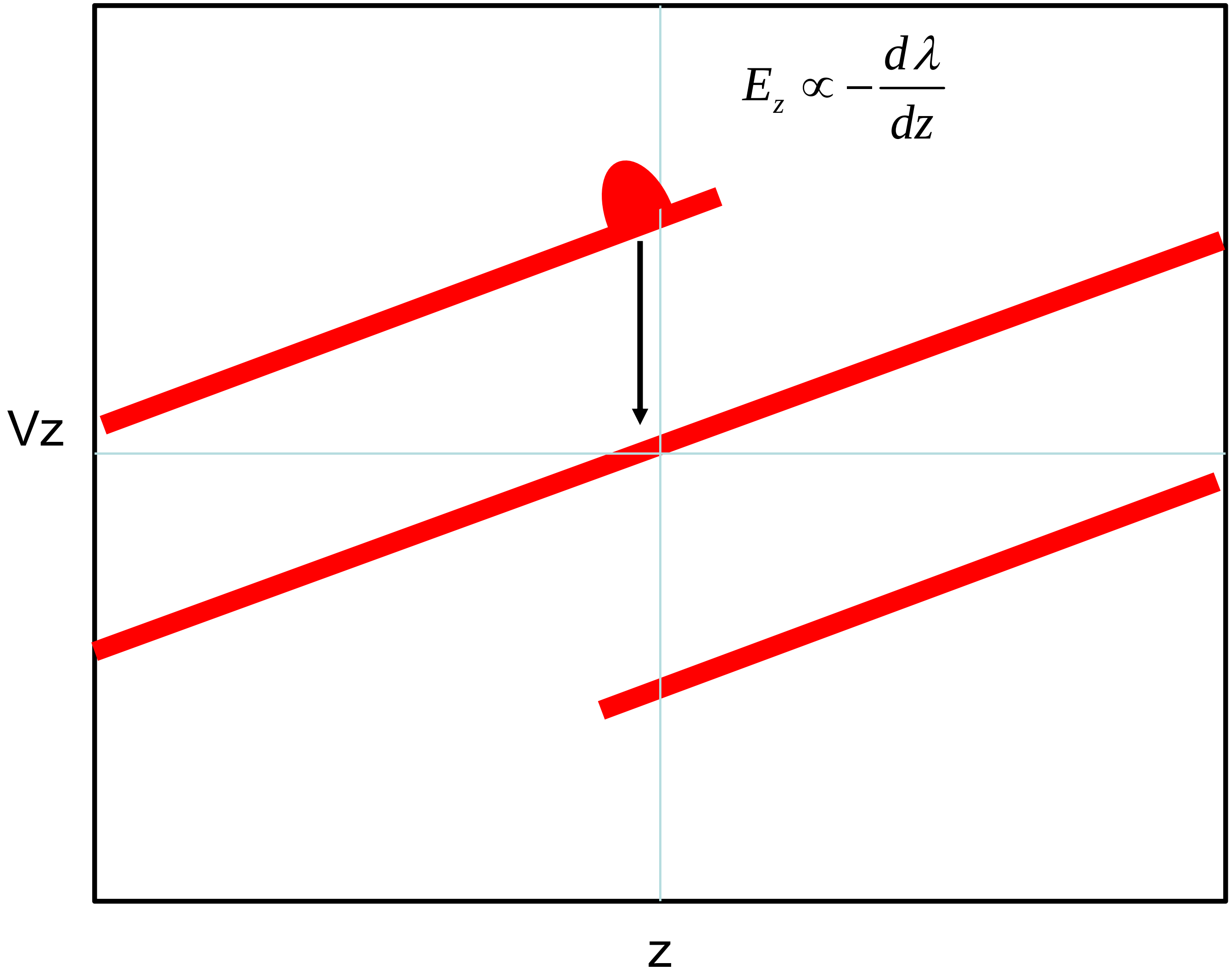

Density perturbations create axial electric fields that perturb other streams close in proximity.
This creates other density modulations that further seed others. This self-amplification creates high-frequency modulations in the beam.

Signature of the Onset in the Current Profiles

Current Profiles from a Wall Current Monitor

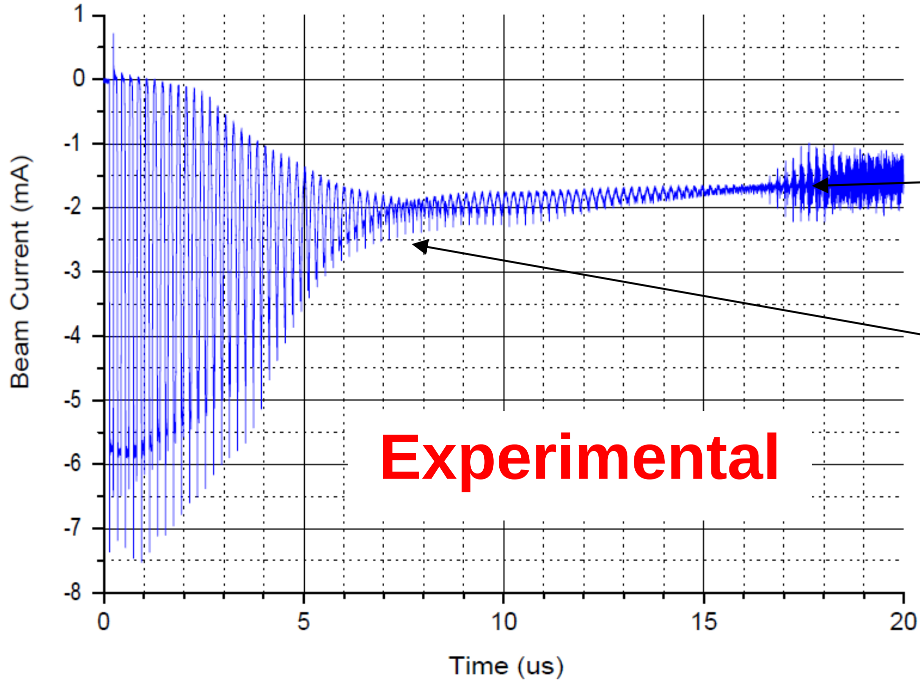

Onset

Beam becomes “DC”

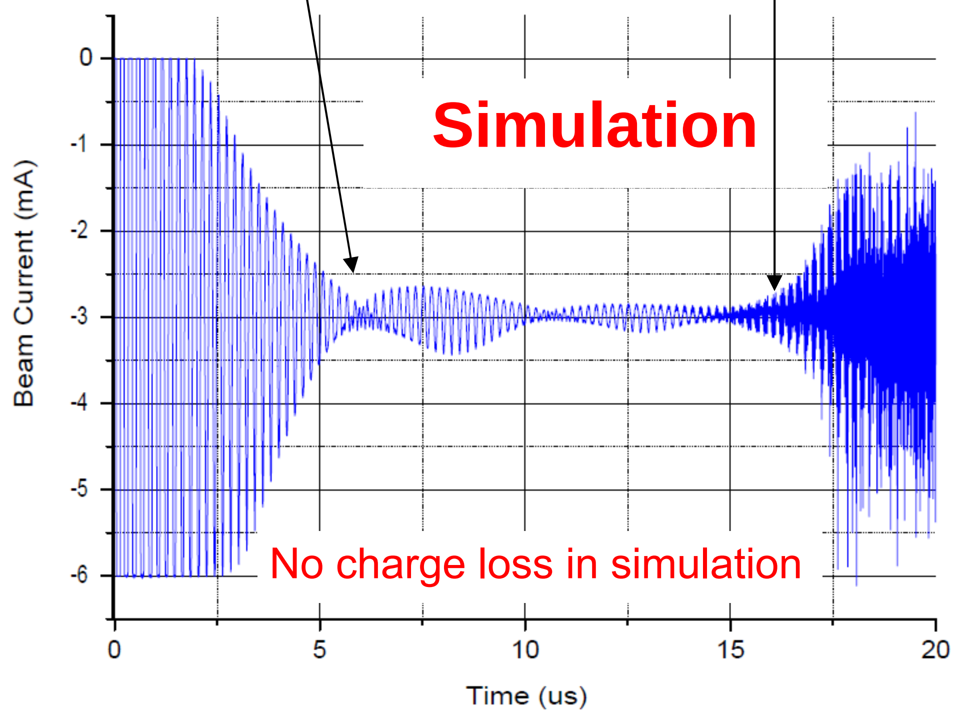

6 mA beam

$\eta = 0.50$

Fill Factor Dependence on the Number of Filamentations

The growth rate of the modulations in phase space is also dependent on the fill factor

Phase Space (6 mA beam)

70 ns long bunch

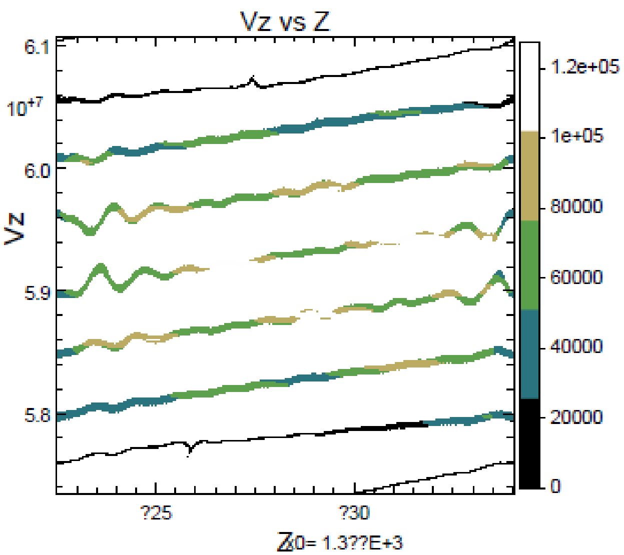

ΔL > 7C $\eta = 0.35$

130 ns long bunch

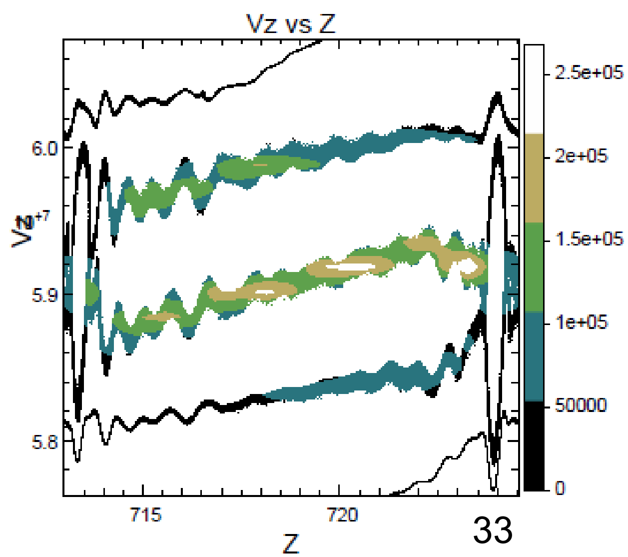

ΔL > 3.5C $\eta = 0.66$

100 ns long bunch

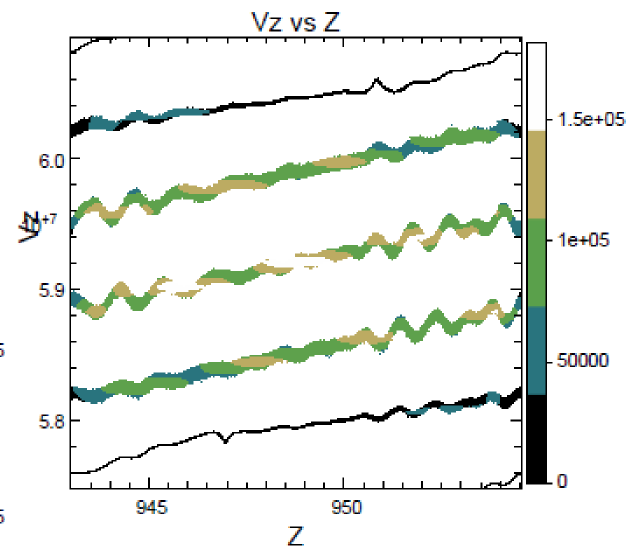

ΔL > 5C $\eta = 0.50$

Fill Factor and Current Dependence on the Onset

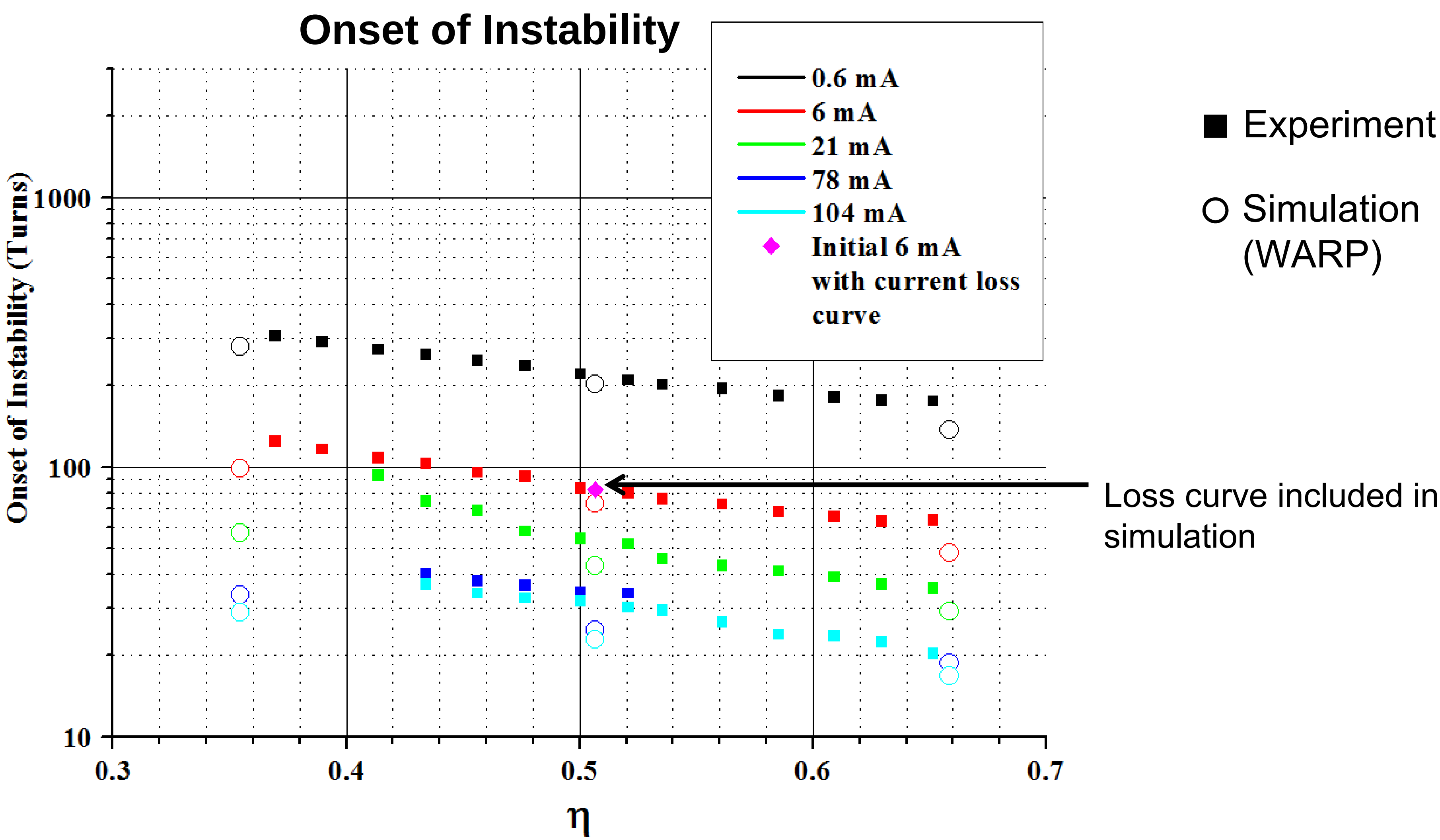

$$\eta = \text{fill factor} = \frac{\text{bunch length}}{\text{period of revolution}}$$

-B.L. Beaudoin, I. Haber, R.A. Kishek, and T. Koeth, *"Experimental Observations of a Multi-stream Instability in a Long Intense Beam,"* Proceedings of the 2013 International Particle Accelerator Conference, Shanghai, China, May 2013, 2044 (2013).

Extending to Multiple Short Bunch Trains

Multi-Bunch Train

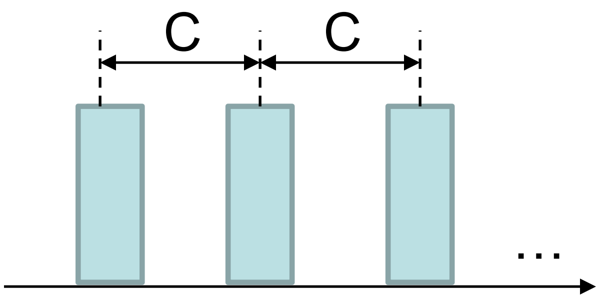

For multiple bunch trains, C is the pulse to pulse spacing

$$C = (20ns)v_o = 1.167m$$

$$\eta = \frac{12.57ns}{197.39ns} = 0.0636$$

Experimental Observation

7.7 mA beam
3 pulse bunch train at 50 MHz

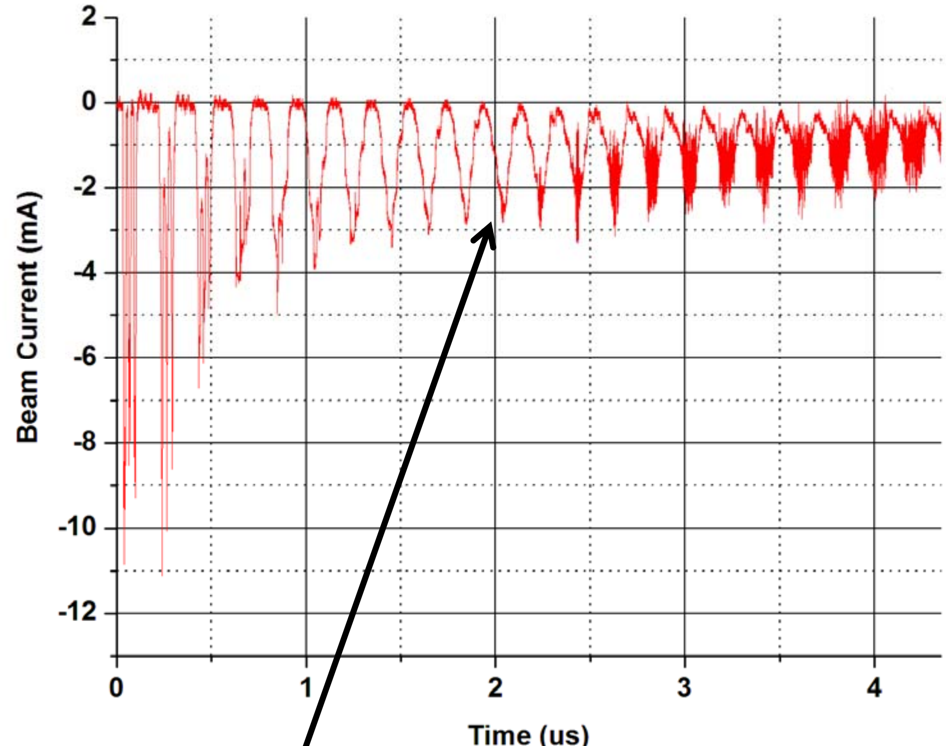

Onset of instability
s_{onset} = 132.7 m
$turns_{onset}$ = 11.5

Longitudinal Dynamics with Barrier Buckets

Longitudinal Physics

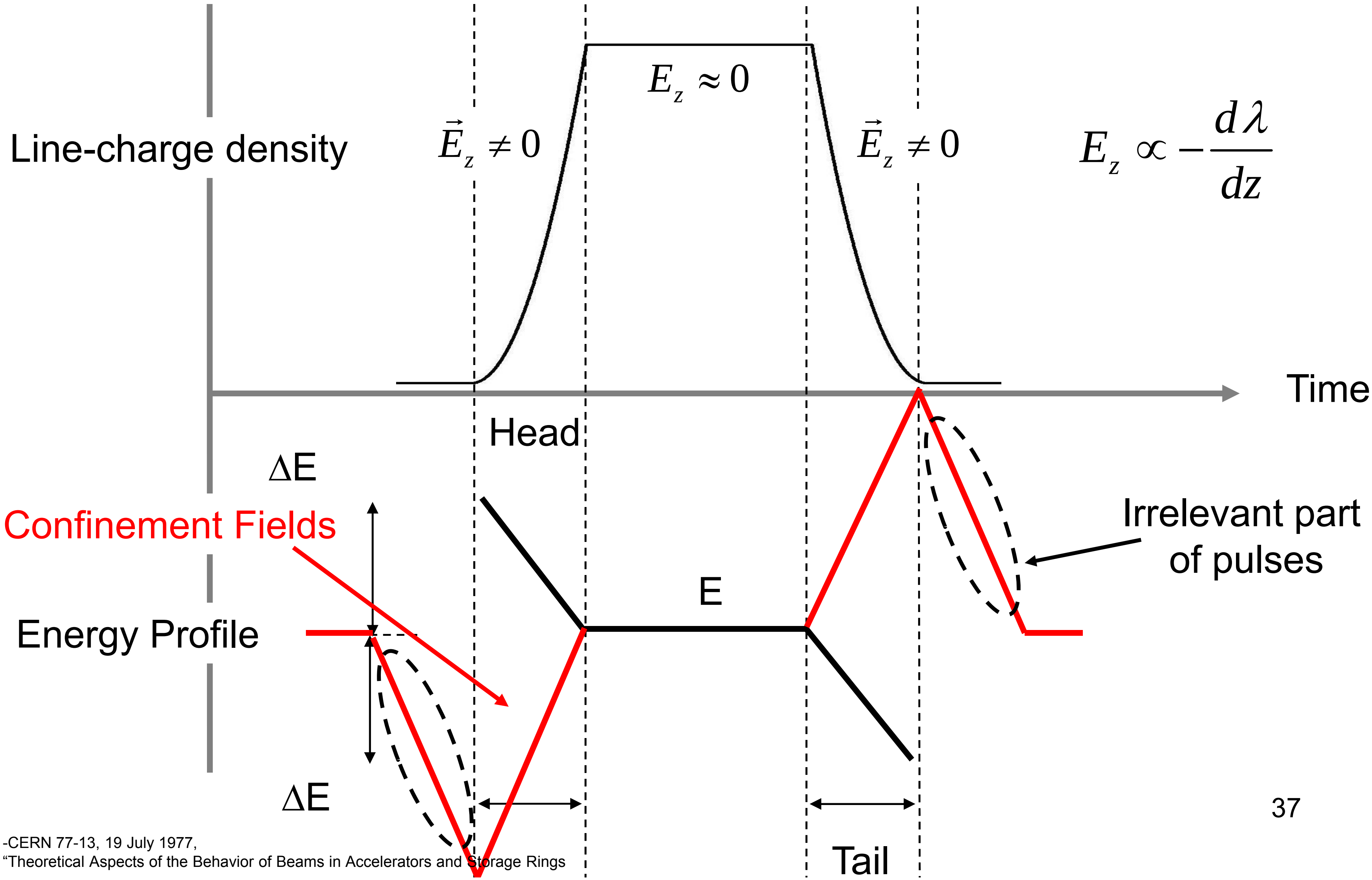

-CERN 77-13, 19 July 1977,
"Theoretical Aspects of the Behavior of Beams in Accelerators and Storage Rings

Barrier Buckets to Confine Beam-Ends

Induction Cell in between Quadrupoles

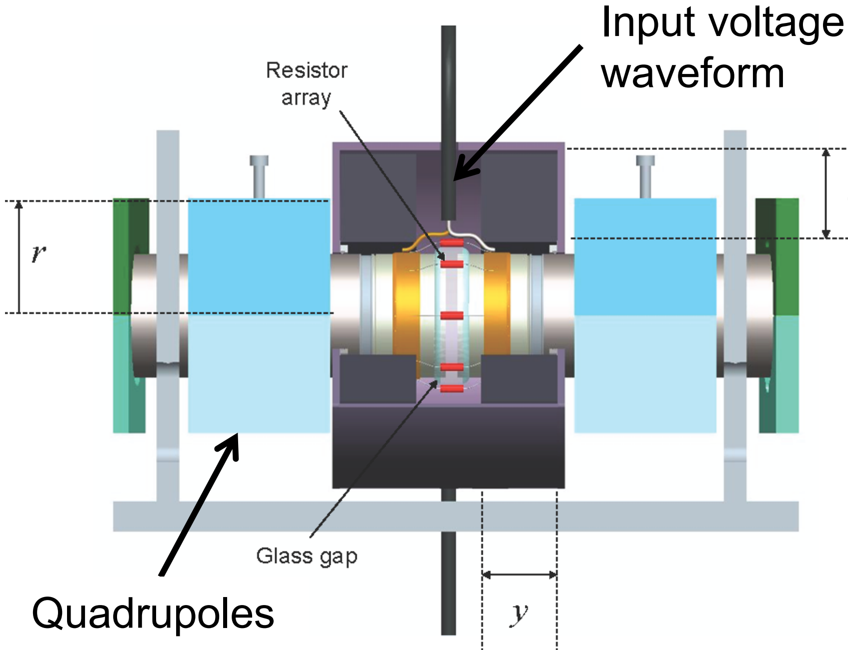

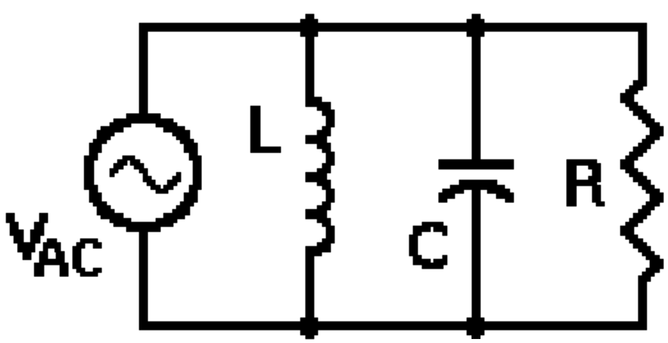

Barrier fields synchronized to revolution frequency

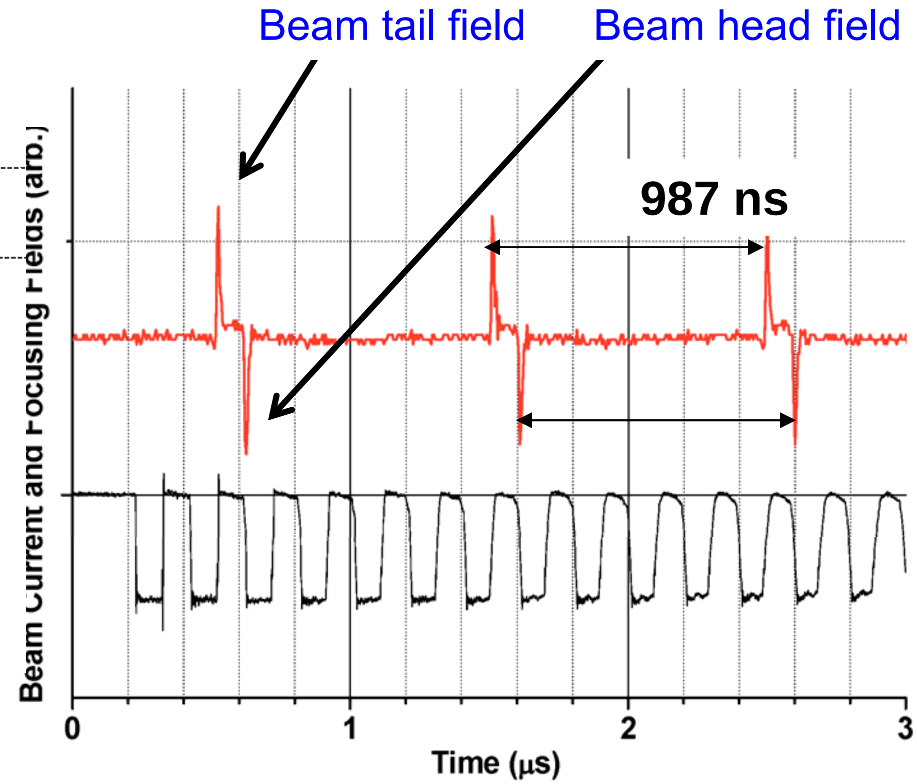

Beam revolution frequency 5.066 MHz

Bunch Shape Diminishes as a Result of Longitudinal Space-Charge Forces

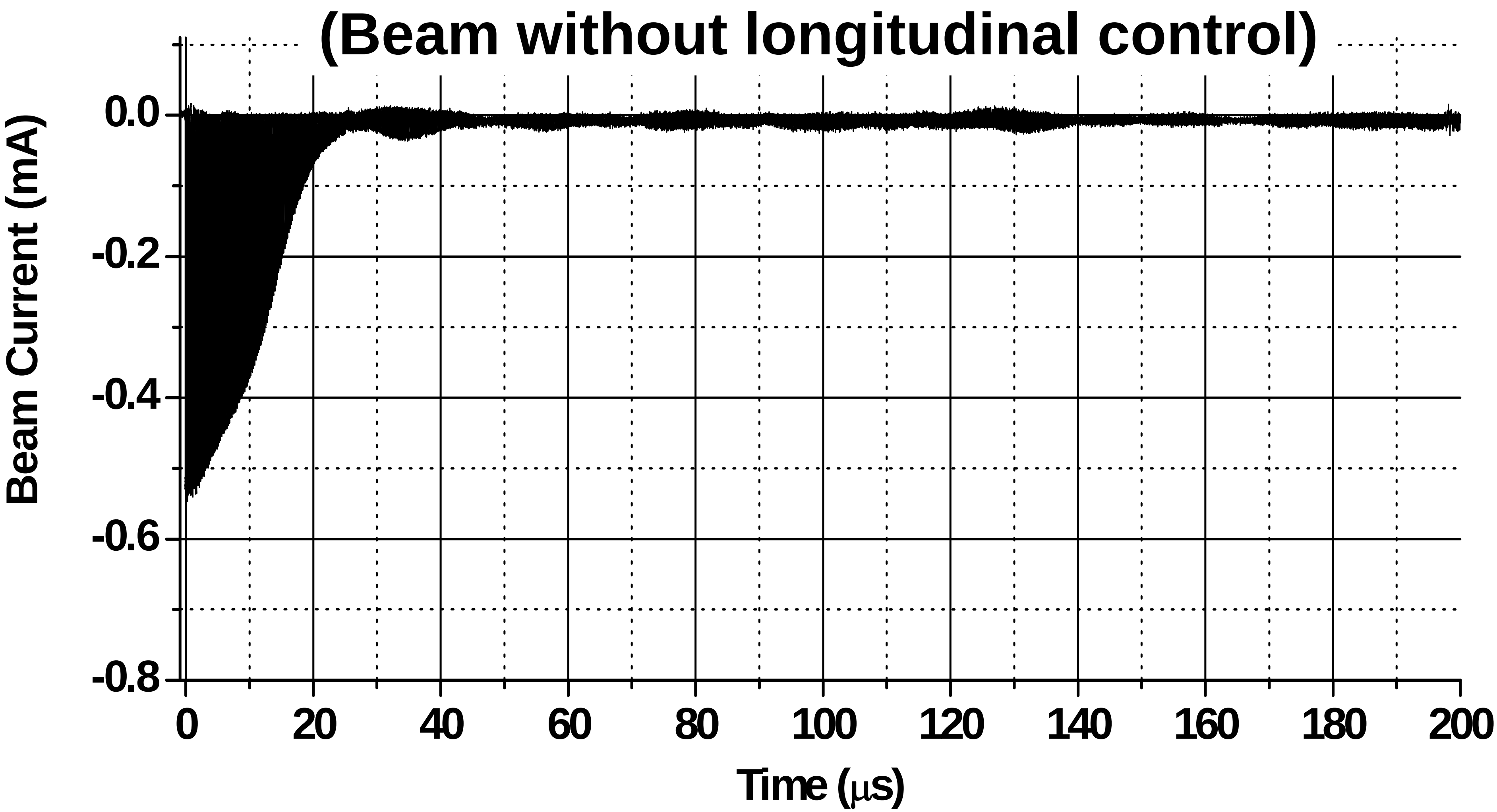

Bunch Lifetime is Extended with Longitudinal Control

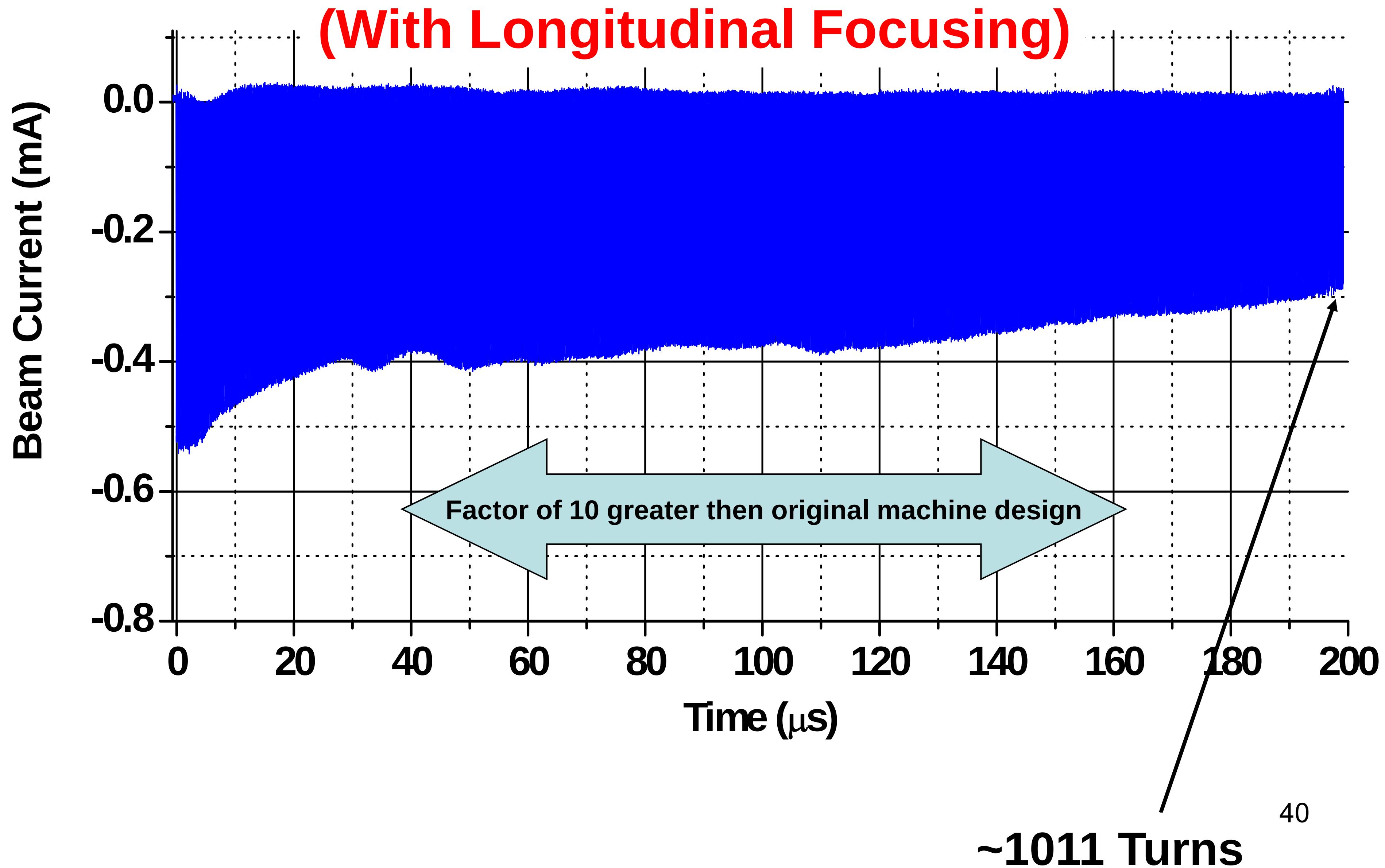

Experimental Results of Longitudinal Bunch Shape

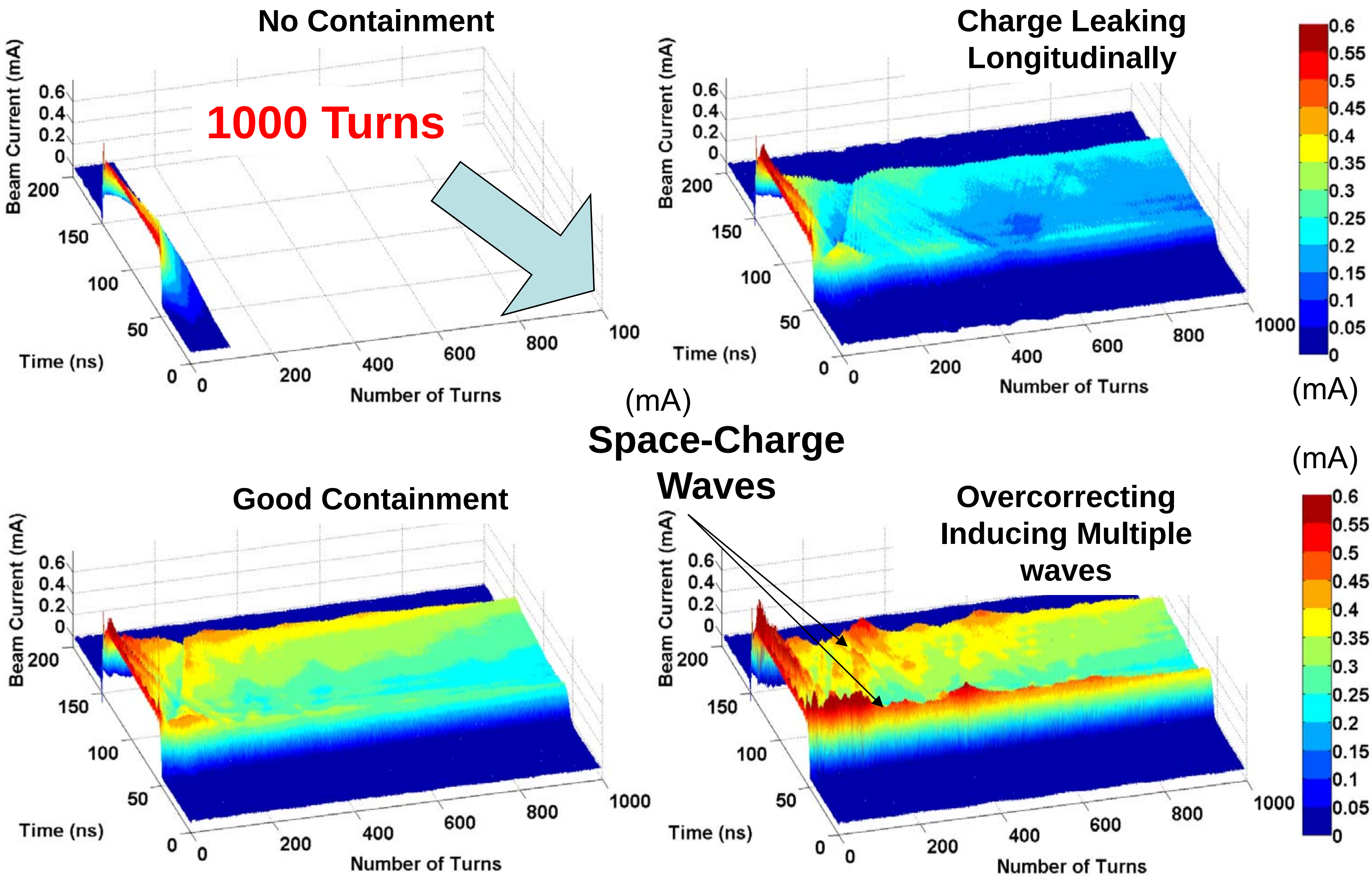

Waves Propagate/Reflect Along a Confined Bunch

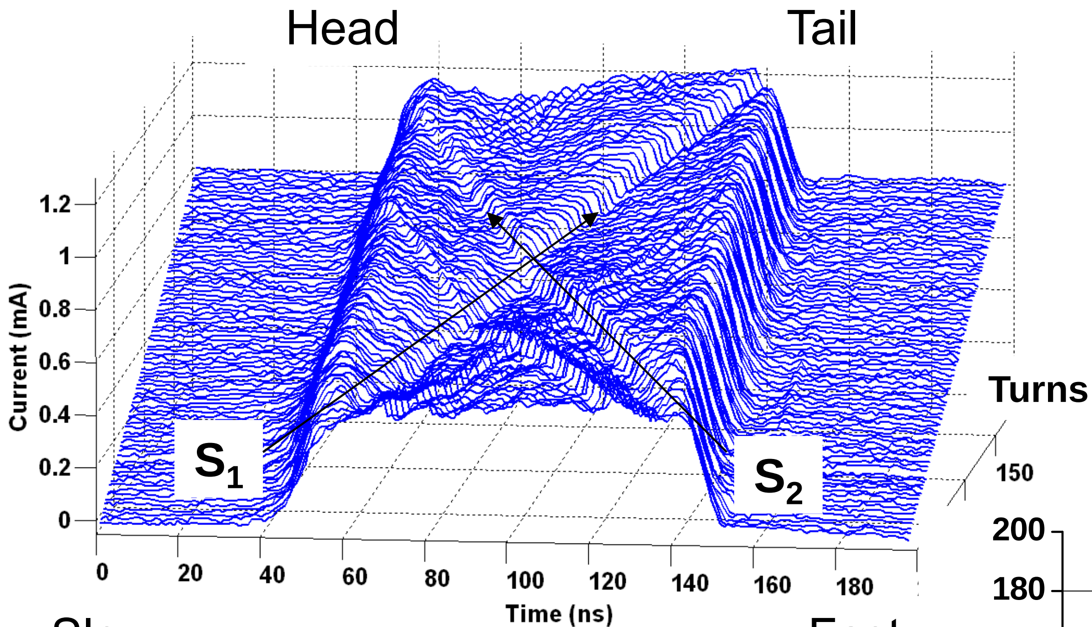

Slow wave

Fast wave

Wave velocity

$$c_s = \sqrt{\frac{qg\lambda}{4\pi\varepsilon_o\gamma_o^5 m}}$$

$$\boxed{c_s = slope \times \frac{\mathrm{v}_o^2}{11.52}}$$

$$0.569ns/turn = 1.68(1\times10^5)m/s$$

$$0.503ns/turn = 1.49(1\times10^5)m/s$$

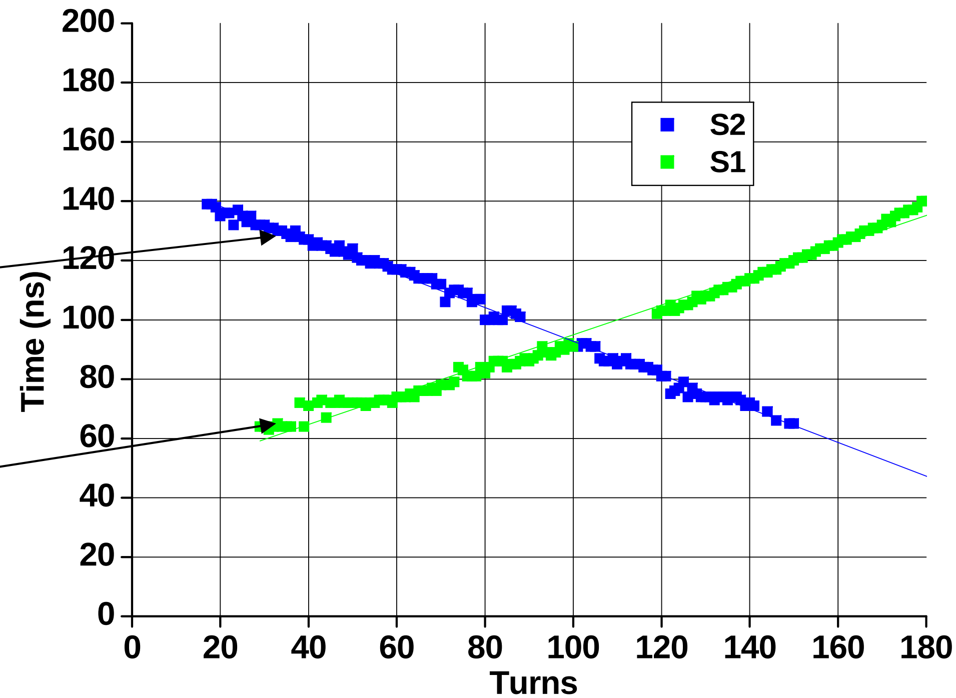

Analogy to Transmission Lines

Reflection Coefficient

$$\Gamma = \frac{Z_L - Z_o}{Z_L + Z_o}$$

Waves moving along a confined bunch corresponds to a wave reflecting on a transmission line

$$\Gamma = 1, Z_L >> Z_o, open\,circuit$$

$$\Gamma = -1, Z_L << Z_o, short\,circuit$$

$$\Gamma = 1$$

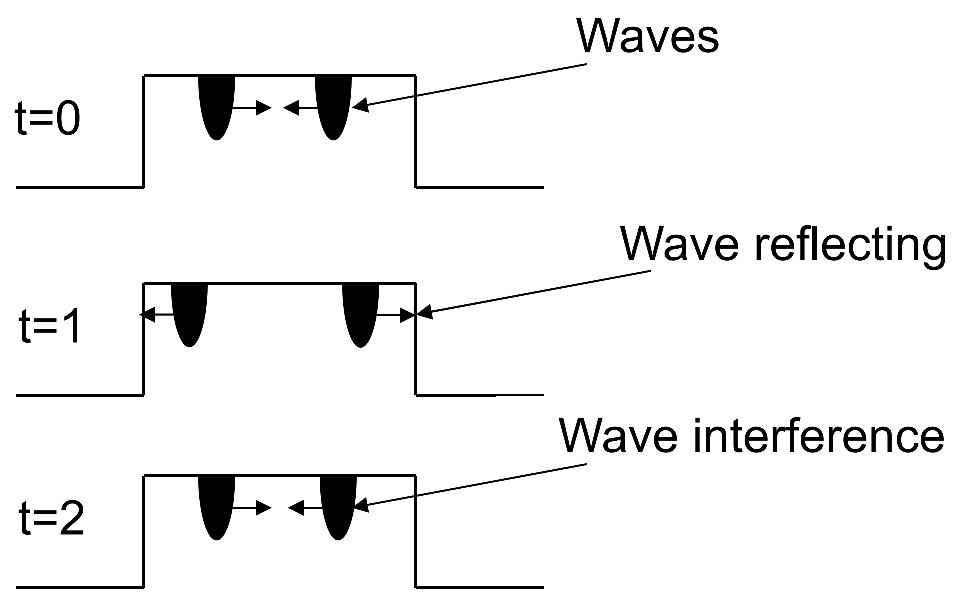

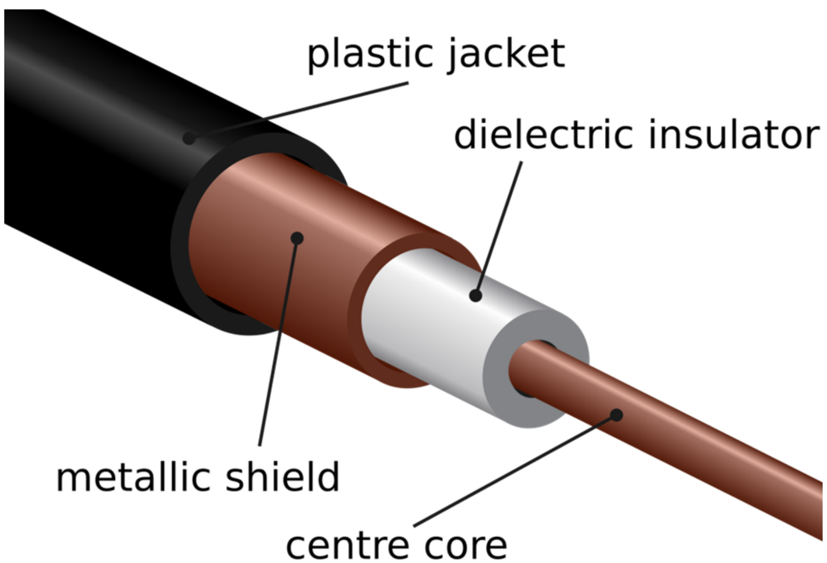

UMER Realignment

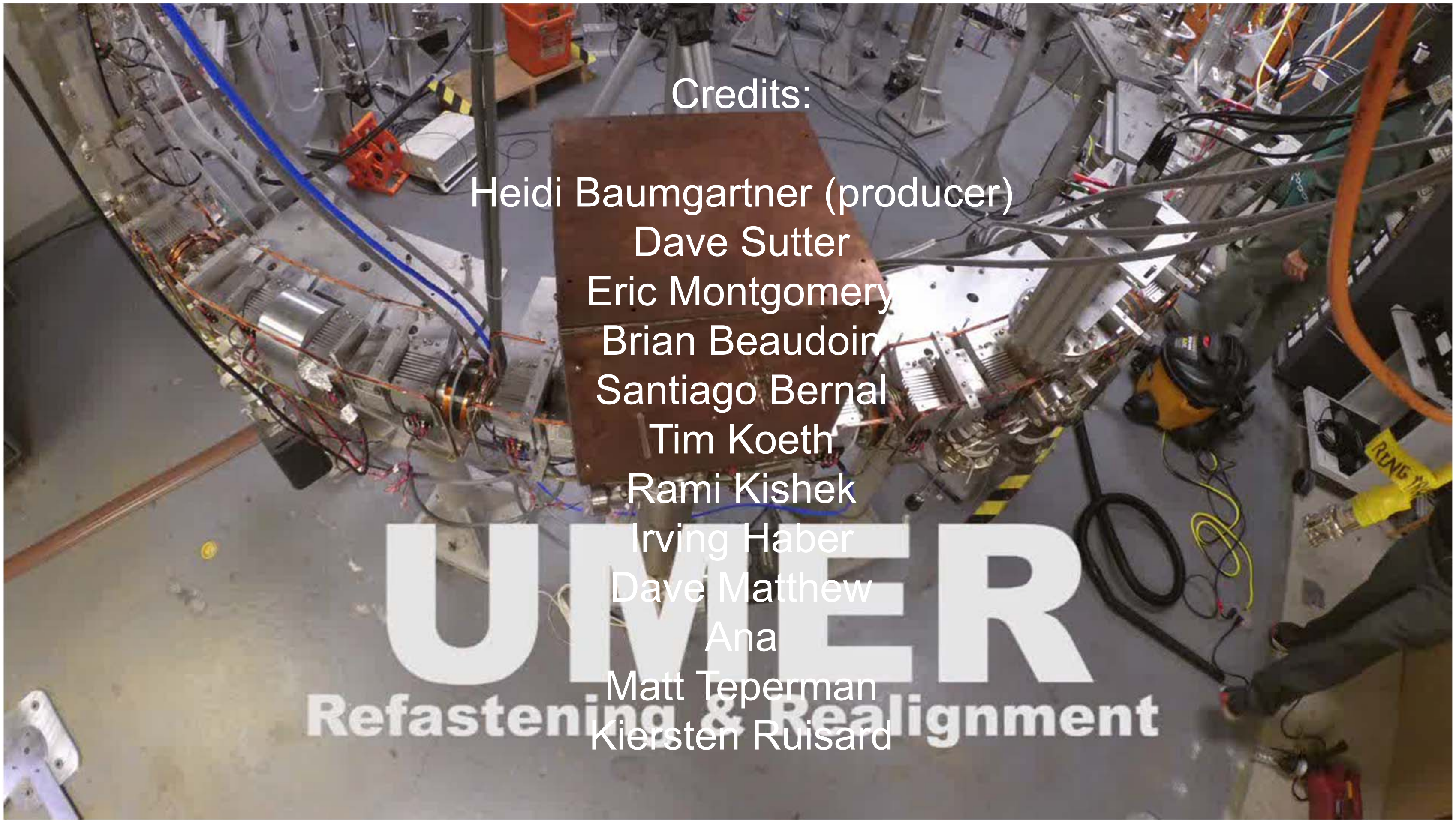

https://youtu.be/EZcCYs80T8k

Additional Slides

Space-Charge Waves on Long Beams

Perturbations to the beam density and/or energy initiates a fast and slow space-charge wave

$$\left(\omega - v_o k\right)^2 = c_{so}^2 k^2 \qquad c_{so}^2 = \frac{qg}{4\pi\varepsilon_0 \gamma_0^5} \lambda_0$$

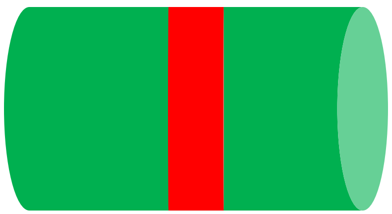

Density and/or energy perturbation

Wave Amplitude for a perturbation

	+F	-F
+S	***Pos. Density Perturbation***	**Neg. Energy Perturbation**
-S	**Pos. Energy Perturbation**	**Neg. Density Perturbation**

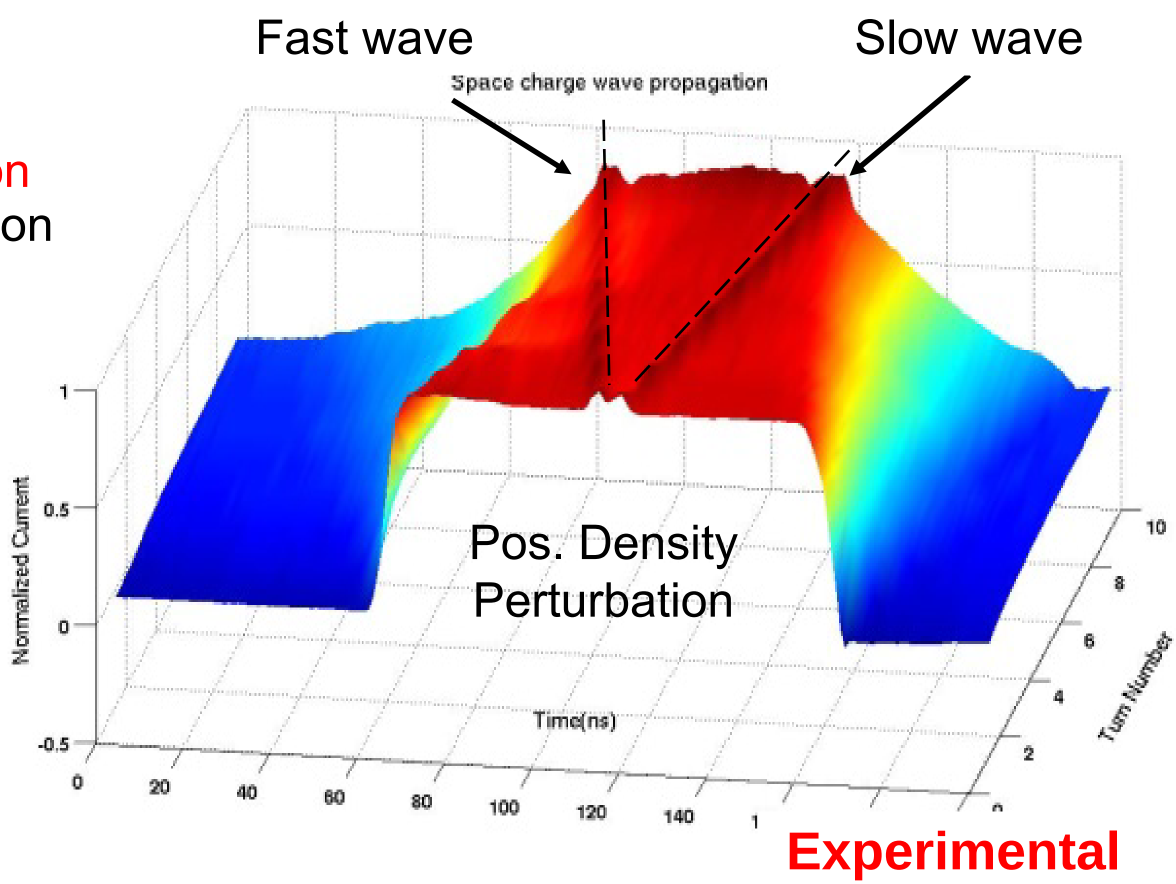

Space-Charge Waves on Long Beams

Perturbations to the beam density and/or energy initiates a fast and slow space-charge wave

$$\left(\omega - \mathrm{v}_o k\right)^2 = c_{so}^2 k^2 \qquad c_{so}^2 = \frac{qg}{4\pi\varepsilon_0\gamma_0^5}\lambda_0$$

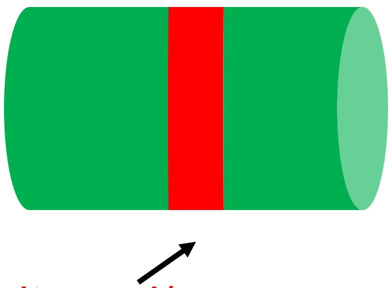

Density and/or energy perturbation

Wave Amplitude for a perturbation

	+F	-F
+S	***Pos. Density Perturbation***	**Neg. Energy Perturbation**
-S	**Pos. Energy Perturbation**	**Neg. Density Perturbation**

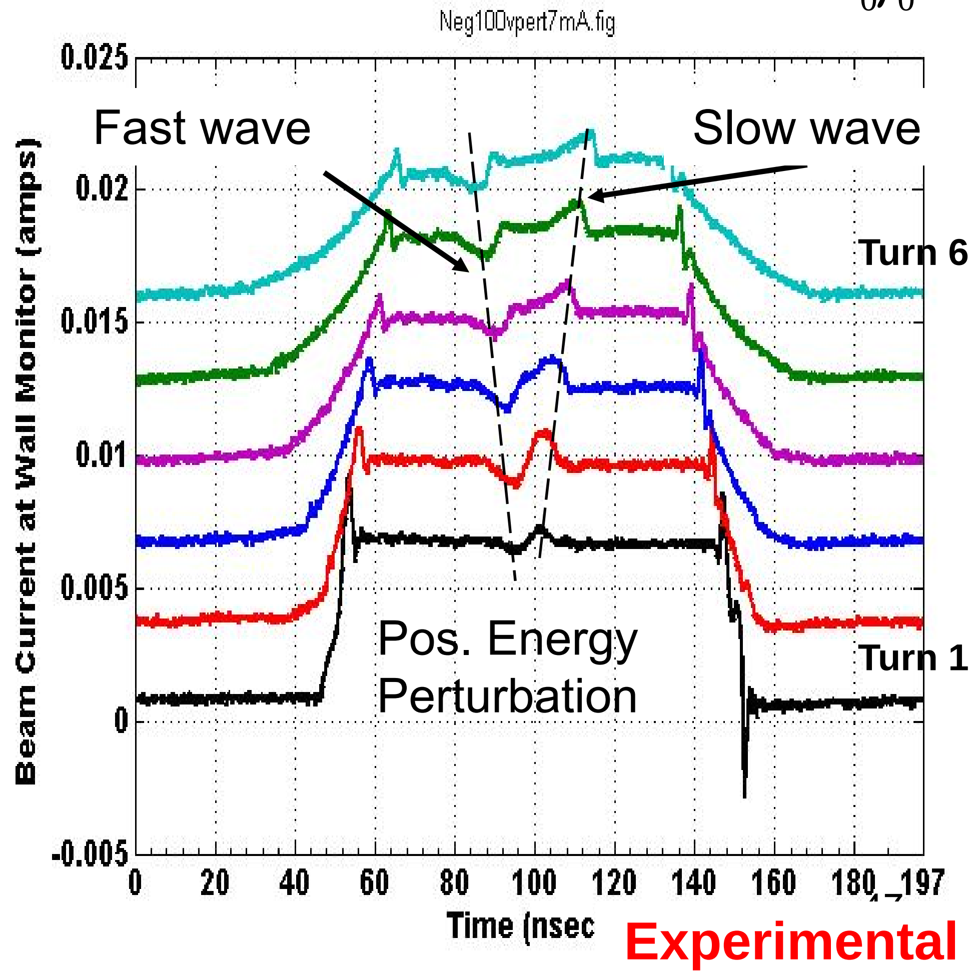

Soliton Wave Trains on Intense Beams

- With a large and narrow perturbation on a long intense beam, the perturbation begins to steepen and spawn soliton wave trains
- The pulse width and amplitude remains unchanged over a long propagation distance

Experimental and Simulation Comparison

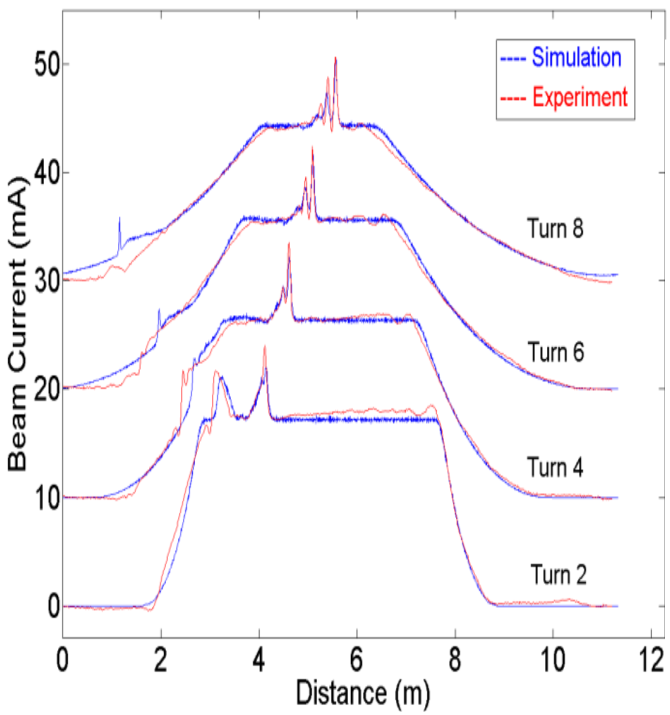

Sub pulses maintain their shape

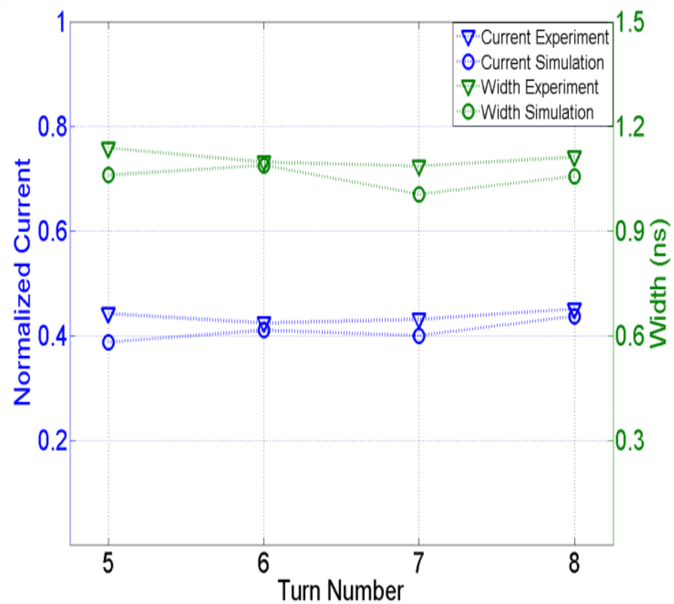

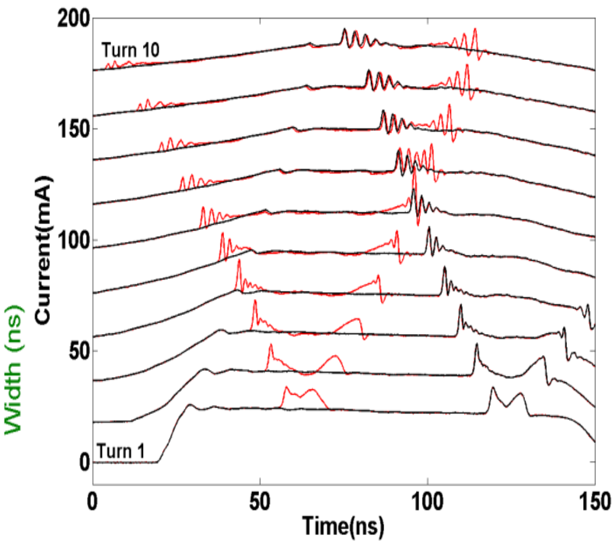

Interaction with other solitons and emerges unchanged

-Yichao Mo, B.L. Beaudoin, D. Feldman, I. Haber, R.A. Kishek, P.G. O'Shea, and J.C.T. Thangaraj, *"Experimental Observations of Soliton Wave Trains in Electron Beams,"* PRL **110**, 084802 (2013).

Soliton Compression

Both focusing ears are placed next to each other in order to create the ramped

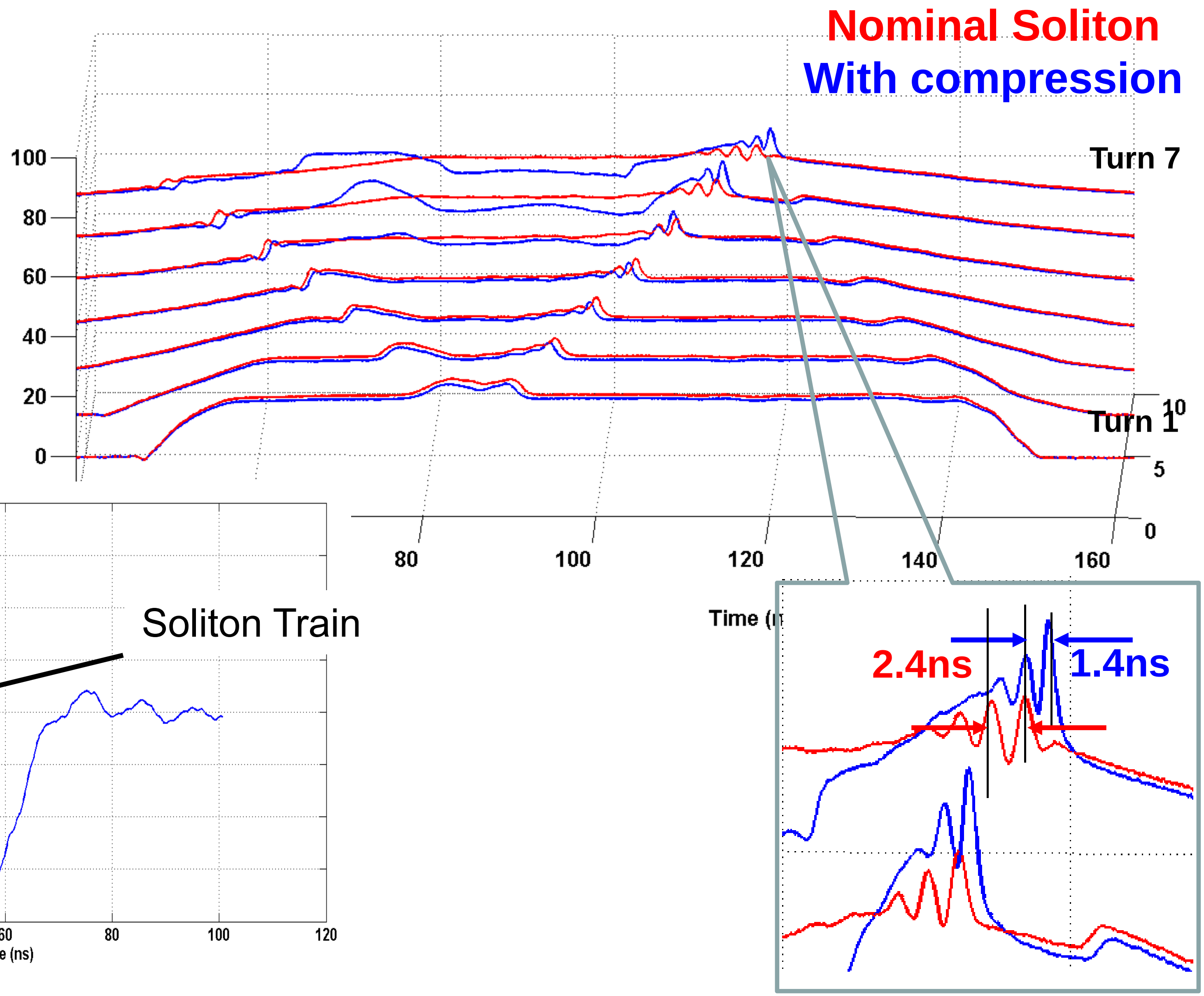

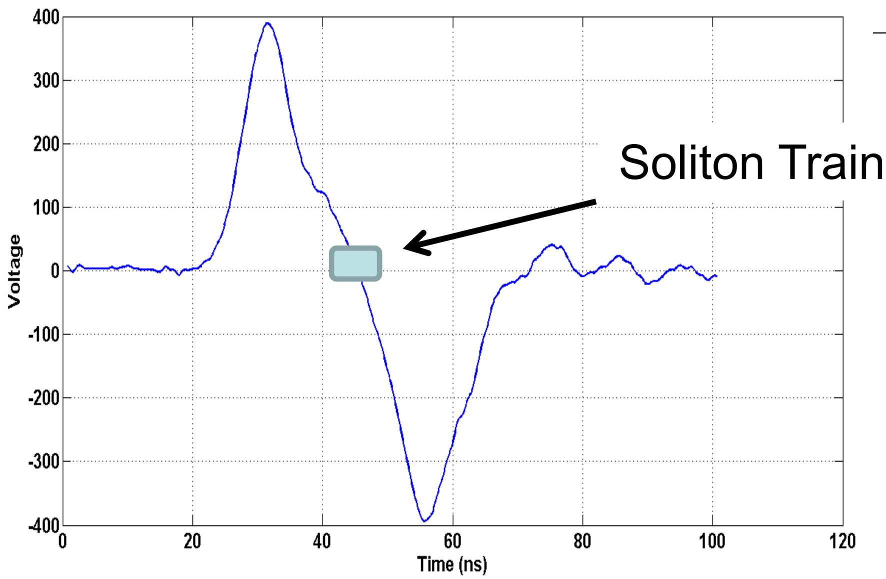

Shock-Wave Bunch Compression

- Bunch compression in barrier system is usually slow
- The presence of longitudinal space-charge improves the efficiency of barrier compression by taking advantage of the shock-front that launches naturally if the barrier moves in a space-charge dominated beam
- The duration depends on the velocity of the shock front

Creating the shock-front

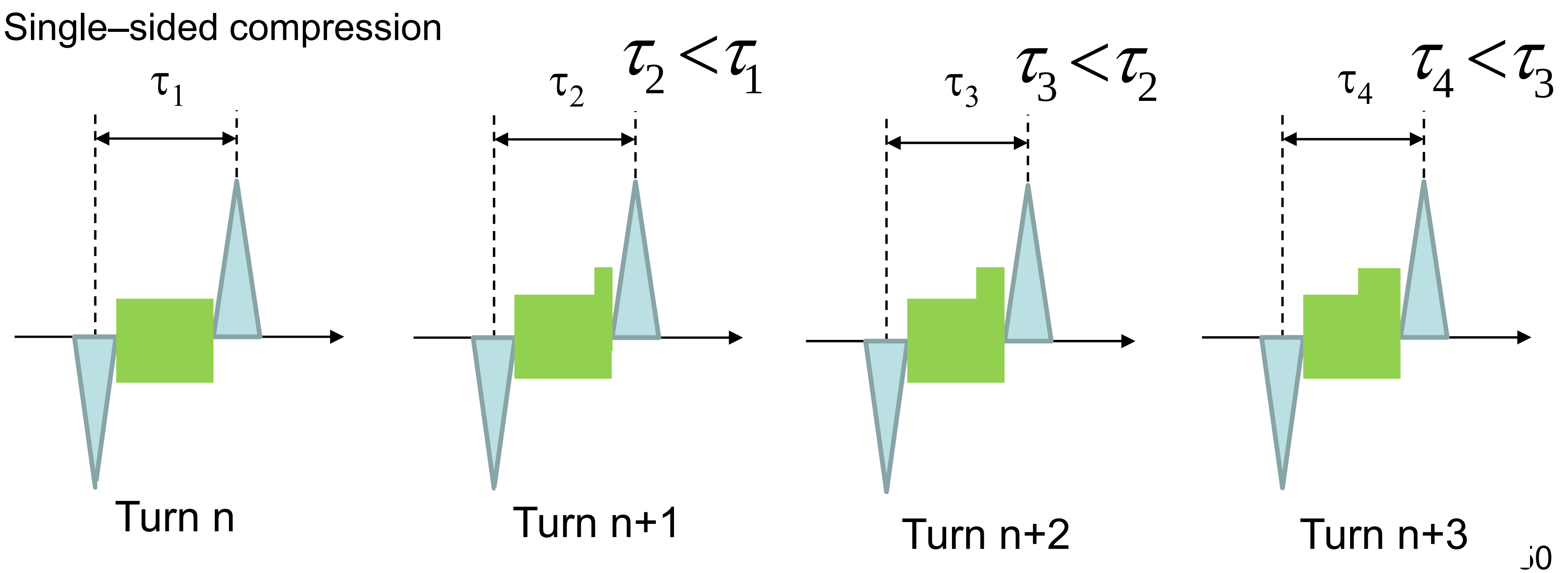

-O. Boine-Frankenheim, PRSTAB **13**, 034202, 2010.

Simulations of Barrier Shock-Compression

The 0.6 mA beam

$$\frac{c_{so}}{V_o} = 0.0049$$

Initially
η = 0.50

Current as a function of time

Turn 45 Turn 46

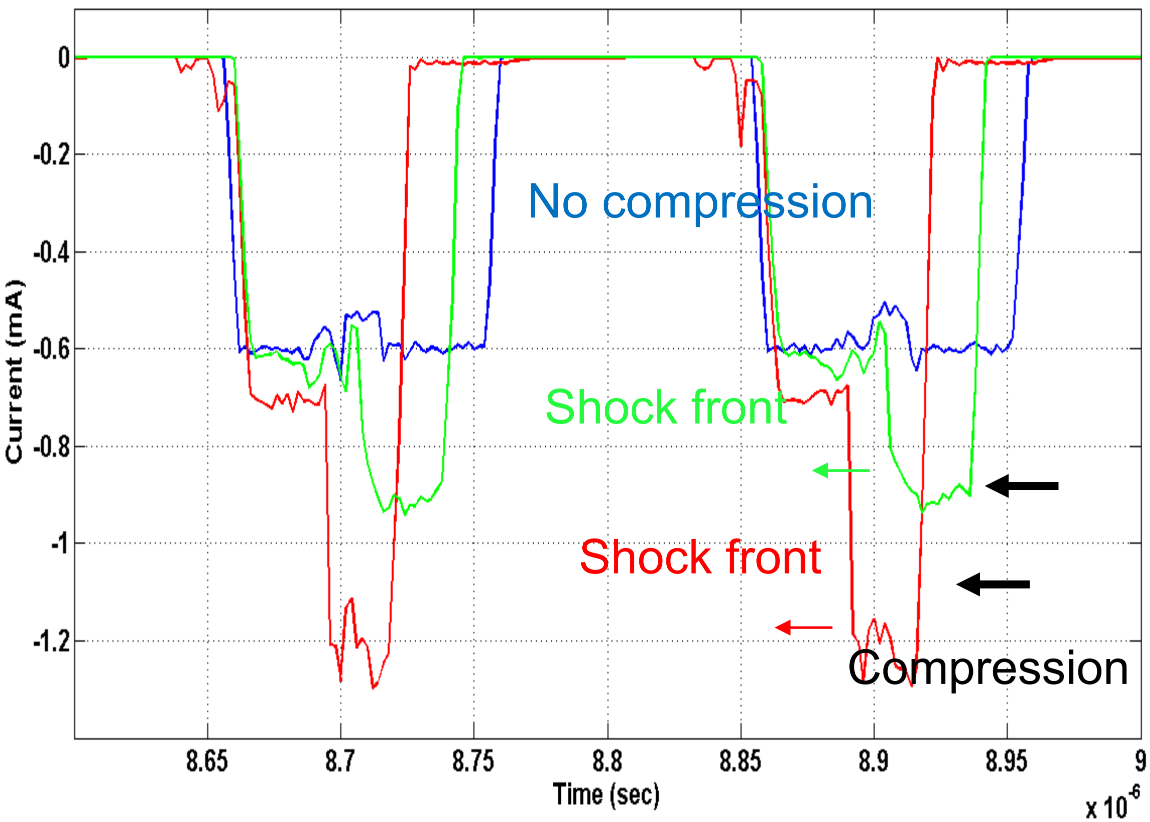

Phase Space

Slightly after Injection

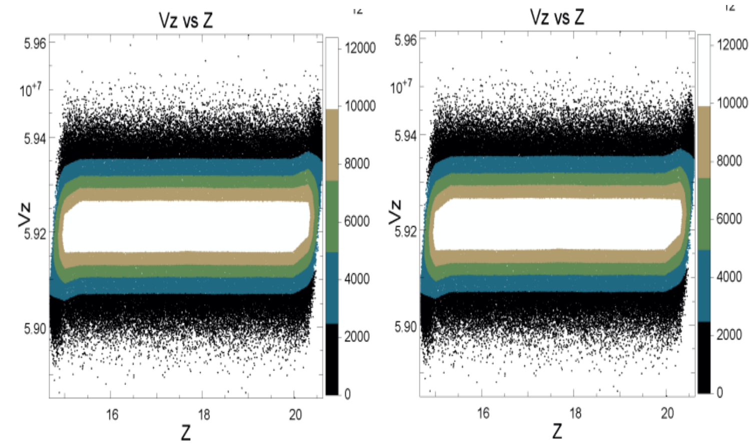

u_b =1.08E5m/s u_b = 2.42E5m/s

Turn 45

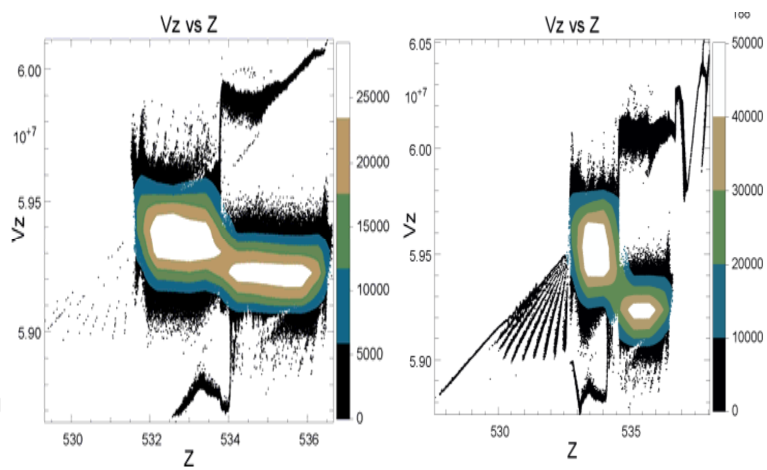

Experimental Results of Symmetric Focusing

$$\frac{c_{so}}{\mathrm{v}_o} = 0.0049$$

$\eta = 0.50$

Heat and Tail fields are independently controlled

Nominally Contained No Compression

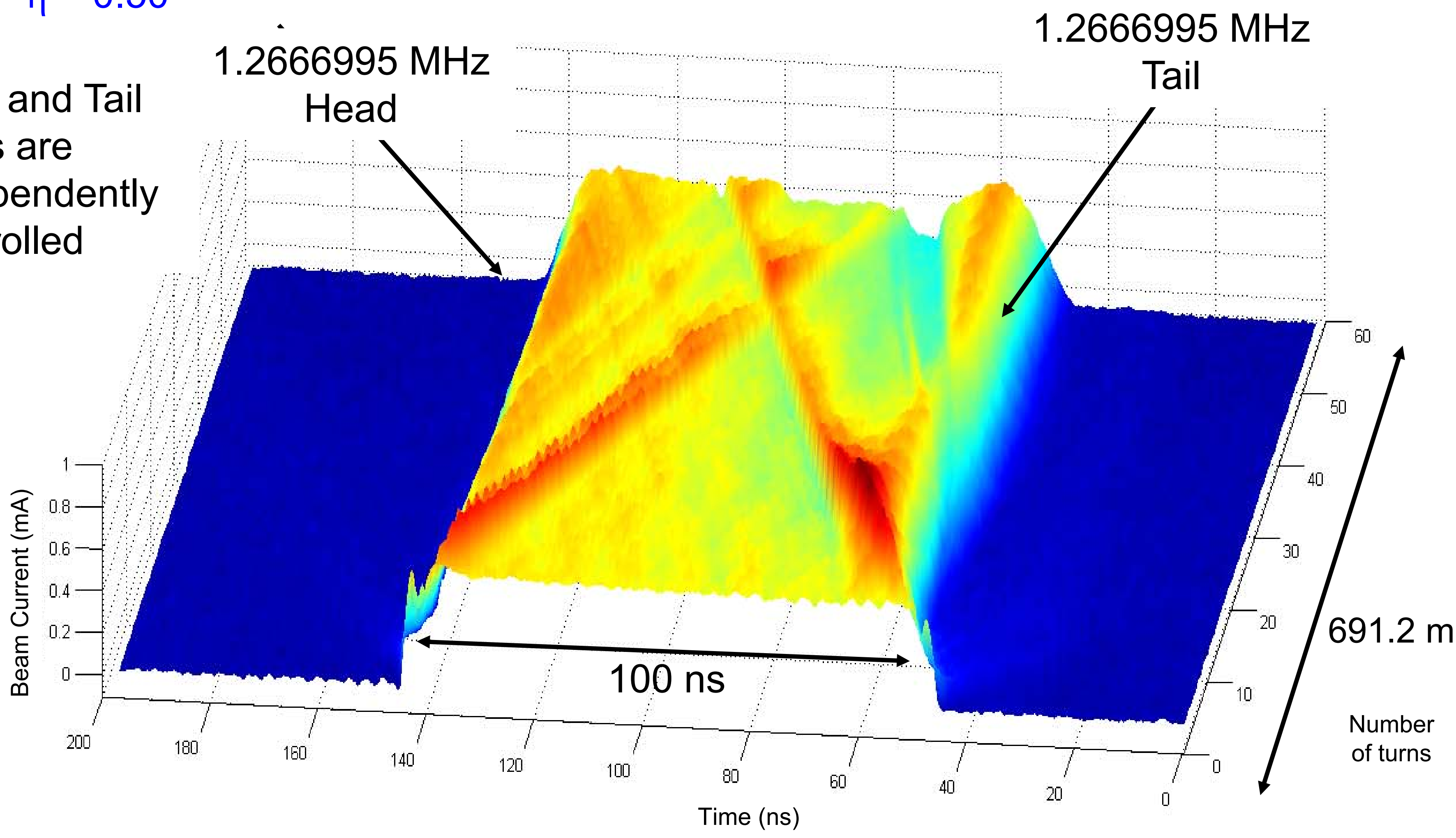

Experimental Results of Asymmetric Focusing

Top View

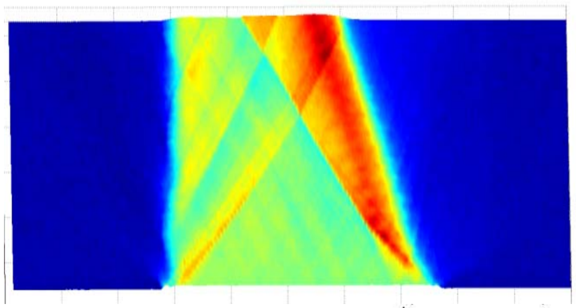

$$\frac{c_{so}}{v_o} = 0.0049$$

$\eta = 0.50$

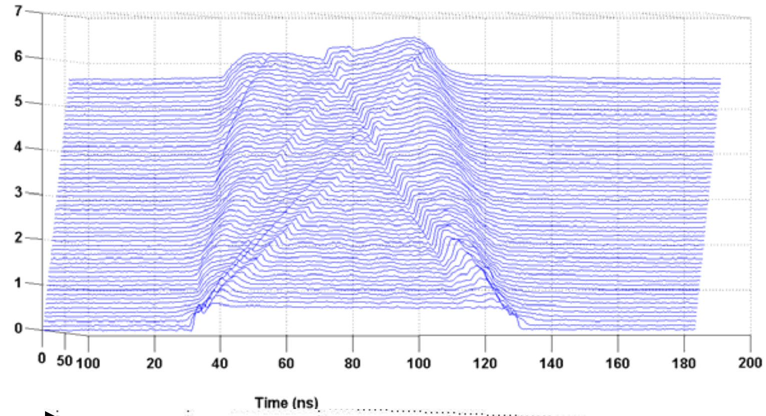

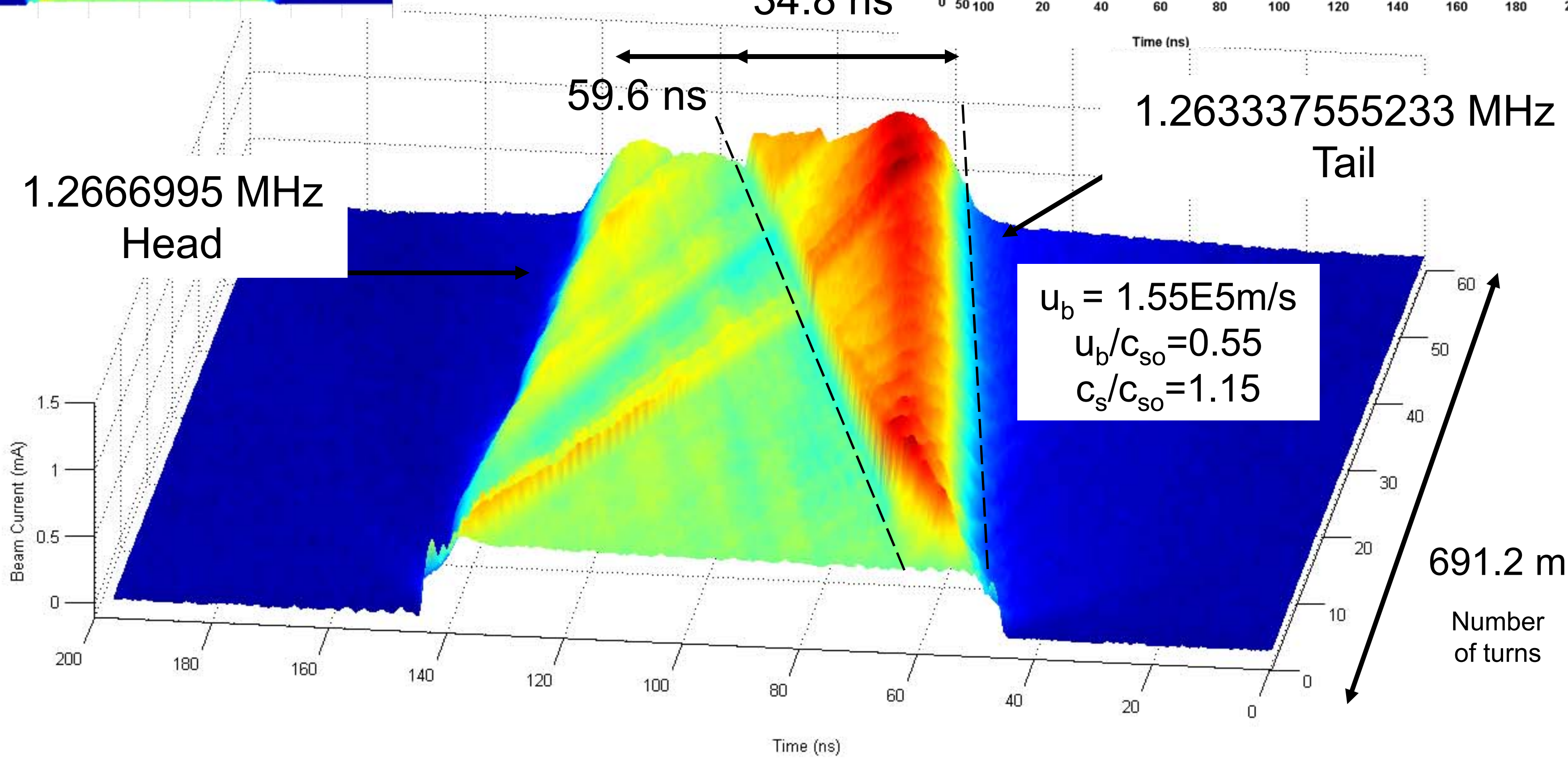

Experimental Results of Asymmetric Focusing

Top View

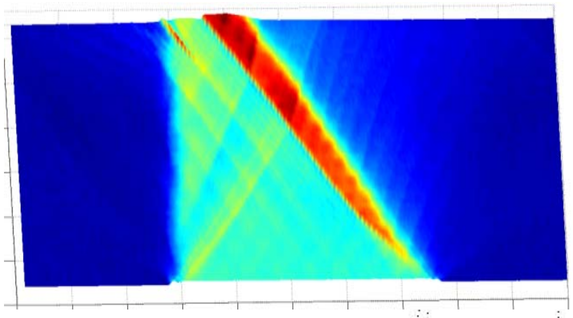

$$\frac{c_{so}}{v_o} = 0.0049$$

$\eta = 0.50$

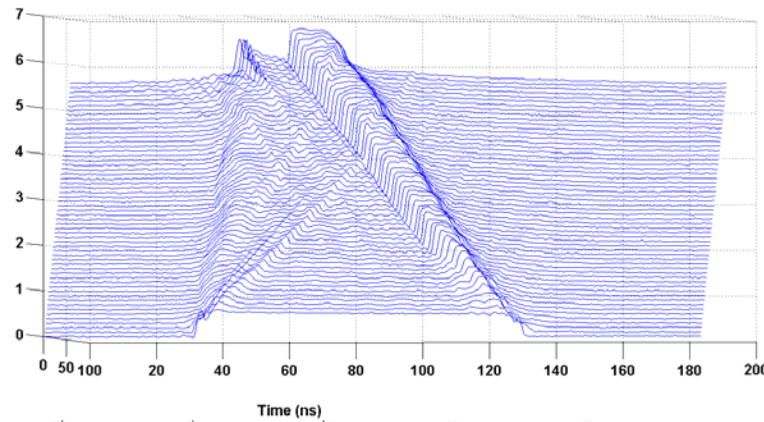

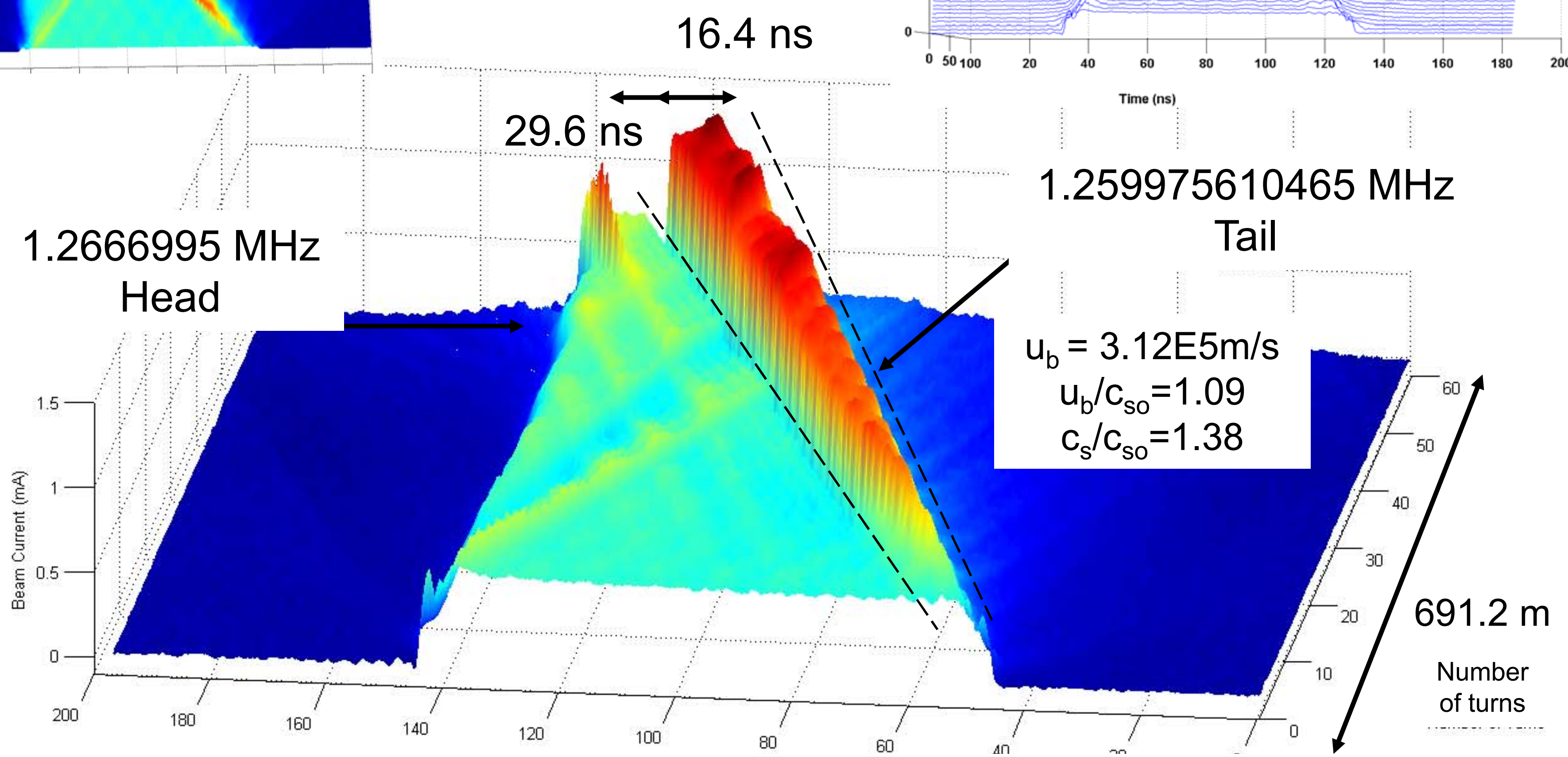

-B.L. Beaudoin, I. Haber, and R.A. Kishek, *"Barrier Shock Compression with Longitudinal Space Charge",* Proceedings of the 2015 International Particle Accelerator Conference, Richmond, VA, USA, May 2015, MOPMA044 (2015).

Shock Velocity as a function of Barrier Velocity

The 0.6 mA beam

$$\frac{c_s}{c_{so}} = 2\sqrt{-Q}\cos\left(\frac{\theta}{3}\right) + \frac{2u_b}{3c_{so}}$$

$$\frac{c_{so}}{v_o} = 0.0049$$

$$\theta = \arccos\left(\frac{R}{\sqrt{-Q^3}}\right)$$

Initially

$\eta = 0.50$

$$R = \frac{1}{27}\left(\frac{u_b}{c_{so}}\right)^3 + \frac{u_b}{12c_{so}}$$

$$Q = \frac{1}{9}\left(\frac{u_b}{c_{so}}\right)^2 - \frac{1}{3}$$

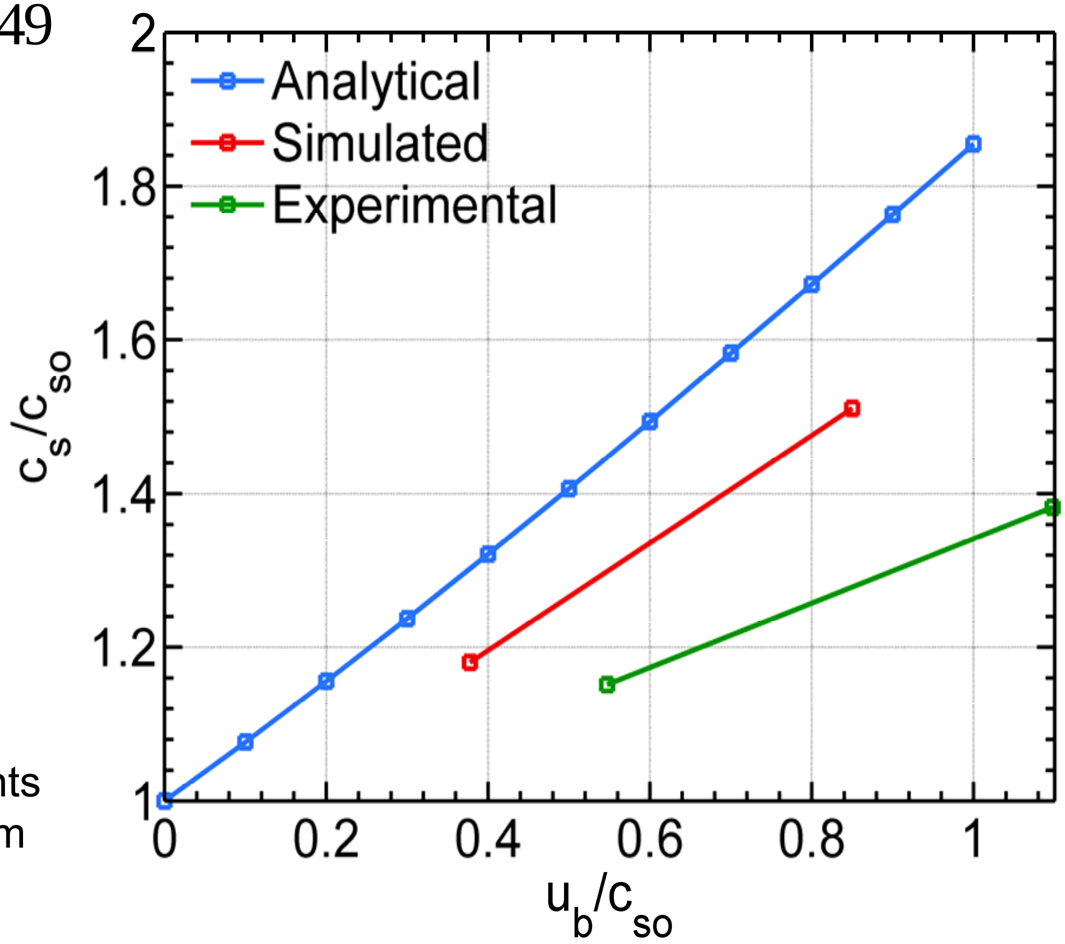

- The peak current increases with barrier velocity u_b
- Expand study to other beam currents to understand dependence on beam intensity

-O. Boine-Frankenheim, PRSTAB **13**, 034202, 2010.

Incorporating Transverse Current Loss into the Simulation Model

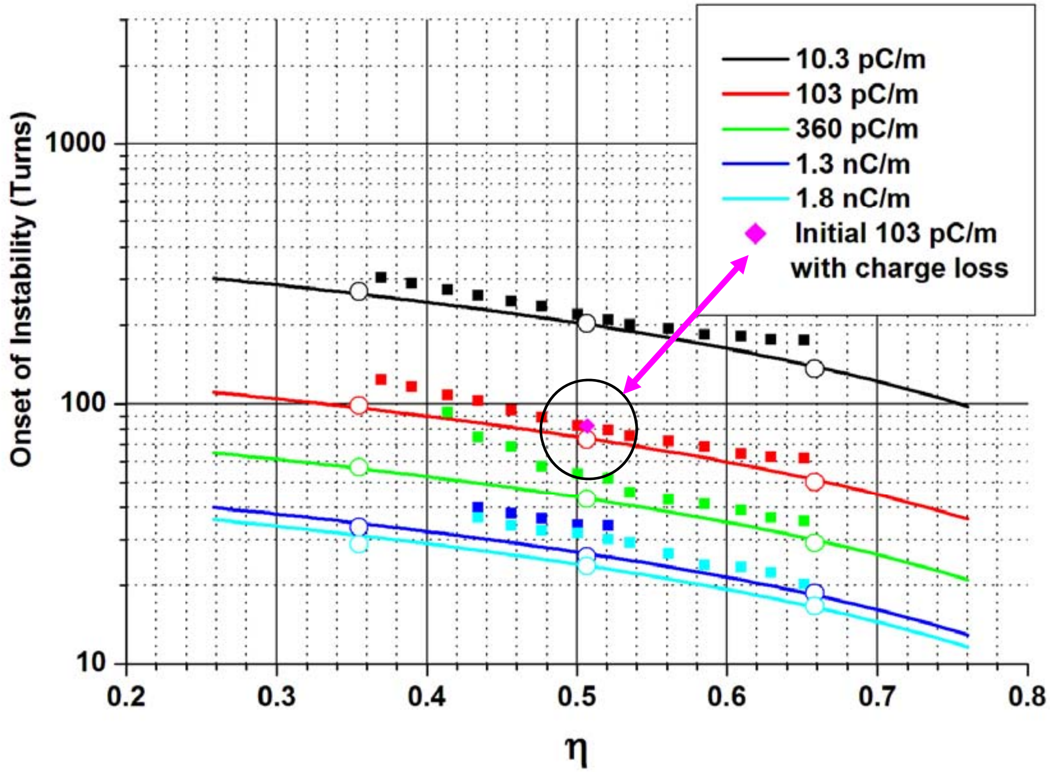

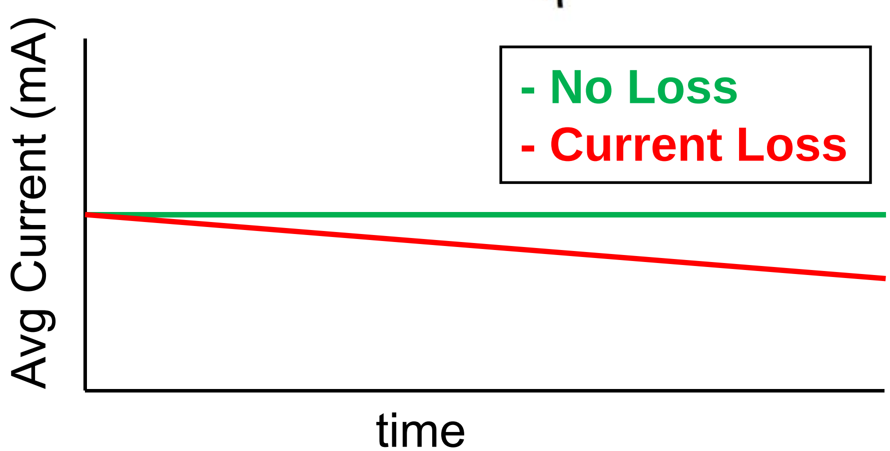

Current loss delays the longitudinal wave velocity, c_s and thus delays the onset of the instability

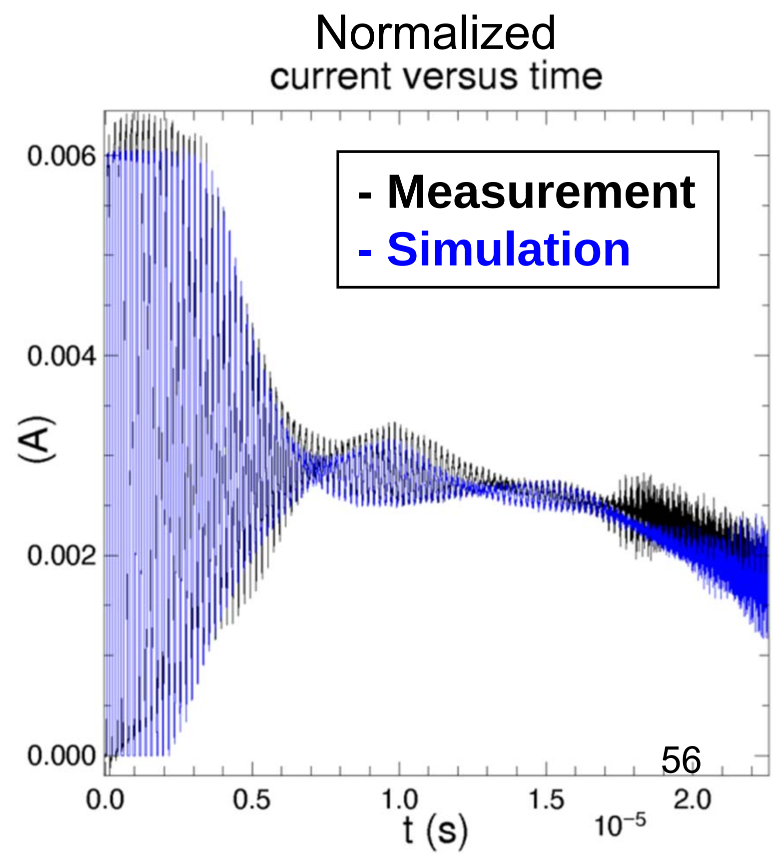

Method to Confirm Beam Size per Turn